HEINRICH HEINE
UNIVERSITÄT DÜSSELDORF

# RAS & RHO signaling in hepatic stellate cells

Dissertation

This dissertation is submitted
for the degree of the *Doctor of Philosophy*
to the Faculty of Mathematics and Natural Sciences
at the Heinrich-Heine-University Düsseldorf

presented by

**Jana Lissy**

from Dormagen, Deutschland

Düsseldorf, March 2019

HEINRICH HEINE
UNIVERSITÄT DÜSSELDORF

# RAS & RHO Signalwege in hepatischen Sternzellen

Inaugural-Dissertation

zur Erlangung des Doktorgrades
der Mathematisch-Naturwissenschaftlichen Fakultät
der Heinrich-Heine-Universität Düsseldorf

vorgelegt von

**Jana Lissy**

aus Dormagen, Deutschland

Düsseldorf, March 2019

aus dem Institut für Biochemie und Molekularbiologie II
der Heinrich-Heine-Universität Düsseldorf

Gedruckt mit der Genehmigung der
Mathematisch-Naturwissenschaftlichen Fakultät der
Heinrich-Heine-Universität Düsseldorf

Referent: Prof. Dr. Reza Ahmadian
Korreferent: Prof. Dr. Lutz Schmitt

Tag der mündlichen Prüfung: 2019

Für meinen wundervollen und besten Freund und Partner

Maik Lissy und unsere Tochter Louisa

´Being confident and believing in your own self-worth is necessary to achieving your fullest potential.´

Sheryl Sandberg

# Table of content

# Abbreviations

| | |
|---|---|
| aa | Amino acid |
| aHSC | Activated HSC |
| E-Ras | Embryonic stem cell-expressed RAS |
| GAP | GTPase-activating protein |
| GDP | Guanosine diphosphate |
| GEF | Guanine nucleotide exchange factor |
| GFAP | Glial fibrillary acidic protein |
| GTP | Guanosine triphosphate |
| GTPase | Guanosine triphosphatase |
| HC | Hepatocyte |
| HCC | Hepatocellular carcinoma |
| HGF | Hepatocyte growth factor |
| HSC | Hepatic stellate cell |
| IGF | Insulin-like growth factor |
| LDs | Lipid droplets |
| LMNB1 | Lamin B1 |
| MSC | Mesenchymal stem cell |
| mTOR | Mammalian target of rapamycin |
| NO | Nitric oxide |
| OCT4 | Octamer-binding transcription factor 4 |
| PDGF | Platelet-derived growth factor |
| PH | Pleckstrin homology |
| PIP3 | Phosphoinositide 3,4,5-trisphosphate |
| PI3K | Phosphoinositide 3-kinase |
| PRAS40 | 40 kDa pro-rich Akt substrate |
| PROTOR | Protein observed with RICTOR |
| PTM | Post-translational modification |
| qHSC | Quiescent HSC |
| RA | RAS association |
| RA | Retinoic acid |
| RASSF | RAS-association domain family |
| RBD | RAS binding domain |
| RE | Retinyl ester |
| RHO | RAS homolog |
| RICTOR | Rapamycin-insensitive companion of mTOR |
| SD | Standard deviation |
| SEM | Standard error of the mean |
| SIN1 | Stress-activated protein kinase interacting protein 1 |
| TGF | Transforming growth factor |
| VIM | Vimentin |
| WNT | Wingless-type MMTV |
| YAP | Yes-associated protein |

# Amino acid abbreviations

| Name | Letter code | Name | Letter code | Name | Letter code | Name | Letter code |
|---|---|---|---|---|---|---|---|
| Alanine | Ala (A) | Glutamic acid | Glu (E) | Leucine | Leu (L) | Serine | Ser (S) |
| Arginine | Arg (R) | Glutamine | Gln (Q) | Lysine | Lys (K) | Threonine | Thr (T) |
| Asparagine | Asn (N) | Glycine | Gly (G) | Methionine | Met (M) | Trypthophan | Trp (W) |
| Aspartic acid | Asp (D) | Histidine | His (H) | Phenylalanine | Phe (F) | Tyrosine | Try (Y) |
| Cysteine | Cys (C) | Isoleucine | Ile (I) | Proline | Pro (P) | Valine | Val (V) |

# Table of figures



# List of tables

# Introduction

## 1.1. Macro- and microanatomy of the liver

The human liver is the largest organ in the body, accounting for approximately 2 -3 % of the body weight. Located in the right-upper quadrant of the abdominal cavity below the right hemidiaphragm, the liver is protected by the rib cage and maintains its position through peritoneal reflections (Abdel-Misih & Bloomston, 2010). The dual blood supply is divided between the hepatic artery, which is responsible for 30 % nutrient poor and oxygen rich blood (60 % oxygen), and the portal vein, contributing to 70 % nutrient rich but oxygen poor blood (40 % oxygen). Portal and arterial blood is mixed in the hepatic sinusoids before it is drained into venous system of the liver (Burt & Day, 2003). The liver is divided into four lobes: right, left, quadrate, and caudate lobe. Based on anatomical aspects on pig dissections, Kiernan in 1833 described the lobules as functional units, which possess a hexagonal structure and are composed of many different cell types (Fig. 1A) (Kiernan, 1833).

The microanatomy of the liver can be directly linked to the function and described as a link of individual cellular components with their relationship and function. Metabolically, the liver is the most active and versatile organ. It is actually the first organ to get in contact with intestinally absorbed nutrients, received toxins, and various products from intestinal microorganisms. Therefore, the liver is responsible for detoxification of various metabolites, protein synthesis, regulation of glycogen storage, decomposition of red blood cells, and the production of biochemicals necessary for digestion. These functions require a complex interaction between individual cells, as well as regulation of blood supply and innervation (Baummann et al., 2008; Rappaport et al., 1954).

The liver lobules are composed of four major parts: 1) Connective tissues, i.e. vessels, ducts and nerve system. 2) Parenchyma, the functional tissue of the liver, consisting of hepatocytes. 3) Hepatic capillaries, known as sinusoids, a complex network of vascular spaces, where the supplied blood from terminal branches of the hepatic artery and portal vein is drained towards the central vein. 4) Space of Disse, the perisinusoidal space between hepatocytes and endothelial cells, which also habits the hepatic extracellular matrix, mostly consisting of fibronectin, collagens (type I, III, IV, V, and VI), laminin, and proteoglycan (Enzan et al., 1997; Iredale et al., 2013; Martinez-Hernandez & Amenta, 1993; Rauterberg et al., 1981) (Fig. 1A).

Hepatic sinusoids consist of five different cell types: hepatocytes, cholangiocytes, sinusoidal endothelial cells, Kupffer cells, and hepatic stellate cells.

*Hepatocytes* (HCs), that occupy about 80 % of the total liver volume, are sandwiched around the liver sinusoids. They are structurally and functionally heterogenic cells depending on their position. The major functions of periportal hepatocytes (zone 1, Fig. 1A) include: gluconeogenesis, β-oxidation of fatty acids, amino acid catabolism, bile secretion, and cholesterol, glycogen and urea synthesis. Whereas

periventricular hepatocytes are involved in glycolysis, lipogenesis, ammonia removal, detoxifications, ketogenesis, glycogen and bile acid synthesis (Gumucio, 1989; Häussinger et al., 1985; Kmiec, 2001; Lamers et al., 1989).

*Cholangiocytes* are a heterogeneous population of epithelial cells, which line the intra- and extrahepatic bile ducts. The main function of cholangiocytes is modification of hepatocyte-derived bile as it is transported from the canaliculi into the bile ducts (named bile ductules). The modification is mostly regulated by peptides, neurotransmitters, and hormones through various intracellular signaling pathways (Tabibian et al., 2013).

*Kupffer cells* (KCs) are liver resident macrophages. They are associated with endothelial cells in the lumen side of the sinusoid and contribute in clearing any bacteria, viruses, dead cells, and tumor cells from the liver. Moreover, they are an important source of cytokines secretion (Dixon et al., 2013).

*Liver sinusoidal endothelial cells* (LSECs) are the most abundant non-parenchymal hepatic cell population. They represent an interface between HCs and hepatic stellate cells on the one side and blood cells on the other side. LSECs are the permeable barrier of the liver and have the highest receptor-mediated endocytosis capacity, thus are responsible for immunological functions such as filtration, antigen presentation and leukocyte recruitment (Poisson et al., 2017; Shetty et al., 2018).

*Hepatic stellate cells* (HSCs), also called Ito cells, lipocytes or fat storing cells, contribute to 5-8 % of the total liver residing cells and are located between the basolateral surface of hepatocytes and sinusoidal endothelial cells in the space of Disse (Fig. 1A) (Kordes & Häussinger, 2013; Sawitza et al., 2009). Functions and responsibilities of HSCs differ in quiescent compared to activated cells, but main functions include storing of vitamin A and secretion of various factors and proteins, including hepatocyte growth factor (HGF) and extracellular matrix (ECM) proteins (Blaner et al., 2009; Schirmacher et al., 1992).

## 1.2. Hallmarks and roles of HSCs

**Quiescent HSCs (qHSCs) in the healthy liver**

Hepatic stellate cells (HSCs) (Ito cells, lipocytes, vitamin A-storing cells or fat storing cells) are located in the space of Disse between fenestrated perisinusoidal endothelial cells and hepatocytes of the hepatic lobule. Kupffer discovered the liver residing stellate cells in the late 19th century by using the gold chloride method. He intended to discover nerve fibers in the liver and by chance he found star-shaped cells and called them stellate cells (German: Sternzellen) (von Kupffer, 1876).

In the healthy liver, HSCs remain in a quiescent, non-proliferating state. They are characterized by their stellate- or star-shaped morphology, a high content of perinuclear, autofluorescent lipid droplets, and expression of neural and mesodermal markers, i.e. desmin and glial fibrillary acidic protein (GFAP) (Gard

et al., 1985; Popper & Greenberg, 1941; Wake, 1971; Yokoi et al., 1984) (Fig 1B). HSCs store about 80 % of the body contained vitamin A mainly as retinyl palmitate in lipid droplets (Hendriks et al., 1988). It is still controversially discussed whether HSCs develop from mesenchymal cells in the septum transversum or from the neural crest, as they contain proteins such as N-CAM, RHON, synaptophysin, and GFAP (Wake, 2006). Recent data suggest, that HSCs represent mesenchymal stem cells (MSC) due to their MSC-related expression profile, the potential to differentiate into adipocytes, and finally their supportive effects on extramedullary hematopoiesis (Castilho-Fernandes et al., 2011; Kordes et al., 2013). Regardless of their origin, during embryogenesis HSCs contribute to organogenesis and liver development through:

I) Progenitor proliferation; HSCs have a profound impact on proliferation of hepatoblasts (epithelial progenitors of hepatocytes and cholangiocytes) by releasing the mitogen factors such as fibroblast growth factor 10 (FGF10) (Berg et al., 2007), hepatocyte growth factor (HGF), which they produce in concert with LSECs (Delgado et al., 2009; Lorenz et al., 2018; Schirmacher et al., 1992), and wingless-type MMTV (WNT) (Matsumoto et al., 2008).
II) Cell fate and differentiation; HSCs control hepatoblast differentiation through extracellular matrix (ECM) protein production and NOTCH signaling (Nagai et al., 2002; Zong et al., 2009).
III) Hematopoiesis; HSCs support extramedullary hematopoiesis due to their MSC-like characteristics (Castilho-Fernandes et al., 2011; Kordes et al., 2013).
IV) Homing; the space of Disse displays similarities to the perivascular hematopoietic stem cell niche in the bone marrow and may favor homing of migrating hematopoietic stem/progenitor cells (Kordes & Häussinger, 2013; Kordes et al., 2013).

In the healthy liver, qHSCs contribute to main processes of retinoid storage, as well as to the maintenance and homeostasis of the stem cell niche and therefore to their significant role in liver regeneration. Mammals uptake retinoids from plants as pro-vitamin beta-carotene and retinyl esters (REs) from animal tissues. Excessive retinoids are stored as REs mainly in the liver but also in adipose tissue. The dietary REs esters are hydrolyzed into retinol and either released into the circulation, or re-esterified and stored in cytosolic lipid droplets (LDs) (Kudo, 1989). Retinoic acid (RA), the biologically active form of retinol, is synthesized in the liver and interacts with retinoic acid receptors (RARα, RARβ, RARγ) and retinoid X receptors (RXRα, RXRβ, RXRγ) and therefore plays an important role as a regulator of cell proliferation and differentiation (Hellemans et al., 2004). Retinoids (REs, retinol, retinal and RAs) are engaged in a large spectrum of physiological processes, e.g. development, organogenesis, differentiation, vision, reproduction and immunity (Blaner et al., 2009; Duester, 2008; Zhou et al., 2012). As the space of Disse displays similar characteristics to the perivascular hematopoietic stem cell niche, it provides soluble factors and cell-cell contacts, which are critical factors for stem cells maintenance

and self-renewal of the stem cell-like HSCs. HSCs appear to be the producers of HGF of the healthy liver, which is essential for hepatocytes homeostasis (Ramadori et al., 1992; Schirmacher et al., 1992). Moreover, characteristics of undifferentiated HSCs are controlled by several signaling pathways, such as WNT, NOTCH, JAK-STAT, BMP, Activin/transforming growth factor (TGF)/Nodal and hedgehog, whereas WNT and NOTCH signaling pathway are responsible for the maintenance of the stem cell niche and the quiescence of HSCs (Kordes & Häussinger, 2013; Kordes et al., 2008; Reya et al., 2003; Sawitza et al., 2009). In addition to their supportive role within the stem cell niche of the liver, HSCs also possess characteristics of stem cells, i.e. the expression of octamer-binding transcription factor 4 (OCT4) and CD133 (cluster designation 133) genes, and react as multipotent cells with the potency to differentiate *in vivo* and *in vitro* into other cell lineages, such as hepatocyte-like, endothelial-like cells, adipocytes, and undifferentiated embryonal sarcoma cells (Kordes et al., 2013; Kordes et al., 2014; Kordes et al., 2007; Sawitza et al., 2015; Tanaka et al., 2012; L. Yang et al., 2008).

Their fundamental role in the support of the liver stem cell niche, the release of cytokines and growth factors, which promotes the regeneration of hepatic epithelial cells, as well as the potential to differentiate into other liver cells, point out their importance in liver regeneration, which was also recently shown *in vivo* (Kordes et al., 2014; L. Yang et al., 2008; Yin et al., 2013; Zaikina et al., 2017). However, during the regression of liver damage, the number of activated hepatic stellate cells (aHSCs) is greatly reduced by the induction of cellular senescence and apoptosis, or by the return to the quiescent state (Friedman, 2008; Kisseleva et al., 2012; Troeger et al., 2012).

**Activated HSCs (aHSCs) in liver injury and regeneration**

Liver injury can be caused by massive alcohol consumption, virus mediated chronic liver injury, medication and genetic diseases. As a consequence apoptotic or necrotic hepatocytes release factors, which activate HSCs and trigger their transdifferentiation into contractile, proliferative, and migrating cells, so-called activated HSCs (Fig. 1C and Fig. 1D) (Tsuchida & Friedman, 2017). Activated HSCs are distinct from myofibroblasts in their vitamin A content, contractile activity, and relative responsiveness to cytokines, particularly TGF (Castilho-Fernandes et al., 2011; Friedman, 2008). They show a reduction in retinoic acid level (Friedman et al., 1993; Ohata et al., 1997), up-regulation of various genes, i.e. α-smooth muscle actin (α-SMA) and collagen type I, and down-regulation of GFAP (Gard et al., 1985; Kordes et al., 2007; Ramadori et al., 1990). Besides the *in vivo* activation following liver injury, HSCs also activate *in vitro* by culturing freshly isolated HSCs on plastic dishes, where they show similar characteristics to the *in vivo* activation models (De Minicis et al., 2007; Nakhaei-Rad et al., 2016).

Activated HSCs represent well-known extracellular matrix (ECM) producing cells. ECM production is important for maintenance of tissue structure and function (Jones et al., 1993; D. R. Wang et al., 2004). In acute liver infection, HSCs protect HCs against toxins of ectopic pathogens by releasing collagen type

I and contributing to scar tissue formation (Bansal, 2016; Friedman, 2008). However, apart from the protective function of scar tissue, in chronic liver injuries, dysregulation of fibrosis can occur thus resulting in excessive scar formation which interferes with the normal liver function. In some pathophysiological conditions, a lasting activation of HSCs causes the accumulation of ECM in the liver and initiate liver diseases like fibrosis and even cirrhosis and hepatocellular carcinoma (HCC) if it remains untreated (Dechene et al., 2010; Pellicoro et al., 2014).

Liver regeneration is a highly organized tissue regrowth process, driven by parenchymal cells (HCs) and non-parenchymal cells (i.e. HSCs, KCs, LSECs, and lymphocytes), which restores the liver mass by cell proliferation. However, two different models of liver regeneration are known. Regeneration after partial hepatectomy (PHx) (two-third of the liver mass is removed), where the remaining diploid hepatocytes enter into the cell cycle and start proliferation to compensate for the loss of liver tissue. The other model of regeneration takes place after liver injury caused by toxins or viral infections, where hepatocytes are injured and therefore progenitor cells as well as oval cells are required to differentiate into HCs, LSECs and biliary cells (Michalopoulos, 2010; Michalopoulos & DeFrances, 1997). Notably, there are growing numbers of evidences indicating the pivotal contribution of other liver cell types, especially HSCs, in supporting hepatocytes upon liver regeneration, by providing high levels of hepatocyte growth factor (HGF), cytokines, chemokines, NOTCH signaling activity and modulation of the ECM composition (Fig. 1C) (Bansal, 2016; Friedman, 2008; Geffers et al., 2007; Roskams, 2008; Sawitza et al., 2009; Yin et al., 2013). HSCs serve as liver stem cells within the space of Disse as a stem cell niche by providing soluble factors and an appropriate microenvironment for cell-cell communication (Kordes & Häussinger, 2013; Kordes et al., 2014; Sawitza et al., 2009). Similar to oval cells, they are multipotent cells and possess stem cell properties as described before. In addition transplanted HSCs transdifferentiate into progenitor cells during liver regeneration (Kordes et al., 2014; L. Yang et al., 2008).

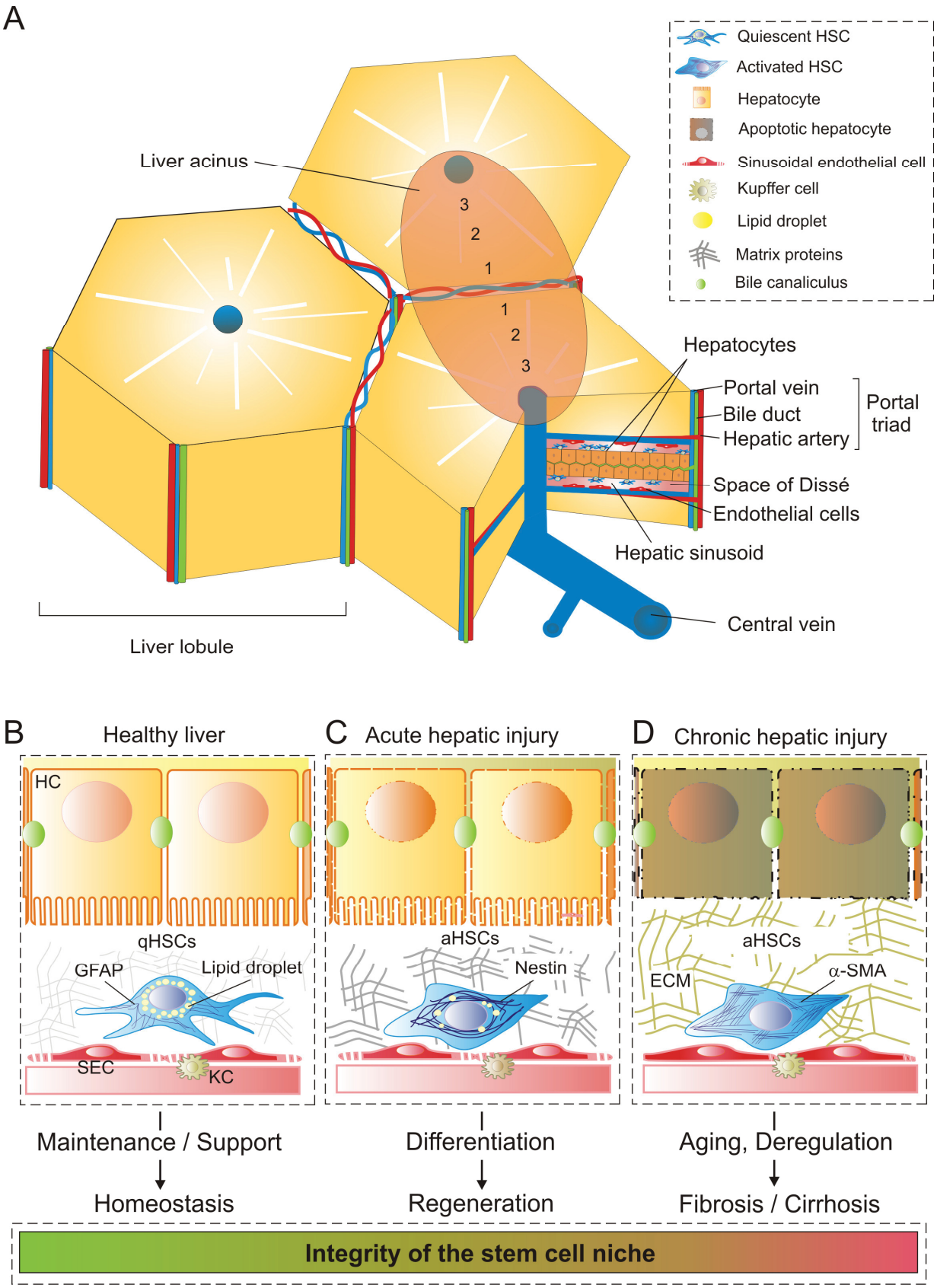


***Figure 1: Microanatomy of the liver and liver residing cells.*** (A) Illustration of liver three lobules and acinus, zone 1 to 3 with a schematic view of sinusoidal space, liver resident cells, Disse space, and blood vessels. (B) Quiescent HSCs (qHSCs) in a healthy liver. (C) Activated HSC (aHSCs) in regeneration. (D) Activated HSC (aHSCs) in liver fibrosis.

## 1.3. Postulated signaling pathways in HSCs

The most exciting aspects of HSCs are their bilateral roles during physiological and pathophysiological situations as positive or negative players. Therefore, there is a pivotal need to further understand the molecular mechanisms that govern the fate and contribution of HSCs in different cellular circumstances. Pathways such as RAS-MAPK, PI3K-AKT, JAK-STAT3, HIPPO-YAP, NOTCH, WNT and Hedgehog, in response to growth factor activation of platelet-derived growth factor (PDGF), transforming growth factor beta (TGFβ) and insulin-like growth factor (IGF), are reported to regulate the plasticity of HSCs during liver development, hemostasis, repair and fibrosis (Carloni et al., 2002; de Souza et al., 2015; Kordes et al., 2008; Lakner, 2010; Mannaerts et al., 2015; Reimann et al., 1997; G. Xie et al., 2013). In addition, it has been shown that supply of nitric oxide (NO) prevents liver damage and that NO is a potent modulator of HSC contractility and may regulate this function by autocrine mechanisms (Nanji et al., 1995; Rockey & Chung, 1995). However, it remains unclear how cross-talks between different signaling pathways modulate the HSC fate decision, as well as the involvement in quiescence and activation of HSCs. The next section shall give an overview about Ras and RHO signaling pathways and their possible role in the regulation of activation of HSCs.

## 1.4. Ras as the prototype of a superfamily

The RAS superfamily comprises more than 150 small GTPases that have been identified in different eukaryotes, ranging from yeast to human (Bourne et al., 1990; Rojas & Valencia, 2014; Wennerberg et al., 2005). The history of the RAS protein family dates back to the 1960s, when Jennifer Harvey and later Werner Kirsten discovered highly oncogenic Harvey and Kirsten murine sarcoma viruses (Ha-MSV and Ki-MSV) causing rapid tumor formation in rats (Harvey, 1964; Kirsten & Mayer, 1967). Later, these viral oncogenes, named Harvey and Kirsten Ras (H-Ras and K-Ras), along with their neuroblastoma Ras (N-Ras) viral oncogene homolog, were further characterized and assigned to the Ras superfamily as the founding members (Colicelli, 2004). Proteins of the RAS superfamily act as molecular switches cycling between a GTP-bound (active) and a GDP-bound (inactive) state (Fig. 2) (Wittinghofer & Vetter, 2011). Based on the sequence, structure and functional similarities, they are divided into five major families: RAS, RHO, RAB, ARF and RAN (Wennerberg et al., 2005). This superfamily plays a major role in signal transduction by transducing signals from receptors at the membrane to downstream effectors and can therefore regulate a variety of cellular processes. RAS GTPases are involved in regulation of transcription, cell proliferation, survival, differentiation and lipid synthesis, whereas RHO GTPases regulate actin organization and the cytoskeleton. RAB and ARF GTPases play a role in vesicular trafficking, regulating endocytosis and secretory pathways. RAN GTPases are involved in nuclear-cytoplasmic transport and mitotic spindle organization (Amin et al., 2013; Coleman et al., 2004; Nakhaei-Rad et al., 2018; Rajalingam et al., 2007).

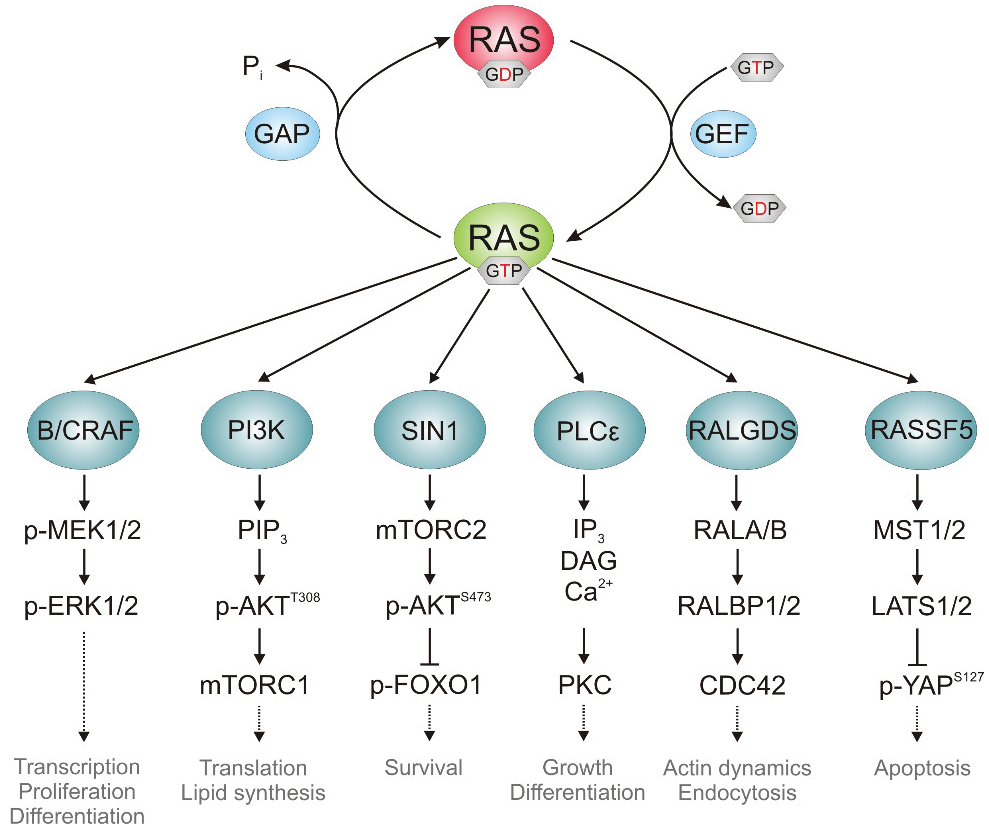


***Figure 2: Schematic view of the RAS GTPase cycle and its downstream signaling pathways.*** RAS proteins cycle between a GDP-bound (inactive) and a GTP-bound (active) form, catalyzed by the two regulatory proteins GEF and GAP. They mainly pass the signal to downstream effectors and exert their cellular function when bound to GTP and anchored to the plasma membrane *via* posttranslational modifications.

The proteins of the RAS superfamily share a highly conserved guanine-nucleotide binding (G) domain comprising five central motifs, G1 to G5, and a variable C-terminal membrane anchoring region, divided into the hypervariable region (HVR) and the CAAX motif. X-Ray structures show the G1 region as a loop ($^{10}$GxxxxGK(S/T)$^{17}$), which is responsible for binding to the phosphates of GTP or GDP (Bourne et al., 1990, 1991; Nakhaei-Rad et al., 2018; Saraste et al., 1990; Schlichting et al., 1990). Substitution of Gly 12 to any other amino acid (except proline) leads to hyperactivation and is mostly found in cancers (Bos, 1989; Tidyman & Rauen, 2009). G2 and G3 motifs, also called switch I and switch II, are dynamic regions changing their confirmation and orientation upon GTP binding and additionally provide the effector binding sites. G4 and G5 motifs are responsible to sense and stabilize the guanine nucleotide binding of the G domain (Bourne et al., 1990; Wittinghofer & Vetter, 2011).

An important biochemical feature of almost all RAS superfamily proteins is their post-translational modification of the C-terminal CAAX (C=Cys, A=aliphatic, X=any amino acid) tetrapeptide sequence by lipids. These post-translational modifications are essential for facilitating membrane association and

subcellular localization needed for biological functions (Ahearn et al., 2012; Wennerberg et al., 2005). The CAAX motif and its upstream HVR are the recognition sites for either prenylation or palmitoylation of RAS and RHO proteins. Most of the RHO proteins terminate with Leu at the X position of the CAAX motif and are modified by geranylgeranyltransferase I (GGTase I), which catalyze the covalent addition of a geranylgeranyl isoprenoid to the Cys residue. Ras proteins, which mainly do not terminate with a Leu, are modified by farnesyltransferase (FTase), which catalyze the addition of a farnesyl isoprenoid to the Cys of the CAAX motif. Although the prenylation modification is needed for plasma membrane localization, it is not sufficient, and a second signal is required for membrane targeting; Palmitoylation modification of Ras proteins occurs at one or two Cys residues upstream of CAAX motif in the HVR and can increase their membrane affinity. Palmitoylacyltransferase (PAT) enzyme is responsible for the fatty acid chain attachment (Buss & Sefton, 1986; Nakhaei-Rad et al., 2018; Wennerberg et al., 2005).

Some RAS superfamily members do not appear to be modified by lipids, but still associate with the membrane (e.g. Rit, RhoBTB, Miro and Sar1) and others (e.g. Rab and Rerg) are not lipid modified and are not bound to membrane (Wennerberg et al., 2005).

As mentioned before, RAS superfamily proteins cycle between an active (GTP-bound) state and an inactive (GDP-bound) state. The conformational state of RAS is controlled by two kinds of proteins, GTPase-activating protein (GAP) and guanine nucleotide exchange factor (GEF). While GAPs inactivate RAS proteins by stimulating the slow intrinsic rate of GTP hydrolysis, GEFs activate RAS by increasing the rate of GDP dissociation, allowing GTP to bind (Bourne et al., 1990, 1991; Scheffzek et al., 1997).

## 1.5. RAS family of GTPases

RAS family GTPases control a wide range of cellular functions depending on their tissue expression and localization. Today, 39 members of the RAS family are reported, including H-Ras, K-Ras, N-Ras, Rap1A/B, Rap2A/B/C, RalA/B, RRas subgroup (RRas, TC21 and MRas), Rheb, DiRas (Rig), RasD (AGS1/DexRas), Rasl10, E-Ras, and Rit (Rojas & Valencia, 2014). The best investigated RAS proteins are H-Ras, N-Ras and K-Ras4B, share overlapping functions, including cell proliferation, differentiation and apoptosis. However, different RAS isoforms exhibit a particular pattern of expression, different regulators and specific microdomains or subcellular localization, indicating their functional specificity as well as redundant roles (Castellano & Santos, 2011; Ichise et al., 2010; Lau & Haigis, 2009; Leon et al., 1987; Omerovic et al., 2007).

### 1.5.1. Embryonic-stem cell-expressed Ras (E-Ras)

Embryonic stem cell-expressed Ras (E-Ras) was introduced by Yamanaka and colleagues in 2003 as a novel member of the Ras family, specifically expressed in undifferentiated mouse embryonic stem cells. E-Ras expression seemed to be critical for maintenance of growth and tumor-like properties in these cells (Takahashi et al., 2003). Later E-Ras expression was also detected in some tumor cell lines, e.g. colorectal carcinomas, breast cancer, pancreatic carcinomas (Ikink et al., 2018; Yasuda et al., 2007) and gastric cancer, where it may play a role in cancer cell survival and metastases (Kubota et al., 2010). In addition, E-Ras expression was also found in gastric cancer tissue and various neuroblastoma cell lines that have been suggested to promote transforming activity and may be the driver of cancer and resistance to chemotherapy (Aoyama, 2010; Ikink et al., 2018; Kaizaki et al., 2009). Recently, we have demonstrated expression of E-Ras in quiescent hepatic stellate cells (HSCs), where it controls distinct pathways, including PI3K/AKT and MST/YAP, and seems to be critical for maintenance of the HSC quiescence in the liver (Nakhaei-Rad et al., 2016).

Sequence comparison between E-Ras and other Ras isoforms highlighted additional regions and motifs, such as the unique N-terminus of E-Ras that is not present in other Ras-like proteins. The 38 aa N-terminal extension of E-Ras might modulate its cellular localization through interaction with potential adaptor/scaffold proteins via putative PXXP and RRR motifs, as significant differences in localization of the N-terminal mutants of E-Ras were observed (Nakhaei-Rad et al., 2015). Besides a unique N-terminal extension, E-Ras harbors a significant amino acid deviation compared to other Ras proteins. The deviation in the phosphate binding loop from Gly to Ser at position 50 causes a hyperactivation as a result of GAP insensitivity (Nakhaei-Rad et al., 2015). Substitution of G12 (H-Ras numbering) for any other amino acids in Ras isoforms is frequently associated with tumor formation (Tidyman & Rauen, 2009). Additionally, E-Ras contains different amino acids in the effector binding sites, implicating it may utilize other effectors and therefore activate other downstream signaling pathways as compared to classical Ras proteins such as H-Ras, K-Ras and N-Ras (Nakhaei-Rad et al., 2016; Nakhaei-Rad et al., 2015; Rajalingam et al., 2007). However, the downstream effectors and signaling pathways selective for E-Ras are not fully identified yet.

## 1.6. RHO family of GTPases

The RHO family of GTPases is another subfamily of the Ras superfamily and comprise 20 family members, including the well-studied triad RAC1, RHOA and CDC42. Rho family members can be divided into classic and atypic GTPases. Classic Rho proteins are regulated by GAPs and GEFs, whereas atypical proteins (e.g. RND subfamily and RHOH) are unable to hydrolyze GTP and therefore remain in its constitutively GTP-bound active state (Haga & Ridley, 2016). Most RHO proteins require permanent posttranslational modification by isoprenyl groups to facilitate their localization to the membrane (Mitin et al., 2012). Consequently, these proteins underlie a third control mechanism that is achieved by the function of guanine nucleotide dissociation inhibitors (GDIs), which bind selectively to prenylated RHO proteins and control their localization between cytosol and membrane (S. C. Zhang, K. Nouri, et al., 2014).

Biochemical functions of RHO GTPases include the organization of the actin cytoskeleton, regulation of microtubule dynamics, regulation of several signal transduction pathways that alter gene expression, as well as regulation of enzymatic activities, including ROS (reactive oxygen species) generation and lipid metabolism (Chardin et al., 1989; Illenberger et al., 1998; Jaffe & Hall, 2005; Paterson et al., 1990; Takeya & Sumimoto, 2003). Besides contributing to physiological processes, RHO GTPases have been found to contribute to pathological processes including cancer cell migration, invasion, and metastasis, inflammation, and wound repair (Aspenstrom, 2018; Aspenstrom et al., 2007; Jaffe & Hall, 2005). RHO proteins might be linked to cancer only through their interaction with known oncogenes, such as Ras, as it was shown that RHOA and RAC1 can cooperate with RAS and RAF in tumor progression (Qiu et al., 1995).

### 1.6.1. RHO-related GTP-binding protein RHOQ (TC10)

The small RHO-related GTPase RHOQ, also called TC10, has been classified on the basis of sequence homology to be a member of the RHO family. TC10 plays a role in the regulation of the actin cytoskeleton like other Rho GTPases. Additionally, there is evidence that TC10 is involved in the regulatory mechanism of adipocyte insulin signaling and is a regulator of glucose uptake in a PI3K-independent pathway, but does not participate in insulin signaling in muscle cells (JeBailey et al., 2004; Satoh, 2014). As a consequence of insulin docking to its receptor, TC10 has been suggested to locate to Glut4 (Glucose transporter type 4) storage compartments and stimulate their translocation to membrane in order to enable glucose uptake (Kanzaki & Pessin, 2003). So far, there is no available study about the role and function of TC10 in HSCs.

## 1.7. Ras effectors, scaffold proteins and interactions partners

RAS effectors are defined as proteins with a strong affinity to GTP-bound RAS and binding to the effectors leads to downstream signal transduction. RAS effectors share little sequence homology but all contain either a Ras binding domain (RBD) or Ras association (RA) domain (Herrmann, 2003). Depending on the RAS effector itself, different biological pathways are activated and therefore the cellular outcome may vary (Fig. 2). Among all RAS effectors, the best studied effectors include RAF, PI3K, PLCε, and RALGDS (Marshall, 1996).

Beside RAS effectors, scaffold proteins may also regulate various signaling pathways by interacting or binding to Ras proteins, tethering them into complexes, localizing the complex to specific cellular areas such as the nucleus, mitochondria, Golgi, or plasma membrane and coordinate negative and positive feedback signals (Ferrell, 2000; Shaw & Filbert, 2009). There is an increasing number of Ras scaffold and adaptor proteins, including CAM, GAL1, GAL3, IQGAP1, NCL, NPM1, SHOC2, SHP2, SPRY, SPRED1, and GAB1, that are responsible in modulating and integrating Ras proteins in various signaling networks (Nakhaei-Rad et al., 2018). Future studies will investigate further on modulatory proteins and shed light on the underlying mechanisms of these groups of scaffold proteins.

### 1.7.1. Upstream regulators and substrates of the mTORC2 complex

The mammalian or mechanistic target of rapamycin (mTOR) is a phosphoinositide-3 kinase-related protein kinase, which plays an important role in the regulation of several cellular processes in response to a broad spectrum of intracellular and extracellular stimuli (Brown et al., 1994). It is the catalytic subunit of the two structurally distinct complexes mTORC1 (mTOR complex 1) and mTORC2 (mTOR complex 2). While mTORC1 mediates temporal control of cell growth by activating anabolic processes, mTORC2 facilitates spatial control of cell survival and cell growth mainly by regulating actin cytoskeleton organization K substrate of 40 kDa) and DEPTOR (DEP domain containing mTOR-interacting protein). The components of the mTORC2 complex are mTOR, LST8, DEPTOR, PROTOR1 (Protein observed with Rictor-1), RICTOR (rapamycin-insensitive companion of TOR) and SIN1 (stress-activated protein kinase-interacting protein 1) (Loewith et al., 2002).

While the regulation and cellular function of mTORC1 are well defined, less is known about the regulation of mTORC2. It is suggested that mTORC2 is localized next to the plasma membrane and is activated by growth factors, due to its association with AKT and therefore, may play a role in various cancer types (Guertin et al., 2009; Sarbassov et al., 2005; D. Wang et al., 2016). In addition, a positive feedback loop between AKT and mTORC2 via SIN1 T86 phosphorylation has been reported and is suggested to enhance mTORC2 kinase activity (G. Yang et al., 2015). However, dual SIN1 phosphorylation at positions T86 and T398 mainly by S6K impairs mTORC2 complex integrity and

suppresses its activity towards AKT (Liu et al., 2013; Liu et al., 2014; J. Xie & Proud, 2013) (Fig. 6A). Interestingly, in addition to a CRIM (conserved region in the middle) and a PH (pleckstrin homology) domain, which are responsible for target recognition of the mTORC2 substrate kinases and membrane targeting, SIN1 harbors a RBD (Schroder et al., 2007; Tatebe et al., 2017; Y. Yuan et al., 2015). Until now only a few studies connect Ras proteins with SIN1 interaction and therefore mTORC2 activation via SIN1 RBD *in vivo* as well as *in vitro* (Charest et al., 2010; Kamimura et al., 2008; Khanna et al., 2016; S. Lee, 2005; Nakhaei-Rad et al., 2016). It is even suggested that SIN1 suppresses RAS signaling (Schroder et al., 2007). Thus, upstream regulation of mTORC2 still remains elusive and further studies are needed to shed light into the possible interaction of upstream regulators of SIN1 as well as mTORC2.

### 1.7.2. Arginase 1 (ARG1)

Arginase (ARG) is a manganese-containing enzyme (EC 3.5.3.1) which catalyzes the fifth and final reaction in the urea cycle by hydrolyzing L-arginine into L-ornithine and urea (Krebs & Henseleit, 1932; Wu & Morris, 1998). There are two paralogs which differ in cellular expression, regulation, and localization (Cederbaum et al., 2004; Jenkinson et al., 1996; Zamecka & Porembska, 1988). The cytosolic arginase-1 (ARG1) is mainly expressed in hepatic cells such as hepatocytes and is thought to be primarily involved in ureagenesis, while ubiquitously expressed mitochondrial arginase-2 is involved in ornithine metabolism (Banerjee et al., 2017; Cederbaum et al., 2004; Janne et al., 1991; Lange et al., 2004; Mezl & Knox, 1977). Arginase activity essentially controls nitric oxide (NO) synthesis and vascular functions since L-arginine is the substrate of both arginase and nitric oxide synthase (NOS) (Durante et al., 2007). Thus, arginase has emerged as a promising therapeutic target for various cardiovascular diseases (Bratt et al., 2011; Lange et al., 2004; Pernow & Jung, 2013; Z. Yang & Ming, 2013), but also in atherosclerosis and inflammatory diseases as increased arginase activity may have anti-inflammatory properties and might be protective (Getz & Reardon, 2006; Teupser et al., 2006). Notably, ARG1 deficiency affects the liver-based urea cycle, leading to hyperargininemia with progressive neurological and intellectual impairment and persistent growth retardation (Sin et al., 2013; Sin et al., 2015). It has been shown that constitutively active Ras mutants and different members of the MAPK family play a role in modulating iNOS and arginase expression (Jin et al., 2015). However, the complete regulation and activation of ARG1 still remains elusive and further investigations are needed to understand arginine metabolism and the possible cross-talk to small GTPases.

## 1.8. Aims and objectives

Hepatic stellate cells play pivotal roles in liver development, immunoregulation, homeostasis, regeneration, and pathology. In addition, they emit a remarkable plasticity in their phenotype, expression profile and function. After activation HSCs contribute either in liver regeneration or in pathological situations, they promote scar formation and liver fibrosis (Fig. 1B, C and D). However, little is known about the intracellular signaling networks which orchestrate HSCs plasticity and their bilateral functions as positive and negative regulators of liver damage responses. Therefore, it is important to consider the impact of different signaling pathways on HSC fate decision and future studies need to focus on finding pharmacological drugs that target HSC activation and shift them to participate in liver regeneration.

In this doctoral thesis, it was the aim to investigate the roles, interaction partners and downstream effectors of the E-Ras signaling pathway that contribute to maintenance of HSC quiescence, play a role during activation of HSCs and may revert activation to quiescence of HSCs. Moreover, it was the aim to generate a new model that will help to a better understand the signaling networks of HSCs. E-Ras appears to play a pivotal role in the fate of HSCs, as it seems important for the maintenance of quiescence in HSCs. However, the regulation, function and particularly downstream effectors of E-Ras especially in HSCs are poorly understood. Therefore, we comprehensively investigated on downstream effectors and their signaling pathways (e.g. mTORC2 pathway) and on other interaction partners that were detected upon mass spectrometry experiments. Furthermore, we analyzed the effects of different cell culture conditions to sustain HSC quiescence in freshly isolated cells that usually tend to activate upon *ex vivo* culture. It was the overall aim to gain more knowledge about the function of RAS-dependent signaling networks in HSCs and help future studies in understanding liver problems and restoring liver regeneration responses.

# 2. Material and methods

# 2.1. Material

## 2.1.1. Antibiotics

| | | |
|---|---|---|
| Ampicillin | Carl Roth GmbH, Karlsruhe | f.c. 100 µg/ml |
| Antibiotic-Antimycotic | Thermo Fisher Scientific, Waltham, MA, USA | f.c. 100 µg/ml |
| Chloramphenicol | Carl Roth GmbH, Karlsruhe | f.c. 34 µg/ml |
| Penicillin/Streptomycin | Thermo Fisher Scientific, Waltham, MA, USA | f.c. 100 U/ml |
| Puromycin | Carl Roth GmbH, Karlsruhe | f.c. 1,5 µg/ml |

## 2.1.2. Antibodies

*Table 1: Primary antibodies*

| Antibody | Company | Catalog number |
|---|---|---|
| α-Actin | Merck Millipore | MAB1501 |
| α-AKT | Cell Signaling | 9272 |
| α-phospho AKT (T308) | Cell Signaling | 2965 |
| α-phospho AKT (S473) | Cell Signaling | 4060 |
| α-Arginase 1 | Santa Cruz | sc-18351 |
| α-αSMA | Dako | M0851 |
| α-E-Ras clone 3.5.8. | Self prepared for WB | |
| α-E-Ras clone 6.5.2. | Self prepared for cLSM | |
| α-FLAG | Sigma-Aldrich | F7425 |
| α-FOXO1 | Cell signaling | 2880 |
| α-phospho FOXO1 (S256) | Cell signaling | 9461 |
| α-GAPDH | Cell signaling | 2118 |
| α-GFAP | Dako | Z0334 |
| α-GST clone 2F3H8 | Self prepared | |
| α-His-HRP | Miltenyi Biotec | 130-092-785 |

| | | |
|---|---|---|
| α-His | Cell Signaling | 2366 |
| α-Histone H3 | Cell Signaling | 9715 |
| α-$Na^+K^+$ ATPase | Merck Millipore | A276 |
| α-Nucleophosmin | Abcam | AB10530 |
| α-Lamin B1 | Abcam | AB16048 |
| α-SIN1 | Cell Signaling | 12860 |
| α-SIN1 | Merck Millipore | 2746272 |
| α-phospho SIN1 (T86) | Cell Signaling | 14716 |
| α-p70 S6K | Cell Signaling | 2708 |
| α-phospho p70 S6K (T389) | Cell Signaling | 9205 |
| α-Vimentin | Cell Signaling | 5741 |
| α-γ-tubulin | Sigma | T5326 |

*Table 2: Secondary antibodies*

| **Antibody** | **Company** | **Catalog number** |
|---|---|---|
| Alexa Fluor 488 goat anti-mouse IgG (2mg/ml) | Thermo Fisher Scientific | A32723 |
| Alexa Fluor 488 donkey anti-rabbit IgG (2mg/ml) | Thermo Fisher Scientific | A21206 |
| Alexa Fluor 488 donkey anti-goat IgG (2mg/ml) | Thermo Fisher Scientific | A11055 |
| Alexa Fluor 546 goat anti-mouse IgG (2mg/ml) | Thermo Fisher Scientific | A32723 |
| Alexa Fluor 546 goat anti-rabbit IgG (2mg/ml) | Thermo Fisher Scientific | A11010 |
| Alexa Fluor 546 donkey anti-goat IgG (2mg/ml) | Thermo Fisher Scientific | A11056 |
| Alexa Fluor 633 goat anti-mouse IgG (2mg/ml) | Thermo Fisher Scientific | A21050 |
| Alexa Fluor 633 goat anti-rabbit IgG (2mg/ml) | Thermo Fisher Scientific | A21070 |
| Alexa Fluor 633 donkey anti-goat IgG (2mg/ml) | Thermo Fisher Scientific | A21082 |
| IRDye 800CW donkey anti-rabbit | Licor | P/N 925-32213 |
| IRDye 800CW donkey anti-goat | Licor | P/N 925-32214 |

| | | |
|---|---|---|
| IRDye 800CW goat anti-mouse | Licor | P/N 925-32210 |
| IRDye 680RD donkey anti-rabbit | Licor | P/N 925-68073 |
| IRDye 680RD goat anti-mouse | Licor | P/N 925-68070 |
| Anti-rabbit | Cell signaling | 7074S |
| Anti-goat | Merck | AP106P |
| Anti-mouse | Dako | P0161 |

## 2.1.3. Bacterial strains

*Table 3: Bacterial strains*

| **Bacterial strain** | **Genotype** | **Supplier** |
|---|---|---|
| *E. coli* BL21 (DE3) pLysS | F-, *omp*T, *hsd*$S_B$ ($r_B$-, $m_B$-), *dcm*, *gal*, λ(DE3), pLysS, $Cam^r$. | Promega, Madison, WI, USA |
| *E. coli* HD10Bac | *F-* mcr*A Δ(*mrr-*hsd*RMS-mcrBC*) Φ80*lacZΔM15 *Δ*lac*X74* recA1 endA1 araD139 *Δ(*ara*,* leu*)*7697 gal*U* gal*K λ*-rps*L* *nup*G*/*pMON14272/pMON7124 | Thermo Fisher Scientific, Karlsruhe |
| *E.coli* Rosetta (DE3) | $F^-$ *ompT, hsd*$S_B$ ($r_B$-, $m_B$-),*gal dcm* (DE3), pRARE ($Cam^R$) | Merck, Darmstadt |
| *E.coli* Codon Plus (DE3) | F– *ompT, hsdS* ($r_B$-, $m_B$-), *dcm*$^+$, $Cam^r$ gal λ(DE3) *endA* Hte [*argU proL* $Cam^r$] [*argU ileY leuW* Strep/$Spec^r$] | Agilent Technologies, Santa Clara, CA, USA |
| *E.coli* XL1-Blue | *recA1 endA1 gyrA96 thi-1 hsdR17 supE44 relA1 lac [F´proAB lacI*$^q$*Zdelta-M*15 Tn*10, (Tet*$^r$*)].* | Agilent Technologies, Santa Clara, CA, USA |
| *E.coli* HST-08 (Stellar) | F-*, endA1, supE44, thi-1, recA1, relA1, gyrA96, phoA, Φ80d lacZΔ M15, Δ(lacZYA-argF)* U169*, Δ(mrr-hsdRMS-mcrBC), ΔmcrA, λ-* | Takara Bio Inc., Kusatsu, Japan |

## 2.1.4. Buffers and solutions

Following buffers and solutions were used in this work:

| | |
|---|---|
| Acidic mixture | $H_2SO_4$, $H_3PO_4$ and $H_2O$ (1:3:7) |
| Blocking buffer milk (Western blotting) | 5 % milk powder in TBS-T |
| Blocking buffer Licor (Western blotting) | 1:3 Odyssey Blocking Buffer in TBS |
| Destaining solution | 20 % (v/v) Methanol<br>10 % (v/v) Acetic acid |
| FISH buffer | 50 mM Tris-HCl pH 7.5<br>100 mM NaCl<br>2 mM $MgCl_2$<br>1 % Igepal CA-630<br>10 % Glycerol<br>20 mM beta-Glycerolphosphate<br>1 mM ortho-$Na_3VO_4$<br>1 Tablet Protease-Inhibitor<br>Add 100 ml $dH_2O$ |
| Laemmli buffer 5x (SDS-PAGE) | 10% (m/V) SDS<br>5% (m/V) β-Mercaptoethanol<br>50% (m/V) Glycerol<br>125 mM Tris-HCl (pH 6.8)<br>0.1% Bromphenolblue |
| Phosphate buffered saline (PBS) | 1.5 mM $KH_2PO_4$<br>2.7 mM KCl<br>8.1 mM $Na_2HPO_4$<br>137 mM NaCl (pH 7.4) |
| Resolving buffer (SDS-PAGE) | 250 mM Tris-HCl (pH 8.0)<br>192 mM Glycerol<br>0.01 % (m/V) SDS<br>20 % Methanol |
| Running buffer (10x) (SDS-PAGE) | 250 mM Tris-HCl pH 8.0<br>1.92 M Glycine<br>1 % (v/v) SDS |
| Stacking buffer (SDS-PAGE) | 0.5 M Tris-HCl (pH 6.8)<br>0.4 % (m/V) SDS |
| Staining solution | 40 % (v/v) Methanol<br>10 % (v/v) Acetic acid<br>4 g/L Coomassie brilliant blue R250<br>4 g/L Coomassie brilliant blue R250 |

| | |
|---|---|
| Standard puffer (E-Ras purification) | 500 mM NaCl<br>150 mM Tris-HCl pH 7.5<br>5 mM $MgCl_2$<br>3 mM DTT<br>5 % Glycerol<br>0.1 mM GTP |
| Transfer buffer (Western blotting) | 250 mM Tris-HCl (pH 8.0)<br>192 mM Glycerin<br>0.01% (m/V) SDS<br>20% Methanol |
| Tris buffered saline (TBS) | 10 mM Tris-HCl (pH 7.4)<br>150 mM NaCl |
| TBS-T | 1% Tween-20 in TBS |

## 2.1.5. Cell lines and primary cells

*Table 4: Cell lines and primary cells*

| **Cell line / Primary cells** | **Description** |
|---|---|
| COS7 | SV40-transformed fibroblast cell line derived from African green monkey (ATCC number: CRL-1651) |
| HEK293T | Immortalized human embryonic kidney cell line (ATCC number: CRL-1573) |
| HepG2 | Human liver cancer cell line derived from male human with hepatocellular carcinoma (ATCC number: HB-8065) |
| HSCs | Primary hepatic stellate cells from *Rattus norwegicus* provided by the local animal facility of the Heinrich-Heine-University Düsseldorf, Germany |
| NIH3T3 *rn* E-Ras | Fibroblast cell line derived from Swiss albino mouse embryo tissue, stably transduced with *rn* E-Ras (Nakhaei-Rad et al., 2015) |

## 2.1.6. Chemicals

*Table 5: Chemicals*

| Chemical | Manufacturer | Storage |
|---|---|---|
| β-Glycerolphosphate | Merck, Darmstadt | RT |
| β-Mercaptoethanol | Merck, Darmstadt | 4°C |
| Acetone | Roth, Karlsruhe | 4°C |
| Acrylamide | Merck, Darmstadt | 4°C |
| Albumin linoleic acid | Merck, Darmstadt | 4°C |
| Ammonium persulfate (APS) | Merck, Darmstadt | -20°C |
| Coomassie Brilliant Blue G250 | Roth, Karlsruhe | RT |
| Coomassie Brilliant Blue R250 | Roth, Karlsruhe | RT |
| $ddH_2O$ | Merck, Darmstadt | RT |
| Dithiothreitol (DTT) | Gerbu Biotechnik, Wieblingen | -20°C |
| Deoxynucleoside triphosphate (dNTPs) | Qiagen, Hilden | -20°C |
| Dimethylsulfoxid (DMSO) | Merck, Darmstadt | 4°C |
| Donkey serum | Abcam, Berlin | -20°C |
| Dulbecco's Modified Eagle's Medium (DMEM) - high glucose | Gibco, Thermo Fisher Scientific, Karlsruhe | 4°C |
| Ethylenediaminetetraacetic acid (EDTA) | Merck, Darmstadt | RT |
| Ethanol | Roth, Karlsruhe | RT |
| Fetal Bovine Serum (FBS) | Thermo Fisher Scientific, Karlsruhe | -20°C |
| Gene Ruler 1kb DNA Ladder | Thermo Fisher Scientific, Karlsruhe | 4°C |
| Glutathione sepharose 4B | GE Healthcare. Freiburg | 4°C |
| Glycerol | Roth, Karlsruhe | RT |
| Goat serum | Abcam, Berlin | -20°C |
| GTP | Merck, Darmstadt | -20°C |
| Hydrochloric acid (HCl) | Roth, Karlsruhe | RT |
| IGEPAL CA-630 | Merck, Darmstadt | RT |

| | | |
|---|---|---|
| Insulin solution, human | Merck, Darmstadt | 4°C |
| Iscove´s Modified Dulbeccos´s Medium (IMDM) | Gibco, Thermo Fisher Scientific, Karlsruhe | 4°C |
| Isonitrosopropiophenone | Merck, Darmstadt | 4°C |
| Isopropanol | Merck, Darmstadt | RT |
| Isopropyl β-D-1-thiogalactopyranoside (IPTG) | Gerbu Biotechnik, Wieblingen | -20°C |
| ITS liquid media supplement (100x) | Merck, Darmstadt | 4°C |
| Laminin-521 | Biolamina, Sundbyberg, Sweden | -20°C |
| LB broth | Merck, Darmstadt | RT |
| Magnesium chloride ($MgCl_2$) | Merck, Darmstadt | RT |
| mantGTP | Jena Bioscience, Jena | -20°C |
| mantGppNHp | Jena Bioscience, Jena | -20°C |
| Methanol | VWR, Darmstadt | RT |
| Nitrogen, liquid | Linde, Pullach | |
| PageRuler Prestained | Thermo Fisher Scientific, Karlsruhe | 4°C |
| Potassium chloride (KCl) | Merck, Darmstadt | RT |
| ProLong Gold antifade mountant without DAPI | Thermo Fisher Scientific, Karlsruhe | -20°C |
| Protease Inhibitor Cocktail (complete, EDTA free) | Roche, Penzberg | 4°C |
| QIAzol lysis reagent | Qiagen, Hilden | 4°C |
| Retinol | Merck, Darmstadt | -20°C |
| SOC medium | Merck, Darmstadt | -20°C |
| Sodium chloride (NaCl) | Merck, Darmstadt | RT |
| Sodium hydroxide (NaOH) | Merck, Darmstadt | RT |
| Sodium dodecyl sulfate (SDS) pellets | Roth, Karlsruhe | RT |
| Sodium orthovanadate | Merck, Darmstadt | -20°C |
| Tetrahydrofuran | Merck, Darmstadt | 4°C |

| | | |
|---|---|---|
| Tetramethylethylenediamine (TEMED) | Merck, Darmstadt | 4°C |
| Tris | Roth, Karlsruhe | RT |
| Triton X-100 | Merck, Darmstadt | RT |
| Tween-20 | Merck, Darmstadt | RT |
| Trypan blue | Bio-Rad Laboratories GmbH, München | RT |

## 2.1.7. Constructs

ARG1 (P05089; aa 1–322), human E-Ras FL (Q7Z444; aa 1–233), human E-Ras *Nex* (aa 1–38), rat E-Ras FL (D3ZTE4; aa 1-227), rat E-Ras *Nex* (aa 1–38), G domain (aa 39–201), and ΔC (aa 1–201), human RIT1 ΔC (Q92963; aa 1-200), $RIT1^{G30V}$ FL (aa 1-219), human $H\text{-}Ras^{G12V}$ FL (P01112; aa 1-189), SIN1-$RBD^{RR311,312,EE}$ (Q9BPZ7; aa 266-373), and SIN1-$RBD^{FSL289\text{-}291REE}$ (Q9BPZ7; aa 266-373),were cloned into pcDNA3.1-Flag, pMal-c5X-His, pGEX-4T1-N-TEV vector or pFastBacHTB. Plasmids were used for protein expression in *Escherichia coli* and insect cells or, transfection in eukaryotic cells.

## 2.1.8. Consumables

*Table 6: Consumables*

| **Consumable** | **Manufacturer** |
|---|---|
| Biacore Sensor Chip CM5 | GE Healthcare, Freiburg |
| Biacore Sensor Chip L1 | GE Healthcare, Freiburg |
| Cell culture plates and dishes | TPP, Trasadingen, Schweiz |
| Cryo tubes | VWR, Darmstadt |
| Eppendorf tubes (0.5 ml, 1.5 ml, 2 ml) | Eppendorf GmbH, Hamburg |
| Falcon tubes (15 ml, 50 ml) | BD Biosciences, Franklin Lakes, USA |
| Gloves Nitra-Tex | Ansell Healthcare, Brüssel, Belgien |
| MicroAmp Optical 96-Well Reaction Plate | Applied Biosystems, Warrigton, UK |
| Nitrocellulose membrane (0.45 µM pore size) | Roth, Karlsruhe |
| Stripette Costar | Corning Incorporated, Coming, USA |

| | |
|---|---|
| TC10 System Counting Slides Dual Chamber | Bio-Rad Laboratories GmbH, München |
| Transwell Corning Costar cell culture inserts TC treated | Merck, Darmstadt |
| Whatman paper | VWR, Darmstadt |

## 2.1.9. Devices

*Table 7: Devices*

| **Device** | **Manufacturer** |
|---|---|
| Ätka Prime | GE Healthcare, Freiburg |
| Äkta Purifier | GE Healthcare, Freiburg |
| Äkta Start | GE Healthcare, Freiburg |
| Biacore X100 Plus | GE Healthcare, Freiburg |
| Centrifuge 5427 R | Eppendorf GmbH, Hamburg |
| Centrifuge 5804 R | Eppendorf GmbH, Hamburg |
| Chromatopac C-R8A | Shimadzu, Kyoto, Japan |
| Confocal microscope LSM-510 | Zeiss, Jena |
| Confocal microscope LSM-550 | Zeiss, Jena |
| Electrophoresis chamber | Bio-Rad Laboratories GmbH, München |
| Fluoromax-4 Spectrofluorometer | Horiba, Kyoto, Japan |
| Fridge | Liebherr GmbH, Rostock |
| Freezer | Liebherr GmbH, Rostock |
| Heating Dri-block DB 3 | Techne, Staffordshire, UK |
| Heracell VIOS 250i $CO_2$ incubator | Thermo Fisher Scientific, Waltham, MA, USA |
| Herasafe Cleanbench | Heraeus, Hanau |
| HPLC, LC118, LC166 | Beckman Coulter, Brea, CA, USA |
| INTAS iX imager | INTAS Science Imaging Instruments GmbH, Göttingen |
| Licor Odyssey Fc imager | Licor, Bad Homburg |
| Mastercycler | Eppendorf GmbH, Hamburg |

| | |
|---|---|
| Microfluidizer M110S | Microfluidics Corporation, Newton, MA, USA |
| Mini-PROTEAN Tetra System | Bio-Rad Laboratories GmbH, München |
| Neubauer chamber | LO-Laboroptik, Lancing, UK |
| NanoDrop ND-2000 | Peqlab, VWR Life Science Competence Center, Erlangen |
| pH meter | WTW, Weilheim |
| Pipetus-Akku | Hirschmann Laborgeräte, Eberstadt |
| Pipetts 1000 µl, 200 µl, 20 µl, 2.5 µl | Eppendorf GmbH, Hamburg |
| Photometer | Eppendorf GmbH, Hamburg |
| Power pac 300 | Bio-Rad Laboratories GmbH, München |
| Shaker KS15A | Edmund Bühler, Bodelshausen |
| Shaker Infors HT | Biotron Labortechnik GmbH, Hilden |
| Tecan infinite M200 PRO reader | Tecan, Crailsheim |
| Thermomixer 5436 | Eppendorf GmbH, Hamburg |
| Ultracentrifuge Optima Max-XP | Beckman Coulter, Brea, CA, USA |
| UV spectrometer | Eppendorf GmbH, Hamburg |
| Waterbath | Lauda GmbH, Lauda-Königshofen |
| Zeiss Primovert microscope | Carl Zeiss GmbH, Göttingen |
| 7500 Real-time PCR System | Applied Biosystems, Warrigton, UK |

### 2.1.10. Enzymes

All enzymes (polymerases, restriction enzymes, etc.) were purchased from Thermo Fisher Scientific, Karlsruhe.

### 2.1.11. Kits

*Table 8: Kits*

| Kit | Manufacturer |
|---|---|
| DNA-free DNA Removal Kit | Ambion, Life Technologies |
| Midi-prep, NucleoBOND Xtra mini | Macherey-Nagel, Düren |
| ImProm-II Reverse Transcription System | Promega, Madison, WI, USA |
| QIAprep Spin Miniprep Kit | Qiagen, Hilden |
| QIAquick PCR Purification Kit | Qiagen, Hilden |
| RNeasy Mini Kit | Qiagen Hilden |

### 2.1.12. Oligonucleotides

*Table 9: Primer sequences for Reverse transcriptase polymerase chain reaction*

| Gene | Forward primer | Reverse primer | Product size (bp) |
|---|---|---|---|
| *rn Akt* | GGGGCCACGGATACCATGAA | CACATCCTGAGGCCGTTCCT | 150 |
| *rn Arg1* | TTGGGTGGATGCTCACACTG | GTACACGATGTCCTTGGCAGA | 166 |
| *rn α-Sma* | CTCGGCATCAGGGCGTGAT | CTCTTCTGGTGCTACTCGCAG | 188 |
| *rn Desmin* | GTTTCAGACTTGACTCAGGCAG | TCTCGCAGGTGTAGGACTGG | 106 |
| *rn E-Ras* | CCTTGCCAACAAAGTCTAGCATC | GCCAGCATCTTTGCATTGTGC | 104 |
| *rn Foxo1* | GAACGACCTCATGGACGGAGA | GGGGTGAAGGGCATCTTTGGA | 198 |
| *rn Gfap* | CGGAGACGTATCACCTCTG | TGGAGGCGTCATTCGAGACAA | 123 |
| *rn Hprt1* | AAGTGTTGGATACAGGCCAGA | GGCTTTGTACTTGGCTTTTCC | 145 |
| *rn iNos* | TGGTGAGGGGACTGGACTTTT | TTCTCCGTGGGGCTTGTAGT | 89 |
| *rn Lmnb1* | CCGGGCTCAAGGCTCTCTA | GCGCGGCCTCATACTCTC | 198 |
| *rn mTor* | GTGGGCCGACTCAGTAGCAT | AGGCTCCATATAGGGGCGGA | 180 |
| *rn Npm1* | AACTCTTAGGCATGTCTGGAAAG | GCTGGGGTATCTCGTACAGATTT | 199 |
| *rn Sin1* | GAGACGCAGGGCTACATATACG | GCGGAGTCGTTCTAATCTTTGA | 105 |

| | | | |
|---|---|---|---|
| *rn p70-S6k* | TTTCTGGGGACGAGGTGCTT | AGTTGGGCTGTCGGATTGGA | 143 |
| *rn Vim* | CGGCTGCGAGAAAAATTGC | CCACTTTACGTTCAAGGTCAAG | 124 |

### 2.1.13. Plasmids

*Table 10: Plasmids*

| Vector | Description | Reference |
|---|---|---|
| pcDNA3.1(+) | Mammalian expression vector for transient and stable protein expression | Invitrogen (Carlsbad, CA, USA) |
| pFastBacHTB | Expression vector for transient and stable protein expression in insect cells | Invitrogen (Carlsbad, CA, USA) |
| pGex-4T1-NTEV | Expression vector for transient and stable protein expression in *E. coli* | Modified, originally from Invitrogen (Carlsbad, CA, USA) |
| pMAL-C5X | Expression vector for transient and stable protein expression in *E. coli* | New England Biolabs, Ipswich, MA, USA |

### 2.1.14. Programs

Following programs, versions and homepages were used in this study:

Biacore X100 Evaluation Software Version 2.0.1 (GE Healthcare, Freiburg, Germany)

CoralDRAW X3 (Coral corporation, Ottawa, Ontario, Canada)

EndNote X7 (Thomas Reuter, Carlsbad, CA, USA)

GraFit 5.0.13 (Erithacus Software Limited, Surrey, UK)

GraphPad Prism 6 (GraphPad, La Jolla, CA, USA)

Microsoft Office 2013 (Microsoft Corporation, Redmond, USA)

PyMOL (Richardson Lab, Duke University, NC, USA)

SnapGene (GSL Biotech LLC, Chigago, IL, USA)

Zen 2 (blue edition), V2.0 de (Zeiss, Jena, Germany)

# 2.2. Methods

## 2.2.1. Microbiological methods

### 2.2.1.1. Transformation of E. coli

Transformation of DNA was applied by using standard protocols for competent *E. coli* strains. In brief, plasmid DNA (1 µg) was added to 50 µl of thawed, competent bacteria, followed by an incubation at 42 °C for 42 sec and incubation on ice for 5 min. The transformed bacteria were incubated with 900 µl sterile SOC media (37 °C, 1 h, 150 rpm) for bacterial growth. After centrifugation (2 min, 5000 x g) the pellet was resuspended in 200 µl of LB media and spread on LB agar plates with the considered antibiotics and incubated at 37 °C overnight.

### 2.2.1.2. Cultivation of *E.coli*

*E. coli* strains XL1-Blue and HST-08 were used for DNA amplification and isolation (2.2.1.1) and *E. coli* strains BL21 (DE3) pLySs, Rosetta or Codon plus were used for protein purification. Liquid cultures were inoculated with single colonies from LB agar selection plates or glycerol stocks respectively. Inoculated or transformed bacteria were grown in LB media (37 °C, 150 rpm) with the considered antibiotics (ampicillin 100 µg/ml, tetracycline 20 µg/ml) for amplification or further protein purification. For subsequent protein purification cultures were induced with 0.2 mM IPTG when $OD_{600}$ reached 0.6 to 0.8 and incubated overnight at 20 °C, 150 rpm. 10 to 12 h after induction, cultures were harvested (5000 x g, 10 min) and processed for protein purification.

## 2.2.2. Molecular methods

### 2.2.2.1. Plasmid preparation from *E. coli*

Purification of plasmid DNA was performed with QIAprep Spin Miniprep Kit (Qiagen, Hilden) according to the manufacturers´ recommendations after transformation and cultivation of *E. coli* XL1-Blue or Stellar (2.2.1.1, 2.2.1.2). The procedure of plasmid DNA isolation is based on selective alkaline denaturation of high molecular weight chromosomal DNA while covalently closed circular DNA remains double-stranded (Birnboim & Doly, 1979). Lowering the pH causes precipitation of genomic DNA while plasmid DNA can renature and be isolated with anion exchange chromatography column. Plasmid DNA was solved in $H_2O$ and stored at -20 °C.

### 2.2.2.2. RNA isolation

RNA was isolated by seeding cell lines or primary cells in 10 cm dishes. After reaching complete confluence cells were washed twice with PBS -/- and harvested in 500 µl RLT+ buffer containing 1% β-mercaptoethanol or in 500 µl QIAzol (Qiagen) for HSCs. The cell suspension then was stored in -80°C until the total mRNA-transcripts were isolated according to the instructions of the RNeasy kit (Qiagen). For isolation of the RNA from the cells, the lysate was resuspended with 500 µl of 70% of ethanol. Afterwards the whole sample was transferred into an RNeasy Mini spin column and centrifuged for 30 sec, 10.000 g. The flow through was discarded and 700 µl RW1 buffer was used to wash the RNA (10.000 g, 30 sec). Subsequently the column was washed two times with 700 µl RPE buffer and the flow through was discarded. Excess amount of buffer was discarded after the column was centrifuged again (1 min, 10.000 g). RNA was eluted with 30 – 50 µl RNase-free water (1 min, 10.000 g). The concentration of the eluted RNA was measured using NanoDrop 2000.

### 2.2.2.3. DNase treatment

Possible genomic DNA contaminations were removed using the DNA-free™ DNA Removal Kit (Ambion, Life Technologies, Germany). Contaminating DNA is digested to levels below the limit of detection of routine PCR. For the digestion 2000 - 5000 ng of RNA were mixed with 4 µl 10x buffer, 1 µl RNase inhibitor and 1 µl DNase I. The mixture was filled until 37 µl with water and incubated for 30 min at 37°C. Reaction was stopped by adding 5 µl of DNase inactivation reagent to the mixture and incubated 2 min at RT. Then, sample was centrifuged for 3 min, 10.000 g followed by transferring the supernatant into a fresh tube.

### 2.2.2.4. Reverse transcriptase polymerase chain reaction

DNase-treated RNA was transcribed into complementary DNA (cDNA) using the ImProm-II reverse transcription system (Promega, USA). 1 - 2 µg of mRNA were mixed with 2 µl Oligo (dT) and nuclease free water was added to a final volume of 20 µl. The samples were heated to 70°C for 5 min to denature the RNA secondary structure, immediately followed by 5 min incubation on ice. Afterwards samples were mixed with 4 µl RT buffer, 1 µl dNTPs (10 mM), 0.5 µl RNase inhibitor, 3 µl $MgCl_2$, 0.5 µl $H_2O$, and 1 µl Reverse Transcriptase. Thereupon the cDNA synthesis was performed in a thermocycler with described conditions: 25°C for 10 min, 42°C for 1 h, 70°C for 15 min.

#### 2.2.2.5. Quantitative real-time reverse transcriptase polymerase chain reaction (qPCR)

Quantitative real-time reverse transcriptase polymerase chain reaction (qPCR) was performed using SYBR Green Master mix (Life Technologies, Germany). All primer sequences are listed in 2.1.12. Each sample was mixed according to the chart below:

| Reagent | Volume |
|---|---|
| SYBR Green Master Mix | 10 µl |
| Forward Primer (10 µM) | 1 µl |
| Reverse Primer (10 µM) | 1 µl |
| cDNA (product of 50 ng RNA, 1:10 diluted) | 2 µl |
| $H_2O$ | 6 µl |

The following program was applied using 7500 Real-Time PCR System (Applied Biosystem, Warrington, UK):

| Temperature | Time | |
|---|---|---|
| 95°C | 1 min | |
| 95°C | 15 sec | 40 cycles |
| 60°C | 1 min | |

All samples were measured as triplicates and *Hprt1* was used as the internal control for HSCs. The 2-ΔCt method was employed for estimating the relative mRNA expression levels.

## 2.2.3. Protein biochemical methods

#### 2.2.3.1. Protein purification

Large scale *insect cell* E-Ras expression was conducted according to the established protocol as described before (S. C. Zhang, L. Gremer, et al., 2014). *TNAO*38 insect cells were inoculated at a density of $1.5\times10^6$ cells/ml under optimized virus titration and culture time. Cells were resuspended in lysis buffer, containing 20 mM HEPES-NaOH pH 7.4, 150 mM NaCl, 2 mM β-mercaptoethanol, 5 mM $MgCl_2$, 0.1 mM GTP, 10 mM imidazole and the optimized detergents according to the screening procedure described above. Cells were disrupted by sonication in ice-water mixture. Supernatants were collected by centrifugation and loaded on a Ni-NTA Superflow column (Qiagen, Hilden, Germany). High salt buffer (20 mM HEPES-NaOH pH 7.4, 150 mM NaCl, 2 mM β-mercaptoethanol, 5 mM $MgCl_2$, 0.1 mM GTP, 10 mM imidazole, 350 mM KCl and 1 mM ATP) was used to remove impurities from the target proteins. E-Ras protein was eluted using 300 mM imidazole. The protein solution was concentrated and further purified on a Superdex 75 column (10/300 GL, GE-Healthcare, Uppsala, Sweden) with 20 mM HEPES-NaOH pH 7.4, 150 mM NaCl, 3 mM DTT, 5 mM $MgCl_2$ and 0.5% (w/v) Na-cholate as buffer system.

All other proteins (i.e. ARG1, PI3K RBD, RAF RBD, SIN1 FL and SIN1 RBD mutants) were prepared from *E. coli* as either MBP- or GST-recombinant proteins. Therefore cells were grown at 37°C at a density of $OD_{600}$ 0.5-0.6 and inoculated with 0.2 mM IPTG overnight. Cell pellets were resuspended in lysis buffer containing 150 mM NaCl, 30 mM Tris-HCl pH 7.5 (or pH 8.0 for SIN1-GST constructs), 5 mM $MgCl_2$, 3 mM DTT and disrupted by sonication, homogenization and by using a microfluidizer. Supernatants were collected by centrifugation (20,000 x g, 30 min, 4°C) and loaded on either GSTrap columns (GSTrap FF, GE-Healthcare, Uppsala, Sweden) or Ni-NTA Superflow columns (Qiagen, Hilden, Germany). Eluted protein solutions were concentrated and further purified on a Superdex 75 column (10/300 GL, GE-Healthcare, Uppsala, Sweden). GST-coupled proteins that were cleaved were further purified using GSTrap column (GSTrap FF, GE-Healthcare, Uppsala, Sweden). Protein concentration was measured using Bradford solution at 595 nm in a photometer (Eppendorf GmbH, Hamburg).

#### 2.2.3.2. Sodium dodecyl sulfate (SDS) polyacrylamide gel electrophoresis

The discontinuous sodium dodecyl sulfate polyacrylamide gel electrophoresis (SDS-PAGE) is an analytical method for separating proteins according to their molecular weight. Protein samples are incubated with SDS and β-ME (β-mercaptoethanol) containing Laemmli buffer at 95 °C for 5 min and loaded onto a 7 - 15 % SDS gels. Electrophoresis was performed at 85 V for about 120 min in the Mini Protean Tetra System (Bio-Rad Laboratories, München). Gels were either stained with Coomassie Brilliant Blue (CBB) staining solution for at least 10 min and destained with boiling water or destaining solution, or immunoblotted and stained with antibodies.

#### 2.2.3.3. Detergent free subcellular fractionation of HSCs

Subcellular fractionation of HSCs (d0) was conducted by using a differential centrifugation method combined with detergent-free buffers and sucrose cushions as described previously (Taha et al., 2014). HSCs were homogenized by using a pre-chilled 7 ml Dounce homogenizer in a detergent-free lysis buffer containing 10 mM Tris-HCl pH 7.5, 10 mM NaCl, 0.5 mM $MgCl_2$, and EDTA-free protease inhibitor cocktail (Roche). The homogenates were centrifuged at 2000 x g for 5 min at 4 °C. The pellets were resuspended in 250 mM sucrose solution containing 10 mM $MgCl_2$ and centrifuged through an 880 mM sucrose cushion containing 0.5 mM $MgCl_2$ at 1,200xg for 10 min in order to obtain the crude nuclear and cytoplasmic fractions. The supernatants were further subjected to a 16000 x g centrifugation step for10 min to isolate the heavy membrane pellet and the post-nuclear supernatant. The post-nuclear supernatants were then centrifuged for 1.5 h at 130000 x g. The resulting pellets contained the light membrane fraction and polysomes. Nuclei were resuspended in lysis buffer and gently homogenized using a Balch homogenizer (clearance of 8 mm) for 8-10 up-and-down strokes. Homogenized nuclei

were centrifuged through a cushion of 880 mM sucrose containing 0.5 mM $MgCl_2$ at 2000 x g for 20 min to isolate the nucleolar pellet and post-nucleolar supernatant. The post-nucleolar supernatant was finally centrifuged for 1.5 h at 130000 x g. The resulting pellets contained the nuclear membranes and the supernatants the nucleoplasmic fractions. All fractionation steps were carried out at 4 °C. Protein concentration of all fractions was determined by the Bradford assay.

#### 2.2.3.4. Immunoblotting

Separated proteins were transferred from SDS gels onto nitrocellulose membrane (Amersham, GE Healthcare) was done for subsequent immunoblotting. Transfer was performed at 100 V for 60 min in transfer buffer. The membrane was dried at RT afterwards, followed by blocking for 60 min with 5 % milk or 1:3 Odyssey blocking solution (Licor). Primary antibodies were diluted in 5 % milk or 1:3 Odyssey blocking solution with 0.2 % Tween-20 and incubated overnight. The day after, the primary antibody was removed and membranes were washed three times with TBS-T (1% Tween-20) and were incubated with the secondary antibody for 1 h at RT. Finally, membranes were washed 3 times with TBS-T and developed using either the ECL Prime Western blotting detection reagent (GE Healthcare) together with INTAS Chemo Cam Imager (INTAS Science Imaging Instruments GmbH, Göttingen) or for fluorophore-coupled secondary antibodies Licor Odyssey Fc imager (Licor) was used.

#### 2.2.3.5. Arginase activity assay

Purified human ARG1 from *E. coli* was activated by incubation with 50 mM $MnCl_2$, 10 mM Tris-HCl pH 7.5, at 55°C for 10 min. ARG1 activity was determined as described (Corraliza et al., 1994; Garganta & Bond, 1986) by mixing 50 ng of ARG1 with 25 µl of increasing concentrations of L-arginine (1 mM - 50 mM) at 37°C. Samples of the assay were removed at various time points (1 min intervals) and reaction was stopped by adding 400 µl acidic mixture consisting of $H_2SO_4$, $H_3PO_4$ and $H_2O$ (1:3:7). Urea production was quantified after the addition of 25 µl 9% ISPF (isonitrosopropiophenone, dissolved in 100% EtOH) and incubation for 45 min at 100°C. Reaction was kept in the dark for 10 min at room temperature before absorbance at 540 nm was measured with TECAN Infinite M200 PRO reader. Michaelis-Menten kinetics were measured by plotting the reaction velocity (V0) as a function of the L-arginine concentration Grafit 5.0.13.

### 2.2.3.6. Pulldown

GST-fusion proteins were immobilized on GSH agarose beads and either subsequently mixed with purified proteins or total cell lysates and incubated for 1 h at 4°C to pull-down associating proteins. Afterwards, the beads were washed four times, boiled in 2x SDS-Laemmli buffer at 95°C for 5 min. Finally, samples were separated on sodium dodecyl sulfate (SDS) polyacrylamide gels and either immunoblotted and stained with specific antibodies or directly stained with Coomassie Brilliant Blue (CBB).

### 2.2.3.7. Co-immunoprecipitation

Freshly isolated HSCs or other cells were lysed in immunoprecipitation buffer (IP buffer) (20 mM Tris-HCl, pH 7.4, 150 mM NaCl, 5 mM $MgCl_2$, 0.5% Nonidet P-40, 10 mM β-glycerolphosphate, 0.5 mM $Na_3VO_4$, 10% glycerol, EDTA-free protease inhibitor) and sedimented (12.000 x g, 2 min, 4°C). Supernatant of the total cell lysates were incubated with specific antibodies, IgG control, or GFP-fused nanobeads as described (Nakhaei-Rad et al., 2016) respectively for 1 h at 4 °C on the rotor. For IPs without nanobeads, cell lysates were additionally incubated with protein G beads for 1 h at 4 °C on the rotor. Samples were finally washed five times with IP buffer and eluted proteins were heated in 2x SDS-Laemmli buffer at 95 °C and analyzed by subsequent immunoblotting.

### 2.2.3.8. Mass spectrometry

GST-fused *hs* and *rn* E-Ras N-terminus (Nex) proteins purified from *E. coli* were used to fish binding proteins in HeLa cell lysates. Subsequent samples were subjected to SDS-PAGE and stained with Coomassie Brilliant Blue. For mass-spectrometric analysis GST controls as well as *hs* E-RAS and *rn* E-RAS samples (n=5) were cut in three gel pieces each. The SDS gel pieces were reduced, alkylated, and digested by trypsin and the resulting digest mixtures were analyzed by mass spectrometry as described elsewhere (Poschmann et al., 2014). Peptides extracted with 0.1% trifluoroacetic acid were subjected to a liquid chromatography system (RSLC, Dionex/Thermo Scientific, Idstein, Germany) equipped with an Acclaim PepMap 100 C18 column (75 µm inner diameter, 50 cm length, 2 mm particle size from Dionex/Thermo Scientific, Idstein, Germany) coupled to an Orbitrap Elite mass spectrometer (Thermo Scientific, Bremen, Germany) essentially as described (Poschmann et al., 2014). For protein and peptide identification and quantification raw files were further processed using the MaxQuant software suite version 1.3.0.5 (Max Planck Institute of Biochemistry, Planegg, Germany). Database searches were carried out against the UniProt database (release 06.2013) using standard parameters. Label free quantification was done using the “match between runs” option with a time window of 2 min. Peptides

and proteins were accepted at a false discovery rate of 1% and proteins with quantitative information available for at least three analyzed samples were subjected to subsequent statistical analysis. Protein quantification was performed using the SAM algorithm (Tusher et al., 2001) implemented in Perseus version 1.2.7.4 (Max Planck Institute of Biochemistry, Planegg, Germany) on log transformed data (false discovery rate threshold: 0.01). Missing values were replaced by imputation (width: 0.3; down shift: 1.8).

#### 2.2.3.9. Confocal microscopy

For confocal imaging cells were fixed with 4% paraformaldehyde for 20 min at room temperature. After washing the cells with PBS, they were permeabilized with 0.25% Triton X-100/PBS for 5 min and washed once more with PBS. Cells were blocked for 1 h at room temperature with PBS containing 0.25% Triton X-100 and 3% bovine serum albumin (BSA, Merck), 2 % donkey serum, and 2 % goat serum, then incubated with primary antibodies overnight. Next, cells were washed three times, followed by incubation with secondary antibodies as well as DAPI (4',6-diamidino-2-phenylindole) dye for 2 h at room temperature. The coverslips were mounted using ProLong Gold antifade reagent (Life Technologies Inc.). Confocal images were obtained using a LSM 510-Meta microscope and LSM 550-microscope (Zeiss, Jena, Germany).

#### 2.2.3.10. Fluorescence polarization

To investigate the binding of different RAS proteins to effectors, fluorescence polarization of mantGppNHp or mantGTP labelled RAS was monitored. 2 µM of fluorescently labelled RAS protein (i.e. H-Ras, E-Ras, RIT1) was added to the cuvette containing buffer (150 mM Tris-HCl, pH 7.5, 50 mM NaCl, 5 mM $MgCl_2$, 3 mM DTT). Increasing amount of effector protein was added to the cuvette to saturate the system. The change in the fluorescence polarization was monitored at the excitation and emission wavelengths of 360 nm and 450 nm corresponding to the mant-labelled RAS with Fluoromax-4 spectrofluorometer (Horiba, Kyoto, Japan). Data analysis was done with GraFit 5.0 program (Erithracus Software).

#### 2.2.3.11. Liposome preparation

Liposome assays were performed by mixing, sonicating and extruding a defined amount of various lipids. The lipid mixtures were incubated for different time points and centrifuged at different speeds to separate the liposome pellets and supernatants for optimizing the centrifuging force. The liposomes were prepared as described previously (S. C. Zhang, L. Gremer, et al., 2014). A lipid mixture (500 µg),

containing 20% (w/w) PE, 45% (w/w) PC, 20% (w/w) PS, 10% (w/w) cholesterol, and 5% (w/w) PIP2 or PIP3, was gently dried using light air stream at the bottom of a 2 ml Eppendorf tube. Obtained lipid film was hydrated with 300 µl of buffer, containing 20 mM HEPES-NaOH pH 7.4, 50 mM NaCl, 3 mM DTT, 5 mM MgCl2. Sonication (20 s with minimal power, 50% off and 50% on) was used to dissolve the lipids and promote aggregates formation. Finally, to homogenize the liposome size, we used 200 nM filters in extruders and the sample was filtered for 21 injects.

### 2.2.3.12. Surface plasmon resonance (SPR)

For kinetic analysis of the interaction between E-Ras and ARG1, as well as membrane binding, Biacore X100 system was used together with CM5 or L1 sensor chips (GE Healthcare Life Sciences, Uppsala, Sweden), respectively. For interaction analysis of ARG1 binding toward E-Ras, anti-GST antibody was immobilized to the dextran surface of a CM5 sensor chip using the GST capture kit (GE Healthcare Life Sciences). Afterwards, 10 µM of purified GST-*hs*Nex was introduced to the immobilized GST-antibody at 25°C (30 µl/min). Increasing concentrations of MBP-ARG1 (contact time: 90 sec, 30 µl/min) were injected in a multicycle mode and dissociation was measured at the end of the injection of the last concentration for a period of 300 sec. Liposome binding kinetic was measured in a multicycle model through immobilization of synthetic liposomes on the surface of a L1 chip. After immobilization of liposomes (900 sec, 5 µl/min) different concentrations of prenylated human E-Ras and ARG1 were injected (30 µl/min). Protein association at each defined concentration (0 - 20 µM) was monitored in periods of 120 s and the global dissociation was measured at the end of the final injection in periods of 300 s. The dissociation constants ($K_d$) were calculated using BIAevaluation (version 2.0.1) by the Langmuir 1:1 model and the GraFit 5 version. All SPR measurments were carried out at 25 °C in a buffer, containing 10 mM HEPES, pH 7.4, 150 mM NaCl, 0.05 % (v/v) surfactant P20 (GE Healthcare Life Sciences, Uppsala, Sweden).

### 2.2.3.13. Gene ontology analysis

Gene Ontology (GO) data for the biological processes, molecular function, and cellular location of possible E-Ras Nex interacting proteins, including isoforms, paralogs or related proteins were achieved by using the PANTHER database (Mi et al., 2017) and was done by Dr. Mohammad S. Taha.

## 2.2.4. Cell biological methods

### 2.2.4.1. Cultivation of eukaryotic cells

All eukaryotic cells were cultivating in DMEM high/ low Glucose (Life Technology, Darmstadt) with 10% fetal bovine serum (FBS) (Life Technology, Darmstadt) and 1% penicillin/streptomycin (Life technology, Darmstadt) in 10 cm dishes or T75 flasks. For sub-culturing, cells were washed with PBS and incubated for 5-10 min with 2 ml Trypsin/EDTA (Life Technology, Darmstadt) at 37°C. Afterwards, 8-10 ml of DMEM (+/+) was added and the mixture of detached cells was collected in a 15 ml tube and centrifuged for 5 min at 1200 x g at room temperature. The cells were resuspended in 1 ml DMEM high glucose (+/+) and sub-cultured in a new 10 cm dish or T75 flask containing DMEM (+/+).

### 2.2.4.2. Cell isolation and cultivation of HSCs

Male Wistar rats (500-600 g) were obtained from the local animal facility of the Heinrich Heine University (Düsseldorf, Germany). Rat livers were enzymatically digested with collagenase H (Roche, Germany) and protease E (Merck, Darmstadt) and proceed by density gradient centrifugation to obtain primary cultures of HSCs. Purified HSCs were cultured in Dulbecco's Modified Eagle Medium DMEM (Gibco Life Technologies) supplemented with 2% FBS and 1 % penicillin/streptomycin (Life technology, Darmstadt).

For co-culture experiments, HSCs were seeded in DMEM/F12 with 2 % FBS and 1% penicillin/streptomycin. One day after seeding, hepatocytes obtained from rat livers were seeded above in Transwell system (0.4 µm pore size, Corning, Inc, NY, USA). For treatment with vitamin A and insulin, HSC medium was supplemented with 10 µM retinol (Merck, Darmstadt) and 50ng/ml human insulin solution (Merck, Darmstadt). Medium was exchanged every 48h.

### 2.2.4.3. Transfection of adherent cells

For transient expression of various constructs, 1 – 2 x $10^6$ cells (i.e. COS7, NIH3T3, HepG2, HEK293T) were seeded in 10 cm dishes. Transfection of 10 µg DNA was done on the next day using either Turbofect (Thermo Fisher Scientific), Lipofectamine (Thermo Fisher Scientific) or Jetprime (Polyplus). 4 – 6 h later, medium was changed due to toxicity of transfection reagent. Cells were grown for additional 48 h before further analysis.

#### 2.2.4.4. Cell lysis

For the lysis of the adhered cells, the medium was removed and cells were washed twice with PBS. Afterwards, cells were lysed in the dish with FISH buffer or IP buffer depending on the following experiment. Using a rubber branch the cells were scratched off from surface, collected and harvested by centrifugation at 12000 x g for 2 min at 4°C. Supernatant was transferred subsequently and used for the following experiment. The cell lysis of adhered cells for following RNA isolation the steps are described in 2.2.2.2.

#### 2.2.4.5. Detection of cell number

The number of cells needed for experiments were measured with TC10 automated cell counter (Bio-Rad). Therefore, 10 µl of cell suspension were mixed with 10 µl of Trypan blue and loaded on TC10 system counting slides.

#### 2.2.4.6. Baculoviruses and insect cell culture

Human *E-Ras* gene was subcloned into pFASTBacHTb vector (Invitrogen, Carlsbad, CA, USA) by Dr. Mohammed Akbarzadeh and transformed into *E. coli* DH10BAC strain. Agar plates containing kanamycin, gentamycin, tetracycline, X-gal and isopropyl-β-D-thiogalactoside were used to select recombinant *GTPase* clones. Plasmid-DNA of GTPase-positive clones was isolated for recombinant *GTPase* bacmid extraction and virus generation. The baculoviruses (passage 1) were generated by infecting *Sf*9 insect cells using recombinant *GTPase* bacmids. Viruses were ready to use for large scale expression after two more amplification steps (passages 2 and 3). For large scale *TNAO38 insect cells* were used due to high efficiency compared to *Sf9 cells*. *Sf*9 and *TNAO*38 cells were cultured at 27°C in *Sf*-900 III medium (Gibco), containing penicillin and streptomycin. The multiplicity of infection (MOI) and the time for E-Ras expression were optimized by infecting the *Sf*9 cells at different time points. A sample of transfected culture supernatant was analyzed with immunoblotting using anti-His-HRP antibody.

### 2.2.5. Statistical analysis

Data shown in the graphs are the average of triplicate or quadruplicate experiments. Data are expressed as the mean ± standard deviation or standard error of the mean. Quantitative real-time pcr data was evaluated using GraphPad Prism 6 software. For variance analysis ordinary two-way analysis of variance test was performed using the Sidak's multiple comparisons test. Results were considered significant with $p < 0.05$. (*($p < 0.05$), ** ($p < 0.01$), *** ($p < 0.001$), **** ($p < 0.0001$).

# 3. Results

## 3.1. Direct SIN1 interaction with Ras proteins regulates mTORC2 activity

### 3.1.1. SIN1 contains a Ras-binding domain (RBD) and can interact with Ras GTPases

As it was already reported in 2007 SIN1 possesses four domains, an N-terminal domain (NTD), CRIM (conserved region in the middle) domain, a Ras-binding domain (RBD), and a pleckstrin homology (PH) domain (Fig. 3A). The NTD is responsible for interaction of SIN1 with other mTORC2 associated components, such as mTOR, RICTOR, and DEPTOR, and to enable a functional complex (Y. Yuan et al., 2015), whereas the CRIM domain and PH domain play a role in target recognition of mTORC2 substrate kinases and membrane targeting, respectively (Cameron et al., 2011; Schroder et al., 2007; Tatebe et al., 2017). The role of the SIN1 RBD is unclear, it has been proposed to bind and co-localize with the small GTPases, such as H-Ras (Schroder et al., 2007; Y. Yuan et al., 2015), human Rap1 and *Dictyostelium* RasC (Khanna et al., 2016). Nevertheless, overexpression of SIN1 has also been reported to inhibit Ras-dependent activation of AKT and ERK1/2 (Schroder et al., 2007).

Multiple sequence alignment of SIN1 RBD with the other RBD-containing proteins, e.g. CRAF and PI3Kα, was used to visualize conserved amino acids (highlighted in dark grey) within the domain (Fig. 3A). Next, SIN1 RBD, CRAF RBD and PI3K RBD were cloned into pGEX-4T1-NTEV vector and subsequently purified to obtain GST-coupled proteins for further studies (Fig. 3B). In 2016, E-Ras was postulated to activate the mTORC2 pathway in HSCs (Nakhaei-Rad et al., 2016). Consequently, it was the aim to identify whether SIN1 is a direct interaction partner of E-Ras and other RAS proteins. Therefore, GST pulldown experiments using heterologous expressed and purified E-Ras proteins from *Rattus norvegicus* (*rn*) and *Homo sapiens* (*hs*) with GST-coupled RBD-containing proteins were performed. In both experiments, using *rn* E-Ras or *hs* E-Ras, SIN1 RBD as well as PI3K RBD and CRAF RBD were able to interact with E-Ras. Signal intensities from subsequent immunoblotting indicated a strong interaction between *rn* E-Ras and PI3K RBD, as reported before (Nakhaei-Rad et al., 2016), and similar binding affinity between *rn* E-Ras and CRAF as well as SIN1 RBD (Fig. 3C). Signal intensities between *hs* E-Ras and all three RBD-containing proteins showed comparable amounts. GST was used as a negative control and did not show binding to *hs* or *rn* E-Ras. Furthermore, binding properties of Ras to cellular SIN1 were analyzed by overexpressing and co-immunoprecipitating *hs* H-Ras$^{G12V}$ and *hs* E-Ras$^{WT}$ as EYFP-fusion proteins in COS7 cells. Immunoblotting of subsequent samples showed that E-Ras and H-Ras bound in similar affinity to SIN1 (Fig. 3D).

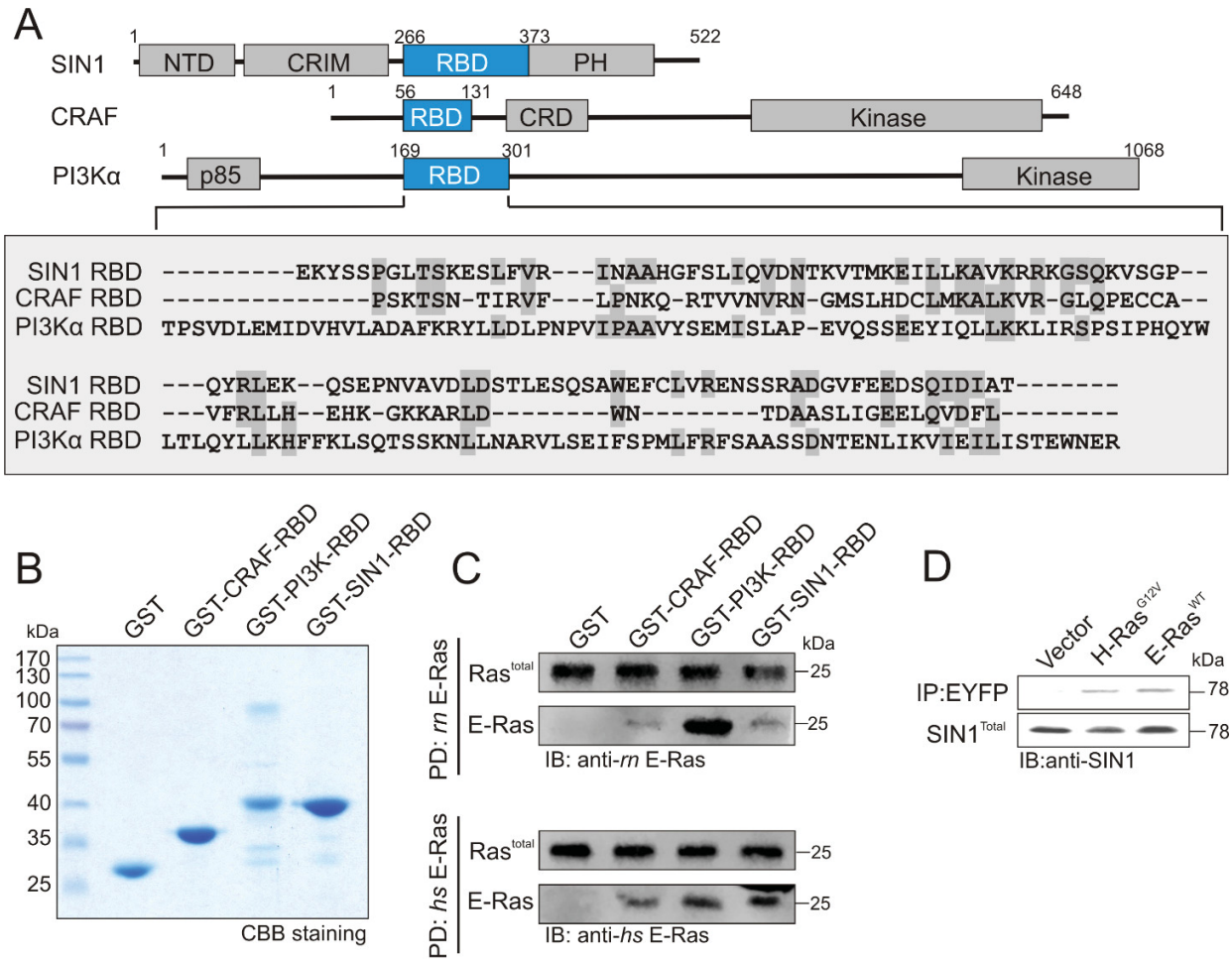


***Figure 3:SIN1 contains a Ras binding domain (RBD) and interacts with E-Ras in pulldown and immunoprecipitation.*** (A) Domain organization of RBD containing proteins and multiple sequence alignment of subsequent RBDs. (B) Purified constructs of GST alone and GST-fused CRAF-RBD, GST-PI3K-RBD, and GST-SIN1-RBD as detected by coomassie brilliant blue (CBB) staining. (C) GST pulldown of purified RBD containing proteins with human and rat E-Ras. (D) Co-immunoprecipitation of endogenous SIN1 with H-Ras$^{G12V}$ and E-Ras$^{WT}$ overexpressed as EYFP constructs in COS7 cells.

## 3.1.2. Analysis of SIN1-RAS interaction using different biophysical methods

Identification of the SIN1 RBD-based interaction with E-Ras in the previous pulldown and immunoprecipitation experiments led to further analysis and characterization of the RBD itself and the binding behavior between SIN1 and E-Ras. Therefore, SIN1 RBD structure in complex with H-Ras was modelled by Dr. Radovan Dvorsky based on sequence homology to the complex of RAF RBD with GppNHp-bound H-Ras (PDB: 4G0N). The interaction interface between H-Ras and SIN1 RBD was analyzed and indicated several SIN1 residues in close proximity which might be responsible for the direct interaction between Ras proteins and SIN1 (Fig. 4A).

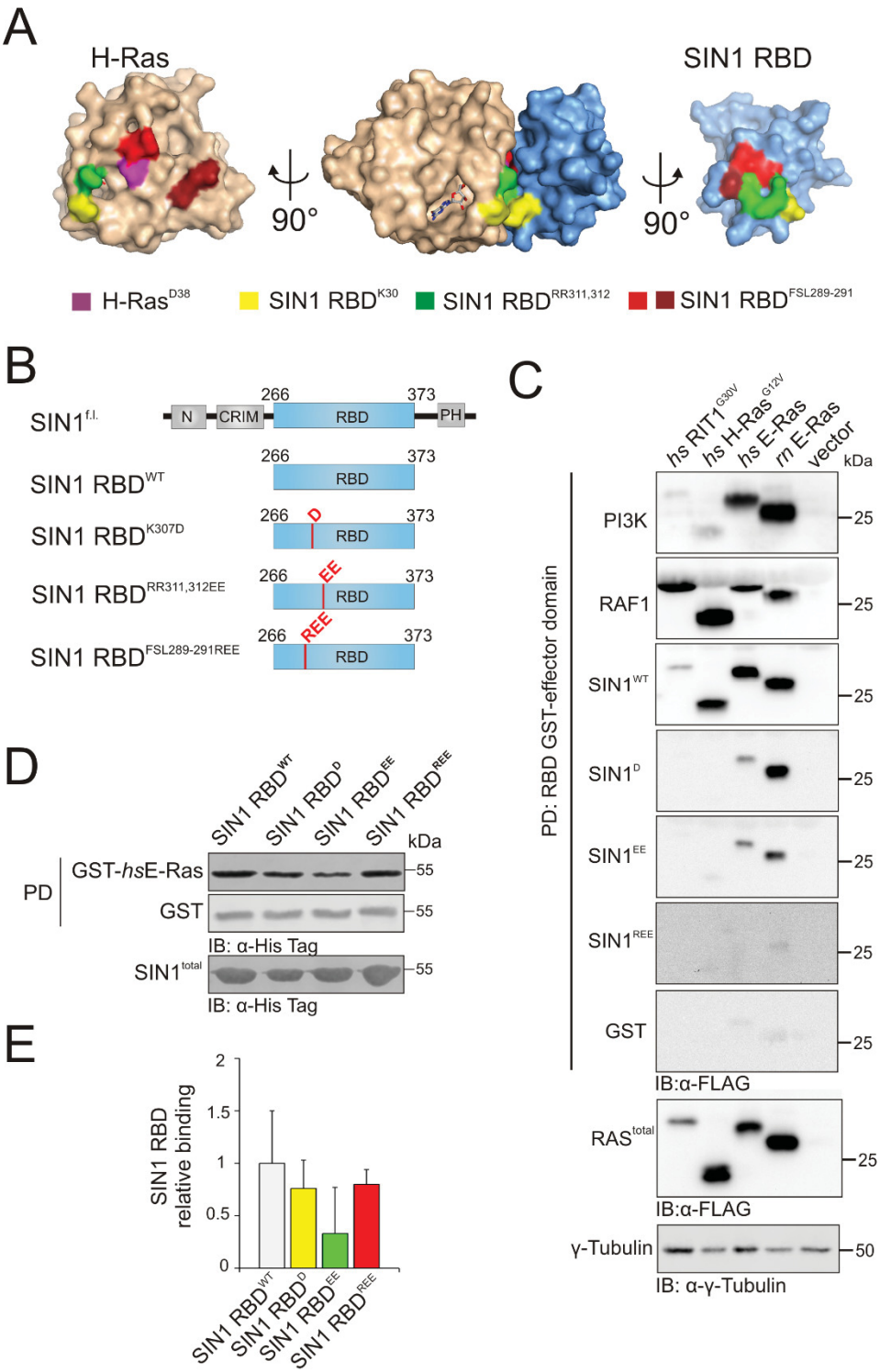


***Figure 4: Direct interaction of SIN1 with E-Ras.*** (A) Surface representation of the interaction of H-Ras (beige) with SIN1 RBD (blue). SIN1 RBD was modelled based on CRAF RBD (PDB: 4G0N). Colored domains indicate predicted residues of SIN1 and H-Ras responsible for interaction. Ras-binding residues of SIN1 RBD are K30 (yellow), R311,312 (green), and FSL289-291 (light and dark red). SIN1 RBD-binding residues of H-Ras are D38 (magenta). (B) Domain organization of human SIN1 with mutations in RBD residues predicted to play a role in interaction. (C) Pulldown of various GST-fused RBDs including PI3K, RAF1, SIN1, SIN1D, SIN1EE, SIN1REE, and GST as control after overexpression of different Ras proteins in *COS7* cells. (D) Pulldown and subsequent immunoblotting of all purified SIN1 RBD constructs with GST-fused human E-Ras and GST alone (E) Quantitative binding analysis of pulldown samples using GST-*hs*E-Ras and SIN1 RBD$^{WT}$ (white), SIN1 RBD$^{D}$ (yellow), SIN1 RBD$^{EE}$ (green), and SIN1 RBD$^{REE}$(red) constructs (N=3). Error bars represent *SD*.

Based on the identified residues in the structural model of SIN1 RBD in complex with H-Ras, three different mutants of the SIN1 RBD were designed (Fig. 4A and 4B): SIN1 RBD$^{K30D}$ (yellow), SIN1 RBD$^{RR311,312EE}$ (green), and SIN1 RBD$^{FSL289-291REE}$ (red). Residues were substituted to amino acids with opposite charge to generate repulsion between the interacting proteins and serve as a proof of principle in following experiments for correct mutational analysis. All three SIN1 mutants were cloned into pGEX-4T1 and pMAL-C5X vectors for subsequent protein expression and purification. In pulldown experiments, using different Ras constructs (i.e. RIT1, H-Ras, and E-Ras) overexpressed in COS7 cells together with all three GST-fused SIN1 RBD mutants and SIN1 RBD$^{WT}$, different signal intensities in subsequent immunoblotting were obtained (Fig. 4C). SIN1 RBD$^{WT}$ showed the highest binding affinity to RIT1$^{G30V}$, H-Ras$^{G12V}$, *hs* E-Ras and *rn* E-Ras. With each introduced amino acid mutation the binding affinity of the respective SIN1 RBD mutant to the different Ras constructs decreased and displayed lower signal intensities in the pulldown precipitates. GST-coupled PI3K RBD, RAF1 RBD, and GST alone were used as positive and negative controls, respectively. Immunoblot using anti-FLAG and anti-γ-tubulin indicated equal amounts of total cell lysate subjected to pulldown analysis. Similar results were obtained in a second pulldown experiment using GST-coupled *hs* E-Ras and GST as control together with purified SIN1 RBD constructs (Fig. 4D). Immunoblotting with anti-HIS antibody showed equal input amounts of SIN1 RBD constructs (30µM) Immunoblotting of pulldown samples with anti-HIS antibody indicated strongest interaction affinity of SIN1 RBD$^{WT}$ to GST-E-Ras (20µM), followed interaction affinity of the SIN1 RBD mutants to GST-ERas in ascending order of introduced number of amino acid mutations (Fig.4D, upper panel), which is also shown in the subsequent statistical analysis performed with three independent pulldown experiments (Fig. 4E).

Furthermore, binding affinity between RAS proteins and various SIN1 constructs were determined in fluorescence polarization experiments. Therefore, *hs*E-Ras was cloned by into pFastBac HTB vector in order to generate Baculoviruses, transduce insect cells (Tnao38 cells) and purify prenylated *hs*E-Ras from insect cells. H-Ras and SIN1 FL were cloned by Dr. Hossein Nakhaeizadeh into pGEX-4T1-NTEV vector and purified from *E. coli*. SIN1 RBD WT and all previously introduced SIN1 RBD mutants were cloned into pMAL-C5X vector and purified as MBP-fused constructs from *E. coli*. Using fluorescence polarization, increasing concentrations of SIN1 constructs were titrated to mantGppNHp or mantGTP labeled *hs*E-Ras (Fig. 5A, B) or H-Ras (Figs. 5C, D) or RIT1 (Figs. 5E, F). Dissociation constants ($K_d$) for binding of SIN1 FL to E-Ras, H-Ras and RIT1 showed comparable ratios (e.g. 10.3 µM, 12.6 µM, and 35.5 µM) as depicted in the column charts (Fig. 5G). The data, which were obtained for the interaction of SIN1 RBD with E-Ras, H-Ras and RIT1 are quite different. While SIN1 RBD$^{WT}$ binds to H-Ras with only 2-fold lower affinity the data obtained for E-Ras and RIT1 showed a drastic reduction the $K_d$ values by 17- and 7-fold (Fig. 5G). This result indicates that either additional binding regions of SIN FL are most

probably missing in SIN1 RBD or the latter is structurally stabilized in the context of the full-length proteins. Dissociation constants ($K_d$) for binding of SIN1 RBD mutants to E-Ras, H-Ras and RIT1 showed comparable reduction in affinity, except for the affinity between E-Ras and SIN1 $RBD^{EE}$ ($K_d$ = 19.7 µM) (Fig. 5G). Data indicates less binding affinity and therefore increased dissociation constants ($K_d$) for truncated SIN1 RBD WT and mutated constructs of SIN1 RBD with E-Ras, H-Ras and RIT1.

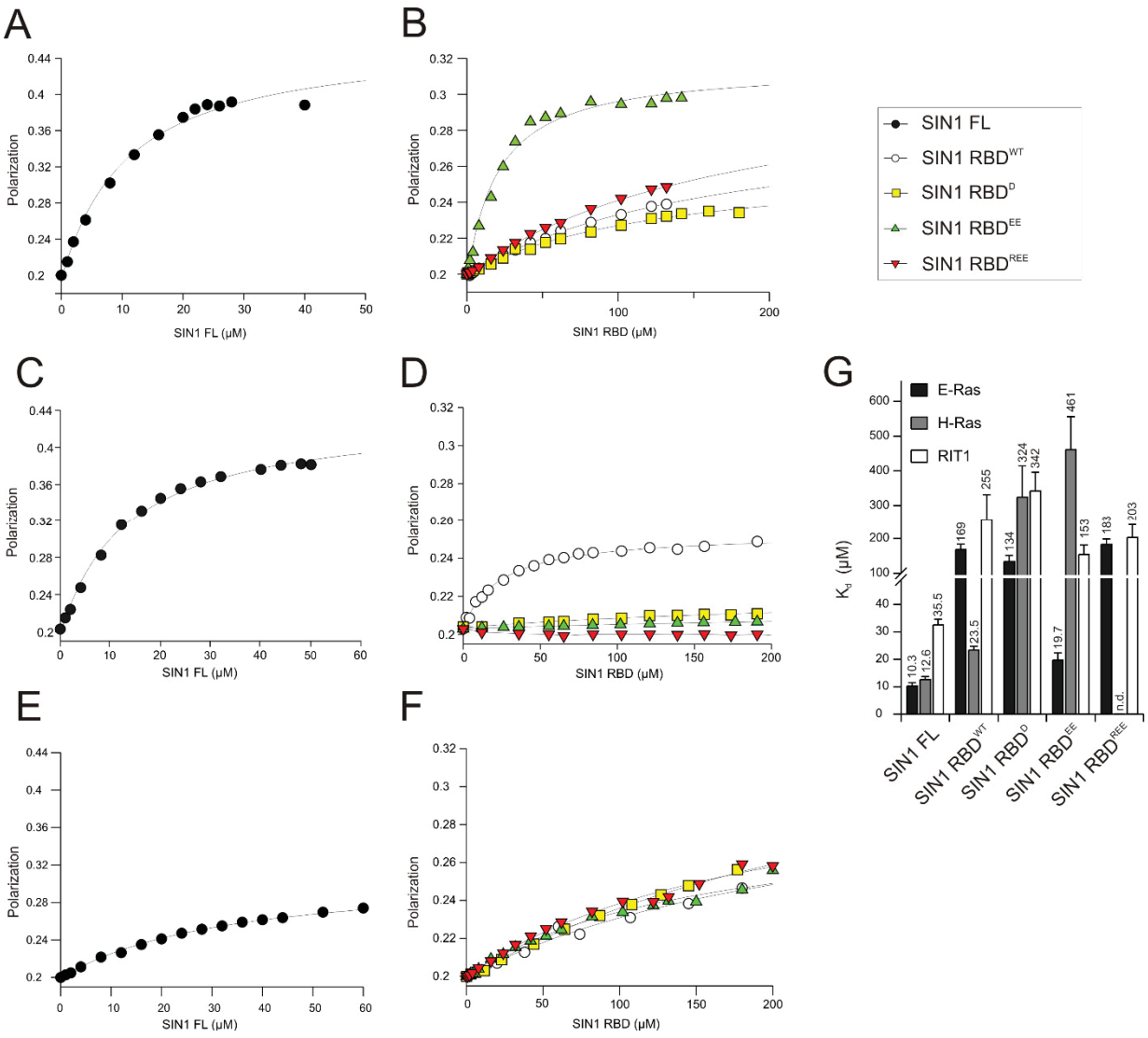


***Figure 5: Fluorescence polarization experiments reveal interaction between RAS and SIN1.*** (A, B) Fluorescence polarization between *hs*E-Ras and SIN1 FL as well as different SIN1 RBD constructs (C, D) Fluorescence polarization between H-Ras and SIN1 FL as well as different SIN1 RBD constructs (E, F) Fluorescence polarization between RIT1 and SIN1 FL as well as different SIN1 RBD constructs (G) Dissociation constants ($K_d$) of fluorescence polarization measurements between *hs*E-Ras, H-Ras and RIT1 with all SIN1 constructs as column charts. Error bars represent S.D.; n.d. not detected.

### 3.1.3. Interaction between E-Ras and SIN1 activates the mTORC2 pathway

While upstream activators of mTORC1 are well characterized, i.e. PI3K and AKT, little is known about the upstream regulators of mTORC2. Many scientists postulate growth factor-induced with PI3K-induced activation of mTORC2, but it still remains unclear (Cota, 2014; Oh & Jacinto, 2011; Sabatini, 2017). Therefore, it was the aim to investigate possible upstream regulators and activators of mTORC2. As E-Ras, H-Ras and RIT1 were found to interact with SIN1 (Figs. 3, 4, 5), an mTORC2 component, it was assumed that these small GTPases may also act as activators of mTORC2 and play a role in the downstream signaling pathway. Therefore, the impact of the previous detected E-Ras-SIN1 interaction was investigated under cell-based conditions. Figure 6A shows signaling pathways and their identified cross-talks downstream of Ras. Recently, an independent negative feedback loop through S6K or AKT was reported, which can directly phosphorylate SIN1 and consequently represses mTORC2 activation (Liu et al., 2014). To investigate whether E-Ras alone can activate the mTORC2 pathway, EGFR signaling and subsequent Ras activation was inhibited by serum starvation. Furthermore, PI3K pathway cross-talks to the mTORC2 pathway were blocked with a pan-PI3K inhibitor. Therefore, COS7 cells were transfected with different FLAG-coupled Ras constructs (i.e. RIT1$^{G30V}$, H-Ras$^{G12V}$, *hs* E-Ras, *rn* E-Ras). 24h after transfection cells were serum starved for additional 24 h and finally treated for 1 h with the pan-PI3K inhibitor GDC-0941 (1µM) or DMSO as control under continuous serum starvation. Resulting signaling profile was investigated by subsequent immunoblotting of various downstream components of the mTORC2 and PI3K/AKT pathways. Phosphorylation of AKT$^{S473}$ can be detected after serum starvation and subsequent GDC-0941 treatment in combination with overexpression of *rn* E-Ras. Phosphorylation level of FOXO1 do not seem significantly decreased after overexpression of various Ras constructs, serum starvation and GDC-0941 treatment compared to DMSO treated control samples. (Fig. 6B). The relative phosphorylation level of protein kinase AKT (p-AKT$^{S473}$ and p-AKT$^{T308}$) in combination with GDC-0941 treatment is increased after overexpression with *hs* and *rn* E-Ras compared to overexpression with RIT1, H-Ras and empty Flag vector (Fig. 6C). This result indicates that E-Ras may be an upstream activator of the mTORC2 complex by binding to SIN1 and resulting in phosphorylation of AKT at position S473, which is known as an activation phosphorylation (G. Yang et al., 2015).

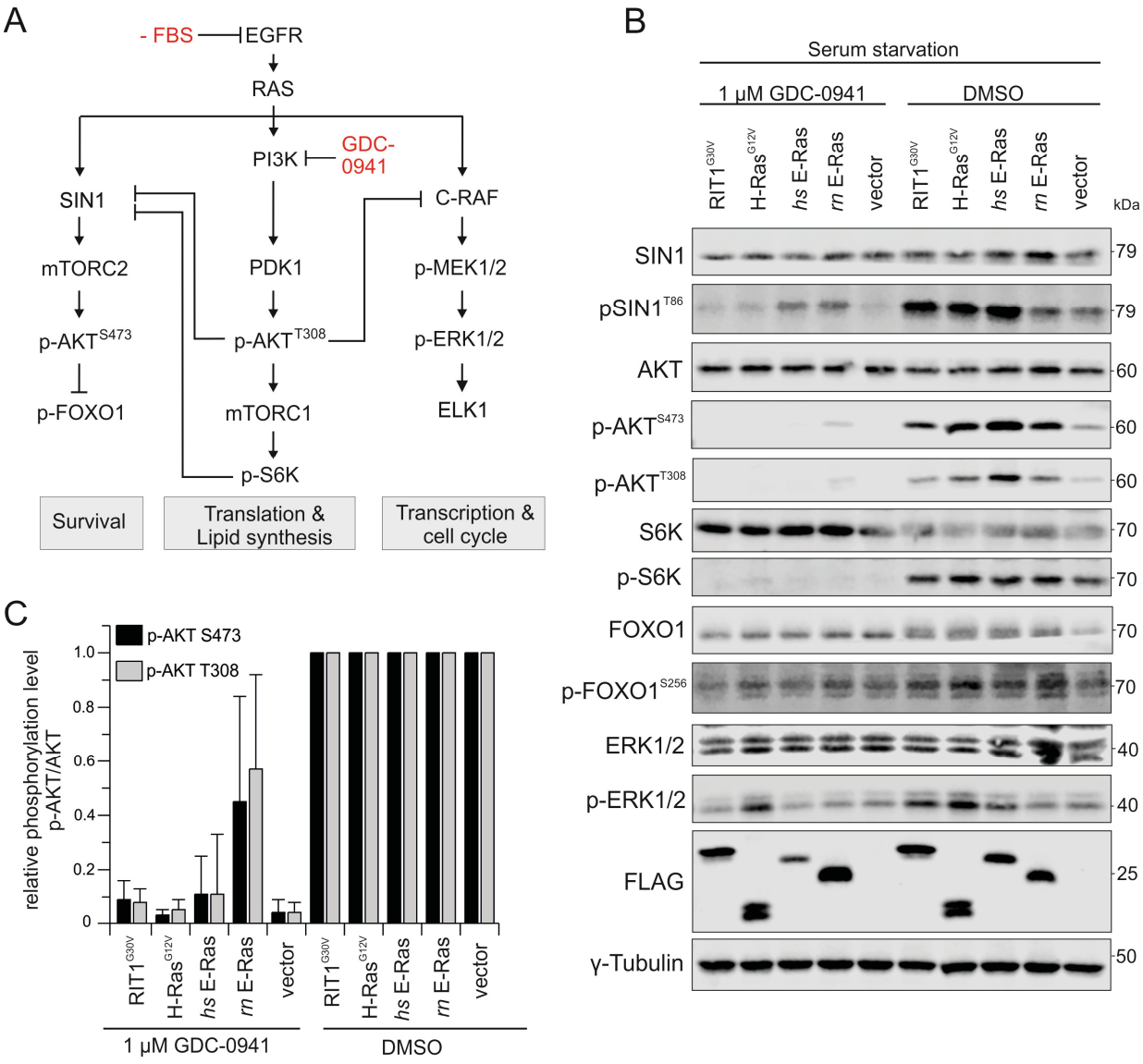


***Figure 6: E-Ras overexpression activates mTORC2 pathway.*** (A) Scheme of Ras downstream signaling pathways including their signaling cross-talks and inhibitors. (B) Immunoblotting of various Ras constructs overexpressed as FLAG-fusion proteins in COS7 cells after serum starvation (24h) and treatment with PI3K inhibitor (GDC-0941, 1 µM, 1h) or DMSO respectively. (C) Relative phosphorylation level of p-AKT S473 and p-AKT T308 in CO7 cells transfected with various Ras constructs and treated with GDC-0941 or DMSO respectively (N=3). Error bars show SD.

### 3.1.4. PI3K/AKT and mTORC2/AKT signaling axes are highly active in HSCs

E-Ras was identified to be up-regulated in freshly isolated, quiescent HSCs on d0 and is postulated to be responsible for the maintenance of quiescence and the fate of HSCs (Nakhaei-Rad et al., 2016). However, the underlying signaling pathways have not been investigated yet. Based on the identified interaction between E-Ras and SIN1 (Figs. 3, 4, 5) and its positive impact on the mTORC2/AKT pathway (Fig. 6), it is assumed that this interaction may regulate major signaling pathways in quiescent HSCs such as survival. Therefore, detailed analysis of signaling pathways downstream of the PI3K/AKT and the mTORC2/AKT axis in HSCs was performed. Freshly isolated primary HSCs were cultivated on plastic dishes for up to 8 days, where they become activated upon ex vivo culture and undergo myofibroblast transition (Kordes et al., 2014; Nakhaei-Rad et al., 2016). HSCs were analyzed at day 0 (d0), day 1 (d1), day 4 (d4) and day 8 (d8) as representatives in the progression from the quiescent to the activated state. Interestingly, in E-Ras expressing quiescent HSCs (d0) high levels of proteins downstream of the mTORC2/AKT axis including SIN1, p-SIN1$^{T86}$, and p-AKT$^{S473}$ were detected, along with low levels of FOXO1 and p-FOXO1$^{S256}$ (Fig 7A). Moreover, immunoblot analysis of proteins downstream of the PI3K/AKT axis displayed up-regulation upon HSC activation (d1-d8), including p-AKT$^{T308}$, p-S6K$^{T389}$. Thus, it is obvious that E-Ras signaling toward PI3K and mTORC2 pathways activates AKT but inactivates FOXO1 in order to maintain HSCs in their quiescent state.

Interestingly, in quantitative mRNA expression analysis, the amount of total proteins displayed quite a different pattern compared to protein levels in immunoblot analysis (Fig. 7B). *Sin1, Akt* and *S6k* expression indicated almost stable expression, whereas *Foxo1* showed, contrary to protein level, up-regulation in d0. *Mtor* expression was up-regulated on d1, which goes along with protein levels detected in immunoblots.

Finally, it was the aim to investigate whether a co-localization of E-Ras and SIN1 *in vivo* in HSCs can be detected in confocal imaging, which may support the role of the E-Ras-SIN1 axis in survival and maintenance of quiescence in HSCs. Therefore, HSCs were cultured either alone as stated above or co-cultured together with hepatocytes in a transwell system up to day 8. Mono-cultured HSCs start to activate upon isolation and culturing. E-Ras expression can only be detected in freshly isolated HSCs on d0. Thus, co-localization of E-Ras and SIN1 was only detected on d0 as indicated by yellow areas (Fig 7C). GFAP expression served as a marker and control for quiescence. Co-culture of HSCs and hepatocytes is postulated to preserve the stem cell niche and provide relevant factors which can antagonize culture-induced HSC activation. Co-localization of E-Ras and SIN1 could not be detected in this set-up, due to high background signals of the antibodies.

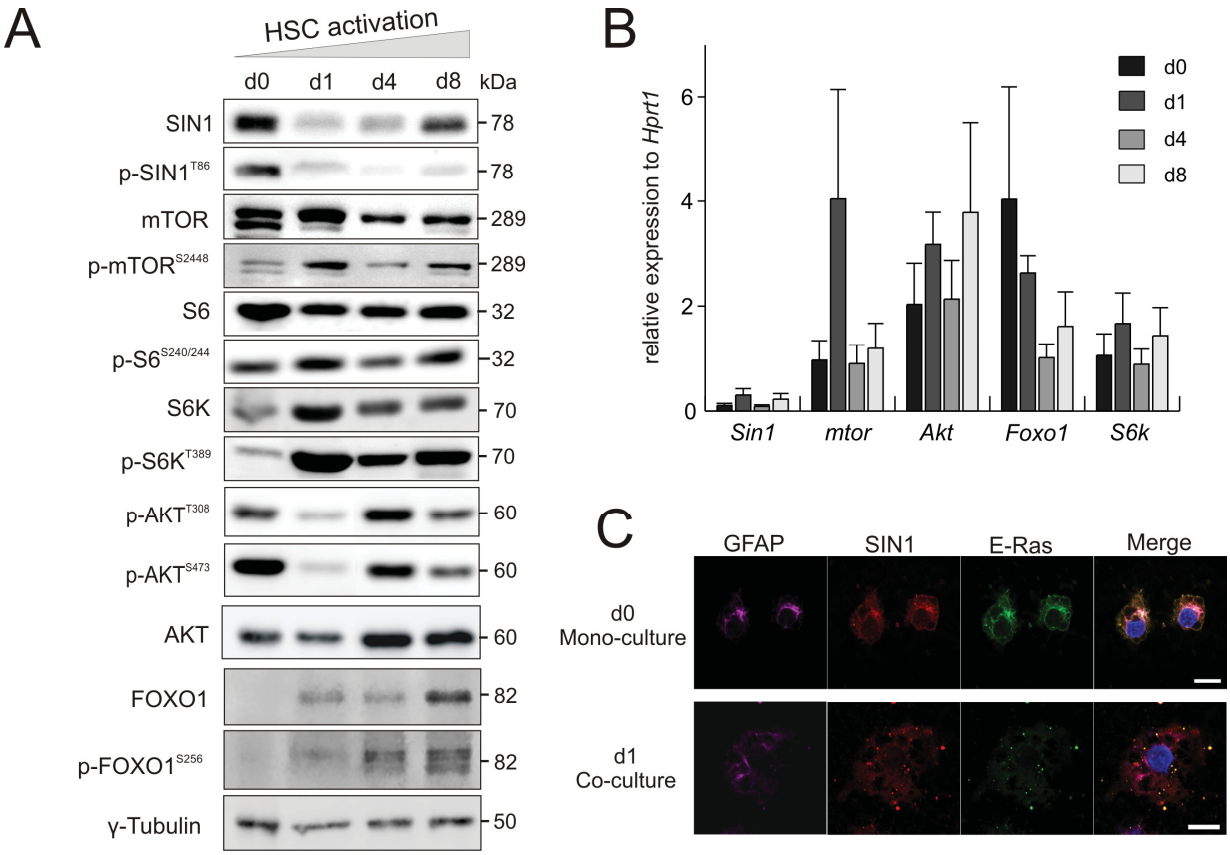


***Figure 7: PI3K/AKT and mTORC2/AKT signaling pathways in quiescent and activated HSCs.*** (A) Immunoblot of total and phosphorylated signaling proteins downstream of PI3K/AKT and mTORC2/AKT axis in quiescent and activated HSCs (d0-d8). (B) Quantitative mRNA expression analysis of signaling proteins downstream of PI3K/AKT and mTORC2 axis in quiescent and activated HSCs (d0-d8) (N=3). Error bars represent *SEM*. (C) Confocal imaging of endogenous GFAP, SIN1 and E-Ras in quiescent HSCs on d0 in mono-cultured HSCs and d1 in co-cultured HSCs. Scale bar, 10 µm.

In conclusion, interaction experiments such as fluorescence polarization, immunoprecipitation and pulldown indicate that SIN1 RBD is able and responsible to bind to RAS proteins (i.e. E-Ras and H-Ras) *in vitro*. Further cell-based analyses in transfected COS7 cells and HSCs also revealed interaction between E-Ras and SIN1. The interaction seems to activate the mTORC2 complex and stimulate downstream signaling including down-regulation of p-FOXO1$^{S256}$ and as a consequence increased survival (Fig. 4A).

## 3.2. E-Ras interacts with Arginase-1 and modulates its activity in quiescent HSCs

### 3.2.1. Novel binding partners of E-Ras

Some members of the RAS family, in spite of sharing a conserved G domain, have additional features outside their G domain that may act as functional regulatory modules (Nakhaei-Rad et al., 2018). The role of E-Ras N-terminus (Nex), an additional 38-amino acid sequence preceding the G domain of E-Ras and showing a sequence identity of 42 % between *hs* and *rn* E-Ras (Fig. 8A), is unclear. In a mutational study, it was proposed that it may modulate E-Ras localization through interaction with potential adaptor/scaffold proteins (Nakhaei-Rad et al., 2015). Thus, protein interaction properties of *hs*Nex and *rn*Nex were investigated by performing affinity pull-down and MALDI-TOF mass spectrometry.

To identify proteins associating with Nex in a proteomic approach, affinity pull-down experiments (N=3) were conducted using total cell lysates and purified GST-*hs*Nex, GST-*rn*Nex and GST, respectively. Pulldown samples were separated in 10% SDS PAGE gels. The gel pieces from each lane of the CBB-stained gels (Fig. 8B, white boxes) were further processed and analyzed by mass spectrometry as described in materials and methods. The bands corresponding to GST-*hs*Nex, GST-*rn*Nex and GST were excluded from the analysis (Fig. 8B, black boxes). All proteins interacting with GST-*hs*Nex and GST-*rn*Nex were detected and individually validated with a high degree of confidence based on the peptide sequences using specific databases and programs as described in materials and methods. The criteria for considering proteins being possible interactors of E-Ras Nex included their presence in all three independent pull-down experiments and their absence in the GST pull-down controls. Contaminant proteins arising from sample handling (such as keratin and bovine serum albumin) were removed. Collectively, a total of 76 potential interacting proteins was found for E-Ras Nex, 35 of them were associated with *rn*Nex, 21 with *hs*Nex, and 20 proteins were found to bind to both Nex peptides (Fig. 8C; Table 11). Table 11 shows protein names, function, molecular weight (kDa), p-values from students t-test, number of counted fragments (MS/MS count), number of peptide sequences that are unique to a protein group (unique peptide), percentage of the protein sequence covered by identified peptides (sequence coverage (%)), Uniprot accession number (Acc. ID). Identified proteins that interact with E-Ras Nex were classified into three gene ontologies, molecular function, biological process, and cellular component (Fig. 8D). The vast majority of these proteins are involved in nucleic acid binding, molecular and catalytic activities, and protein interactions (Fig 8D, left pie chart). They are participating in the control of metabolic processes, cell cycle, organization and biogenesis, as well as cell communication (Fig. 8D, middle pie chart) by localizing in different subcellular compartments, particularly in the cytosol (Fig. 8D, right pie chart).

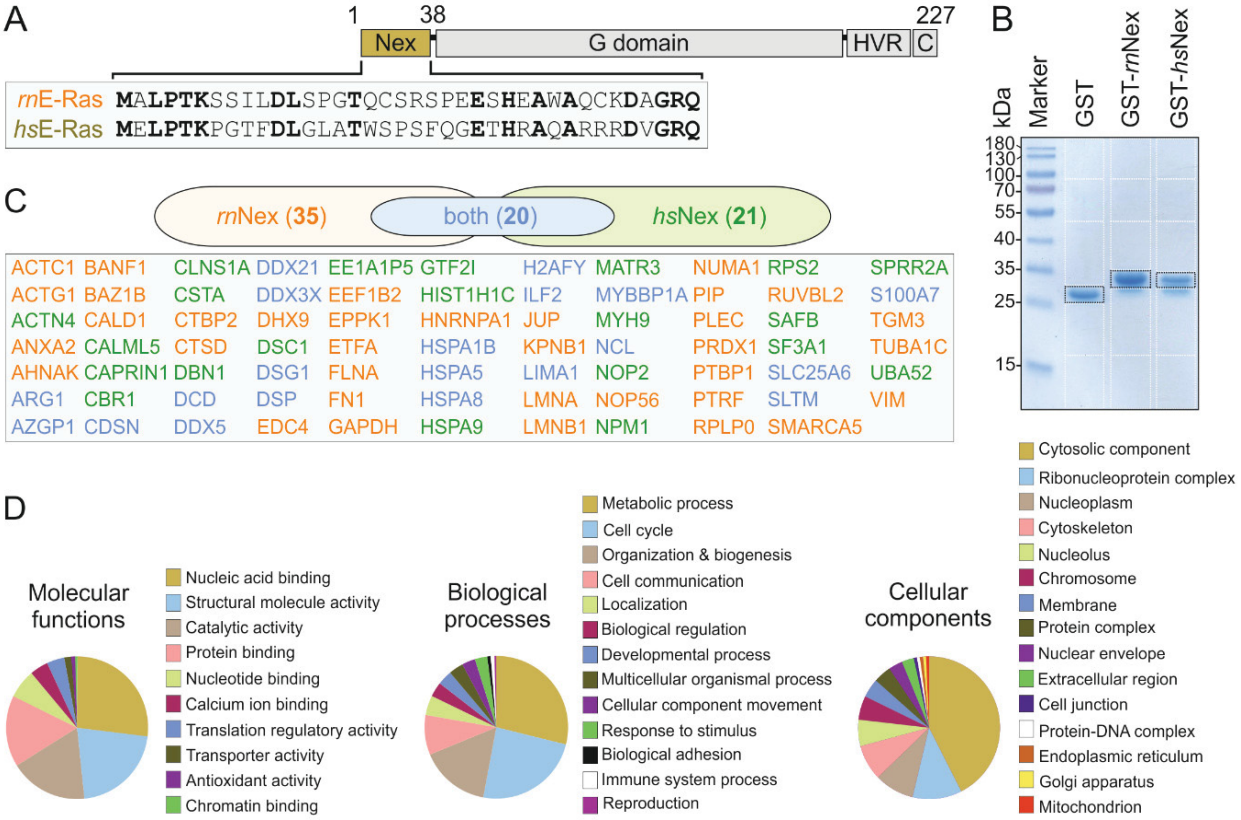


***Figure 8: E-Ras N-terminal extension and its novel binding partners.*** E-Ras contains in addition to its G domain (G), the hypervariable region (HVR), a conserved C-terminal cysteine (C) and an N-terminal extension (Nex). An alignment of E-Ras N-termi of *Rattus norvegicus* (*rn*) and *Homo sapiens* (*hs*) shows a sequence identity (bold amino acids) of 42%. (B) GST-Nex affinity purification. Proteins from total cell lysate were affinity-purified using GST, GST-*rn*Nex or GST-*hs*Nex beads. Bound proteins were resolved on a 10 % SDS gel and stained with colloidal Coomassie blue (CCB). White boxes indicate different gel fragments excised for mass spectrometric (MS) analysis. Black boxes indicate GST, GST-*rn*Nex or GST-*hs*Nex were excluded from MS analysis. Samples from three independent experiments were used for MS analysis. (C) E-Ras Nex binding proteins. Evaluation of MS analysis revealed in total 76 binding partners from which 35 preferentially interact *rn*Nex (red), 21 with *hs*Nex (green) and 20 with both (blue) (for more detail see Table 11). (D) Gene Ontology analysis of identified E-Ras Nex interacting proteins categorized according to biological processes, molecular functions, and subcellular localizations. Thirteen biological processes (left panel) were predominantly classified into metabolic pathways (29 %), cell cycle control (24%) and cellular component and organization (15.9%). From the molecular functions (middle panel), nucleic acid (RNA/DNA) binding proteins (27%), catalytic activity (18%) and protein binding (16%) comprise the major interacting proteins. Cellular components are predominated by cytosolic components (43%).

***Table 11:*** **Mass spectrometry data of detected proteins interacting with *hs*Nex and/or *rn*Nex.** Information about detected proteins including protein and gene name, function, molecular weight (kDa), p-values of *hs*E-Ras Nex or *rn*E-Ras Nex, MS/MS count, number of unique peptides detected, sequence coverage (%) and Uniprot accession number.

| Protein name (gene name) | Function | MW (kDa) | p-values *hs* / *rn* | MS/MS count | Unique peptide | Seq. cov. (%) | Acc. ID |
|---|---|---|---|---|---|---|---|
| 40S ribosomal protein S2 (RPS2) | Translation | 31.3 | 0.231/0.303 | 8 | 3 | 14.3 | P15880 |
| 60S ribosomal protein P0 (RPLP0) | Translation | 34.3 | 0.921/0.545 | 24 | 7 | 36.6 | P05388 |
| 78 kDa ER chaperone (HSPA5) | Chaperone | 72.3 | 0.175/0.651 | 191 | 24 | 45.6 | P11021 |
| Alpha cardiac muscle 1 (ACTC1) | Actin filament | 42.0 | 0.943/0.313 | 8 | 5 | 53.6 | P68032 |
| Actin, cytoplasmic 2 (ACTG1) | Actin filament | 41.8 | 0.783/0.407 | 253 | 2 | 74.4 | P63261 |
| ADP/ATP translocase 3 (SLC25A6) | Apoptosis | 32.9 | 0.097/0.010 | 4 | 2 | 19.5 | P12236 |
| Alpha-actinin-4 (ACTN4) | Actin filament | 104.9 | 0.577/0.732 | 57 | 15 | 35.8 | O43707 |
| Annexin A2 (ANXA2) | Vesicle budding | 38.6 | 0.537/0.112 | 47 | 11 | 35.4 | P07355 |
| Arginase-1 (ARG1) | Metabolism | 34.8 | 0.810/0.879 | 22 | 6 | 22 | P05089 |
| ATP-dep. RNA helicase A (DHX9) | Transcription | 141.0 | 0.670/0.565 | 49 | 21 | 23.9 | Q08211 |
| ATP-dep. RNA helicase (DDX3X) | Immune response | 73.2 | 0.947/0.922 | 25 | 9 | 23.6 | O00571 |
| Barrier-to-autointegration factor (BANF1) | Nuclear transport | 10.1 | 0.649/0.305 | 9 | 2 | 40.4 | O75531 |
| Caldesmon (CALD1) | Actin binding | 93.2 | 0.955/0.261 | 8 | 5 | 13 | Q05682 |
| Calmodulin-like 5 (CALML5) | $Ca^{2+}$ binding | 15.9 | 0.235/0.623 | 25 | 5 | 38.4 | Q9NZT1 |
| Caprin-1 (CAPRIN1) | Translation | 78.4 | 0.114/0.370 | 11 | 5 | 10.7 | Q14444 |
| Carbonyl red. [NADPH] 1 (CBR1) | Differentiation | 30.4 | 0.415/0.753 | 500 | 19 | 74 | P16152 |
| Cathepsin D (CTSD) | Proteolysis | 44.6 | 0.151/0.020 | 4 | 3 | 11.7 | P07339 |
| Caveolae-associated protein 1 (CAVIN-1) | Transcription | 43.5 | 0.507/0.038 | 5 | 3 | 16.7 | Q6NZI2 |
| Core histone macro-H2A.1 (H2AFY) | Transcription | 39.6 | 0.129/0.141 | 10 | 4 | 20.9 | O75367 |
| Corneodesmosin (CDSN) | Cell adhesion | 51.5 | 0.930/0.845 | 9 | 3 | 8.9 | Q15517 |
| C-terminal-binding protein 2 (CTBP2) | Proliferation | 48.9 | 0.335/0.042 | 7 | 4 | 12.4 | P56545 |
| Cystatin-A (CSTA) | Cell adhesion | 11.0 | 0.500/0.688 | 63 | 6 | 67.3 | P01040 |
| Dermcidin (DCD) | Defense response | 11.3 | 0.371/0.375 | 87 | 3 | 22.7 | P81605 |
| Desmocollin-1 (DSC1) | $Ca^{2+}$ binding | 100.0 | 0.405/0.725 | 44 | 5 | 8.3 | Q08554 |
| Desmoglein-1 (DSG1) | Cell adhesion | 113.7 | 0.167/0.136 | 139 | 17 | 25.8 | Q02413 |
| Desmoplakin (DSP) | Cell adhesion | 331.8 | 0.258/0.293 | 147 | 34 | 14.7 | P15924 |
| Drebrin (DBN1) | Actin binding | 71.4 | 0.693/0.976 | 22 | 10 | 31.3 | Q16643 |
| Electron transfer flavoprotein subunit alpha, mitochondrial (ETFA) | Oxidoreductase activity | 35.1 | 0.477/0.220 | 35 | 1 | 6.7 | P13804 |
| Elongation factor 1-beta (EEF1B2) | Translation | 24.8 | 0.590/0.119 | 11 | 3 | 20.4 | P24534 |
| Enhance of mRNA-decapping protein 4 (EDC4) | mRNA degradation | 151.7 | 0.000/0.923 | 47 | 14 | 17.2 | Q6P2E9 |
| Epiplakin (EPPK1) | Interm. filament | 555.7 | 0.996/0.877 | 81 | 30 | 32.7 | P58107 |
| Fibronectin (FN1) | Matrix protein | 262.6 | 0.644/0.514 | 19 | 8 | 7.6 | P02751 |
| Filamin-A (FLNA) | Actin binding | 262.6 | 0.737/0.210 | 167 | 46 | 30.2 | P21333 |
| General transcription factor II-I (GTF2I) | Transcription | 112.4 | 0.274/0.491 | 27 | 7 | 14 | P78347 |
| Glyceraldehyde-3-phosphate dehydrogenase (GAPDH) | Metabolism | 36.1 | 0.644/0.315 | 14 | 4 | 20.5 | P04406 |
| Heat shock 70 kDa protein 1B (HSPA1B) | Chaperone | 70.1 | 0.757/0.685 | 169 | 8 | 49.3 | P0DMV9 |
| Heat shock 71 kDa protein (HSPA8) | Chaperone | 70.9 | 0.911/0.943 | 352 | 25 | 62.7 | P11142 |
| Heterogen. nuclear RNP A1 (HNRNPA1) | mRNA transport | 38.7 | 0.245/0.053 | 15 | 6 | 33.3 | P09651 |
| Histone H1.2 (HIST1H1C) | Transcription | 21.4 | 0.473/0.945 | 29 | 2 | 27.2 | P16403 |
| Importin subunit beta-1 (KPNB1) | Mitosis | 97.2 | 0.626/0.413 | 22 | 4 | 6.3 | Q14974 |

| | | | | | | | |
|---|---|---|---|---|---|---|---|
| Interleukin enhancer-binding factor 2 (ILF2) | Transcription | 43.1 | 0.893/0.952 | 11 | 4 | 17.4 | Q12905 |
| Junction plakoglobin (JUP) | Cell adhesion | 81.7 | 0.382/0.090 | 122 | 16 | 29.9 | P14923 |
| Lamin-B1 (LMNB1) | Nuclear lamina | 66.4 | 0.276/0.164 | 21 | 10 | 30.5 | P20700 |
| LIM domain/actin-binding protein 1 (LIMA1) | Actin binding | 85.2 | 0.435/0.379 | 25 | 8 | 27.6 | Q9UHB6 |
| Matrin-3 (MATR3) | Immune response | 94.6 | 0.344/0.945 | 35 | 10 | 19 | P43243 |
| Methylosome subunit pICln (CLNS1A) | RNA splicing | 26.2 | 0.191/0.608 | 59 | 3 | 27.8 | P54105 |
| Myb-binding protein 1A (MYBBP1A) | Transcription | 148.9 | 0.337/0.271 | 22 | 11 | 11.4 | Q9BQG0 |
| Myosin-9 (MYH9) | Motor activity | 226.5 | 0.549/0.862 | 44 | 14 | 12.2 | P35579 |
| Neuroblast differentiation-associated protein AHNAK (AHNAK) | RNA splicing | 692.1 | 0.475/0.272 | 43 | 29 | 13.7 | Q09666 |
| Nuclear mitotic app. protein 1 (NUMA1) | Meiotic cell cycle | 238.3 | 0.349/0.099 | 51 | 24 | 17.3 | Q14980 |
| Nucleolar protein 56 (NOP56) | rRNA processing | 66.1 | 0.275/0.091 | 15 | 7 | 19.4 | O00567 |
| Nucleolar RNA helicase 2 (DDX21) | Transcription | 87.3 | 0.615/0.609 | 44 | 14 | 27.5 | Q9NR30 |
| Nucleolin (NCL) | Translation | 76.6 | 0.446/0.504 | 13 | 7 | 15.2 | P19338 |
| Nucleophosmin (NPM1) | Transcription | 32.6 | 0.210/0.602 | 73 | 10 | 44.9 | P06748 |
| Peroxiredoxin-1 (PRDX1) | Proliferation | 22.1 | 0.928/0.406 | 28 | 4 | 33.2 | Q06830 |
| Plectin (PLEC) | Actin binding | 531.8 | 0.584/0.373 | 508 | 2 | 43.8 | Q15149 |
| Polypyrimidine tract-bind. protein 1 (PTBP1) | mRNA processing | 57.2 | 0.463/0.171 | 15 | 5 | 17.7 | P26599 |
| Prelamin-A/C (LMNA) | Nuclear lamina | 74.1 | 0.485/0.241 | 86 | 25 | 47.3 | P02545 |
| Probable 28S rRNA (cytosine(4447)-C(5))-methyltransferase (NOP2) | Ribosomal large subunit assembly | 89.3 | 0.047/0.222 | 8 | 6 | 12.1 | P46087 |
| ATP-dependent RNA helicase (DDX5) | Transcription | 69.1 | 0.149/0.136 | 23 | 5 | 21.2 | P17844 |
| Prolactin-inducible protein (PIP) | Host defense | 16.6 | 0.877/0.568 | 26 | 5 | 49.3 | P12273 |
| Protein S100-A7 (S100A7) | Immune response | 11.5 | 0.536/0.469 | 12 | 2 | 22.8 | P31151 |
| Protein-glutamine γ-glutamyltransferase E (TGM3) | $Ca^{2+}$ binding | 76.6 | 0.301/0.196 | 18 | 4 | 10.1 | Q08188 |
| Elongation factor 1-α-like 3 (EEF1A1P5) | Translation | 50.2 | 0.316/0.903 | 23 | 4 | 16.2 | Q5VTE0 |
| RuvB-like 2 (RUVBL2) | DNA repair | 51.2 | 0.367/0.165 | 3 | 3 | 8.6 | Q9Y230 |
| SAFB-like transcription modulator (SLTM) | Apoptosis | 117.2 | 0.183/0.286 | 8 | 3 | 3.1 | Q9NWH9 |
| Scaffold attachment factor B1 (SAFB) | Transcription | 102.6 | 0.063/0.444 | 11 | 3 | 10 | Q15424 |
| Small proline-rich protein 2A (SPRR2A) | Keratinocyte diff. | 8.0 | 0.126/0.623 | 3 | 2 | 43.1 | P35326 |
| Splicing factor 3A subunit 1 (SF3A1) | mRNA processing | 88.9 | 0.549/0.884 | 4 | 4 | 10.1 | Q15459 |
| Stress-70 protein, mitochondrial (HSPA9) | Differentiation | 73.7 | 0.389/0.907 | 108 | 19 | 39.3 | P38646 |
| SWI/SNF-related matrix-ass. actin-dep. regulator of chromatin A5 (SMARCA5) | Transcription | 121.9 | 0.126/0.001 | 5 | 3 | 7.3 | O60264 |
| Tubulin alpha-1C chain (TUBA1C) | Microtubules | 49.9 | 0.974/0.136 | 23 | 5 | 16.9 | Q9BQE3 |
| Tyrosine-protein kinase (BAZ1B) | Transcription | 170.9 | 0.737/0.558 | 7 | 6 | 5.9 | Q9UIG0 |
| Ubiquitin-60S ribo. protein L40 (UBA52) | Translation | 14.7 | 0.336/0.810 | 62 | 5 | 38.3 | P62987 |
| Vimentin (VIM) | Cytoskeleton | 53.7 | 0.935/0.379 | 379 | 45 | 78.1 | P08670 |
| Zinc-alpha-2-glycoprotein (AZGP1) | Cell adhesion | 34.3 | 0.589/0.633 | 17 | 4 | 18.5 | P25311 |

### 3.2.2. Expression and localization pattern of E-Ras binding partners

In order to obtain specific, functional insights related to E-Ras Nex interactions in HSCs, we set out to further investigate proteins detected in mass spectrometry, which are expressed in liver cells or even HSCs. Nucleophosmin (NPM1) is an abundant nucleolar phosphoprotein involved in multiple cellular functions. It is overexpressed in liver cancer cells and is upregulated during HSCs activation (Ji et al., 2012; Xu et al., 2014). Lamin B1 (LMNB1) possesses a transcriptional coregulatory activity and plays an important role in DNA replication, cellular aging, and stress responses. It is also upregulated during HSC activation (Ji et al., 2012; Sun et al., 2010). Vimentin (VIM) is used as a mesodermal marker in HSCs and is upregulated during HSC activation (Niki et al., 1999). The cytosolic arginase-1 (ARG1) is mainly expressed in hepatic cells such as hepatocytes and is thought to be primarily involved in ureagenesis (Banerjee et al., 2017; Cederbaum et al., 2004).

ARG1, NPM1, LMNB1, and VIM were therefore investigated regarding their expression, intracellular localization, and association with endogenous E-Ras in HSCs. Freshly isolated primary HSCs were cultivated on plastic dishes for up to eight days and subsequently analyzed by quantitative real-time PCR at days 1 (d1), 4 (d4) and 8 (d8) in comparison to unseeded HSCs (d0), as representatives of the activated and quiescent state, respectively. *Arg1*, *Npm1*, *Lmnb1*, and *Vim* are differentially expressed in both freshly isolated quiescent (d0) and activated (d8) HSCs. Compared to the other genes, *Lmnb1* expression is low and is only increased in d1. In contrast to *Npm1* and *Vim*, which are transiently increased in their expression during the activation process, *Arg1* revealed the highest expression level in HSC d0 (Fig. 9A). *Arg1* expression rather resembles the *E-Ras* expression in quiescent HSCs with a principle difference, that is, E-Ras expression is suppressed during HSC activation (Nakhaei-Rad et al., 2016). ARG1 and NPM1 significantly have been implicated in different subcellular localization. As stated above, NPM1 is a nucleolar protein in contrast to ARG1, which is a cytosolic enzyme. To experimentally determine compartmentalization of E-Ras, ARG1 and NPM1 proteins in quiescent rat HSCs, we applied a detergent-free fractionation protocol as described before (Taha et al., 2014). $Na^+/K^+$ ATPase, histone H3, actin and GAPDH expression served as internal controls for different fractions. Accordingly, E-Ras, ARG1 and surprisingly also NPM1 were detected in heavy and light membrane fractions (Fig. 9B). Cytoplasmic fraction contained large amounts of ARG1 and traces of E-Ras and also NPM1. E-Ras was not detected in the nuclear fraction but ARG1 and expectedly NPM1. The significance of nuclear ARG1 is unknown (Yan et al., 2010). The same HSCs at d0, which were used for fractionation, were also used in a GST-*rn*Nex pull-down assay to visualize ARG1, NPM1, LMNB1, and VIM binding to E-Ras Nex. Figure 9C shows that all four proteins associated with the E-Ras N-terminal peptide, thus confirming the proteomic data (Fig. 8C).

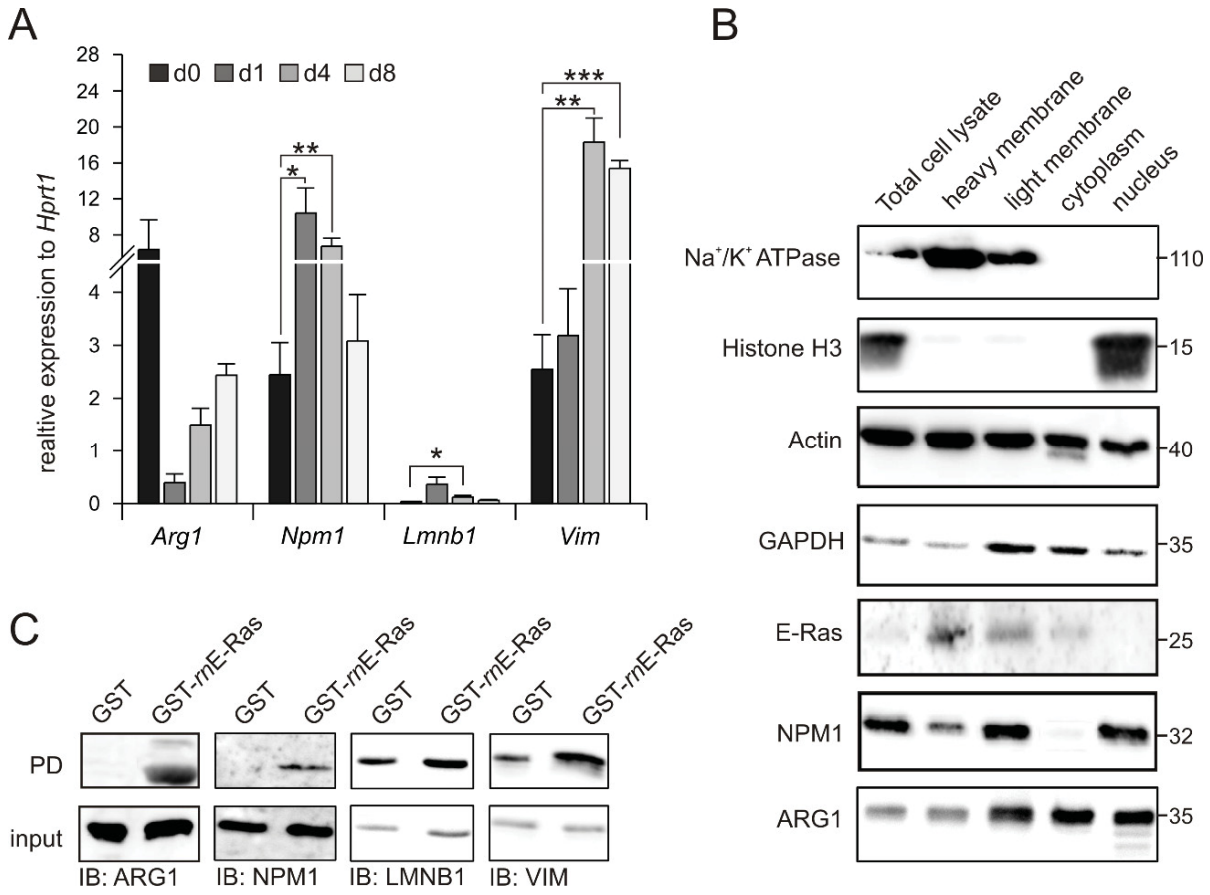


***Figure 9: E-Ras Nex interactions in hepatic stellate cells (HSC).*** (A) Expression pattern of genes related to the E-Ras binding proteins *Arginase 1* (*Arg1*), *Nucleophosmin* (*Npm1*), *Lamin B1* (*Lmnb1*), and *Vimentin* (*Vim*) in HSC at different culture time (day 0 to day 8; N=4; t test; * p<0.05, ** p<0.01; *** p<0.001, Error bars *S.E.M*). (B) Experimental cell fractionation protocol of HSCs at d0 employing several differential centrifugation steps resulted in isolation of five distinct fractions, including heavy membrane (HM; plasma membrane and rough endoplasmic reticulum), light membrane (LM; polysomes, Golgi apparatus, smooth endoplasmic reticulum), cytoplasm (CP; cytoplasm and lysosomes), and nucleus (Nu). TCL stand for total cell lysate. (C) Pulldown experiments using GST-*rn*E-Ras and GST as control in total HSC lysates at d0. Immunoblots (IB) show input samples from TCL and resulting pulldown samples (PD) of GST- *rn*E-Ras and GST to ARG1, NPM1, LMNB1 and VIM.

### 3.2.3. Protein-protein interaction profiling identifies ARG1 as a specific binding partner of E-Ras

In order to obtain functional insights related to E-Ras Nex interactions with ARG1, which was found in proteome analysis, further investigations regarding ARG1 binding to purified E-Ras constructs were done. Association of purified ARG1 with different purified E-Ras variants, including *hs*Nex, *rn*Nex, the full-length E-Ras ortholog *hs*FL, *rn*FL, and a C-terminal truncated variant *rn*ΔC, was first analyzed in GST pulldown assay. Purified GST was used as control. Figure 10A shows that ARG1 bound to all GST-E-Ras variants with higher affinity of human E-Ras than rat E-Ras. For immunoprecipitation (IP) studies E-Ras constructs, i.e. *hs*E-Ras FL, *rn*E-Ras FL, *hs*E-Ras Nex, *rn*E-Ras Nex, *hs*E-Ras ΔN, and *rn*E-Ras ΔN, to ARG1,

293T cells were transfected with EYFP-coupled constructs and analyzed 48h after transfection. GFP-binding protein (GBP)-coupled to sepharose beads were used for IP. IP from total cell lysates (TCL) was carried out for 1h at 4°C, followed by a washing step with IP buffer lacking IGEPAL-630 and a final incubation with 30 µM purified ARG1 MBP-fused for 1 h at 4°C. Immunoblotting of the IP experiment showed high affinity between E-Ras FL and ARG1 as well as similar interaction affinity between E-Ras ΔN constructs and ARG1. In contrast, the binding affinity between E-Ras Nex and ARG1 was lower. The lowest affinity was detected between ARG1 and empty EYFP vector (Fig. 10B). Subsequent kinetics of the E-Ras-ARG1 interaction were investigated using surface plasmon resonance (SPR). In a first approach, different concentration of purified ARG1 (0.7, 1.25, 5, 10, and 20 µM) were injected to immobilized GST-*hs*Nex and resulting interaction kinetic was measured (Fig. 10C, inset). A dissociation constant ($K_d$) of 2.1 µM was determined for *hs*Nex-ARG1 interaction using 1:1 binding Langmuir algorithm model. Farnesylated human E-Ras was purified from insect cells, to analyze the kinetics for the ARG1 interaction with E-Ras FL in the presence of a membrane as natural environment. Therefore, E-Ras FL was immobilized on $PIP_2$-rich liposomes at the L1 sensor chip, and different ARG1 protein concentrations (0.7, 1.25, 5, 10, and 20 µM) were injected in a multicycle model (Fig. 10D). Evaluation of the data by 1:1 binding model yielded an average $K_d$ value of 10 nM, which is 3 orders of magnitude higher as compared to *hs*Nex-ARG1 interaction in Figure 10B. This indicates that other events in addition to *hs*Nex-ARG1 interaction contribute to such a high affinity, including binding of ARG1 itself to liposomes. To measure the association of ARG1 with the liposomes, varying concentrations of E-Ras FL were injected in a multicycle model to immobilized $PIP_2$-rich liposomes, including 0.7 µM ARG1 (Fig. 10E, lower panel). Here, a $K_d$ value of 118 nM was determined for ARG1-liposome interaction. This experiment was repeated under the same condition but in the presence of 30 µM *hs*Nex (Fig. 10E, upper panel), which reduced the overall ARG1 affinity for the liposomes by 20-fold ($K_d$ = 2.3 µM). In a subsequent sedimentation assay, ARG1 binding to liposome was proved once more, even after applying high force of 20.000 g in centrifugation. In addition, results from this liposome assay indicate binding of GST-*hs*Nex to ARG1 as seen in immunoblotting with GST-antibody (Fig. 1F). Subsequent ratios of supernatant to pellet of ARG1 binding to the liposome with and without the addition of GST - *hs*Nex indicated less binding of ARG1 in the presence of GST- *hs*Nex (Fig. 10G).

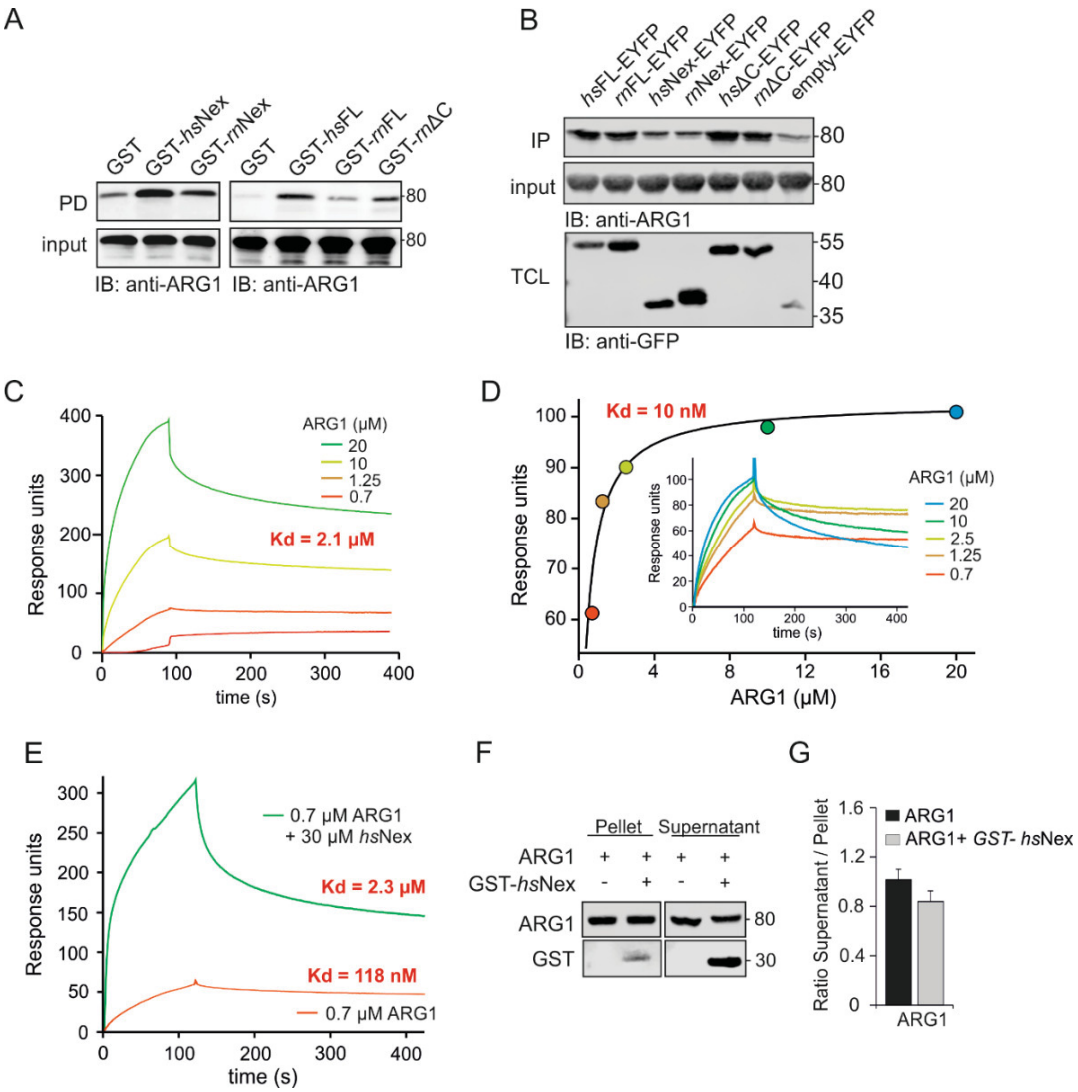


***Figure 10: E-Ras Nex directly binds ARG1.*** Pulldown of purified ARG1 with GST-*hs*Nex and GST-*rn*Nex of E-Ras and *hs* and *rn* GST-E-Ras$^{FL}$ and GST-*rn*E-Ras$^{\Delta C}$. (B) Immunoprecipitation (IP) analysis of *hs*E-RasFL, *rn*E-RasFL, *hs*ERas Nex, *rn*E-Ras Nex, *hs*E-Ras ΔN, *rn*E-Ras ΔN, and empty vector overexpressed as EYFP-fusion constructs in 293T cells with purified ARG1. Proteins retained on GFP-coupled beads were resolved by laemmli buffer and processed for Western blot using a monoclonal antibody against ARG1. (C) Sensogram obtained from the binding of ARG1 (0.7 - 20 µM) to immobilized GST-*hs*Nex on the surface of CM5 sensor chip. (D) Sensogram obtained from the binding of ARG1 (0.7 - 20 µM) to farnesylated E-Ras associated with liposomes immobilized on L1 sensor chip. (E) Sensogram obtained from the binding of 0.7 µM ARG1 to liposomes immobilized on L1 sensor chip in the absence (lower panel) and presence of 30 µM *hs*Nex. (F) Liposome sedimentation assay. 0.2 µM ARG1 was immobilized to liposomes together with GST-*hs*Nex and incubated for 30 min, RT. After sedimentation with 20,000 x g for 30 min immunoblotting was used to show binding affinity of GST-*hs*Nex to ARG1. (G) Ratio of supernatant to pellet from liposome assay indicating ARG1 binding to liposomes with and without the addition of GST– *hs*Nex.

## 3.2.4. Human E-Ras enhances ARG1 enzyme activity

ARG1 was identified by various methods to interact with E-Ras (Fig. 10). It has been shown that constitutively active RAS mutants and different members of the MAPK family play a role in modulating iNOS and arginase expression (Jin et al., 2015).Therefore, it was the aim to investigate whether the interaction between ARG1 and E-Ras has an impact on ARG1 enzyme activity. Thus, increasing concentrations of the substrate L-arginine were mixed with 50 ng of purified ARG1 and reaction was stopped at different time points. Urea production was measured at an absorbance of 540 nm. A plot of the initial reaction velocity versus L-arginine concentration yielded a Michaelis constant ($K_M$) of 27.6 ± 3.9 mM (Fig. 11A), which is in the range of published data obtained for ARG1 purified from rat livers (Garganta & Bond, 1986; Hirsch-Kolb et al., 1970; Muszynska & Ber, 1978). Next, ARG1 activity was measured in presence and absence of purified *hs*Nex and *rn*Nex. As shown in Figure 10B, *hs*Nex significantly increased ARG1 enzyme activity compared to *rn*Nex, which may be attributed to the binding properties of human and rat E-Ras proteins for ARG1 (Fig. 10A). The impact of human E-Ras on ARG1 was further analyzed by increasing concentrations of *hs*Nex (0.5 - 10 µM). Figure 11C shows that *hs*Nex interaction to ARG1 enhances it enzymatic activity in a concentration-dependent manner. These data indicate that E-Ras, particularly human E-Ras, has a direct enhancing impact on ARG1 enzyme activity under cell-free conditions.

In the following E-Ras interaction with ARG1 has been characterized to address the role of E-Ras in the regulation of ARG1 activity in HSCs.

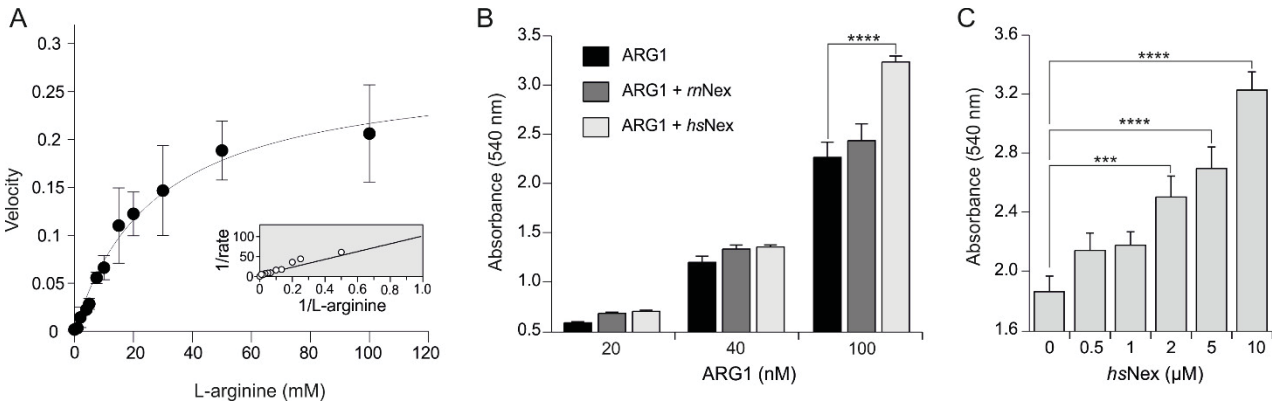


***Figure 11: Impact of E-Ras Nex on the enzymatic activity of ARG1.*** (A) ARG1 enzyme assay. Michaelis-Menten kinetics was measured at various L-arginine concentrations (N=4). A plot of the initial reaction velocity versus L-arginine concentration yielded a Michaelis constant ($K_M$) of 27.6 ± 3.9 mM. (B) Measurement of the ARG1 activity in the presence and in the absence of *hs*Nex and *rn*Nex (N=3). (C) Measurement of ARG1 activity in the presence of increasing hsNex concentrations (N=3). Bars represent mean values with indicated SD.

### 3.2.5. E-Ras colocalization with ARG1 may regulate its enzyme activity in HSCs

The interaction between ARG1 and E-Ras was identified to regulate ARG1 enzyme activity in cell-free conditions. Next, rat HSCs were analyzed regarding an impact of the interaction in cell-based context. Therefore, freshly isolated primary HSCs were cultivated on plastic dishes for up to eight days, where they become activated upon *ex vivo* culture and undergo myofibroblast transition (Kordes et al., 2013). Hence, total lysates of rat HSCs were prepared at different days (d0 – d8) and used for protein detection, analysis of ARG1 enzyme activity, confocal microscopy and immunoprecipitation. Immunoblot analysis in Figure 12A showed that ARG1 protein is expressed at highest levels in quiescent HSCs (d0). ARG1 protein levels transiently decreased in d1 and increased again in the course of time and activation (d4 and d8). This is consistent with the *Arg1* mRNA expression pattern (Fig. 9A). Control experiments showed that E-Ras is only detectable in quiescent HSCs as described before (Nakhaei-Rad et al., 2016). In addition, loss of GFAP, a quiescent HSC marker, and gain of α-SMA, a marker of activated HSCs, was detected upon activation (Fig. 12A). ARG1 expression rather resembles the E-Ras expression in quiescent HSCs with a principle difference, that E-Ras expression is completely suppressed during HSC activation (Nakhaei-Rad et al., 2016). Interestingly, the ARG1 activities in HSC lysates were concomitant with the protein pattern with the highest activity measured in lysates of freshly isolated HSCs (d0), followed by a significant decrease on d1 and d4, before activity started to increase again on d8 (Figs. 12A, B). Given this, it is tempting to speculate that E-Ras may be responsible for the high enzyme activity of ARG1 in HSCs. Immunoblot data (Fig. 12A) were confirmed by confocal imaging, which showed that unlike E-Ras, ARG1 is transiently expressed in HSCs at different days of culture (Fig. 12C). A closer look at freshly isolated HSCs at d0 revealed that E-Ras and ARG1 co-localized in defined regions of the cell (Fig. 12C; white arrows). Total cell lysates of freshly isolated HSCs were then used for immunoprecipitation of endogenous E-Ras and ARG1. Immunoblotting against ARG1 revealed that it was co-immunoprecipitated with E-Ras but not with IgG control (Fig. 12D). Additionally, iNos expression was analyzed in cultivated HSCs d0 to d8 by quantitative real-time PCR and immunoblotting. Both analyses showed that iNos is expressed at the highest levels in HSCs on d1 (Fig. 12E and 12F), followed by decreased expression on d4 and d8. Interestingly, ARG1 expression was completely contrary and showed the lowest expression signals on d1 (Figs. 9A and 12A).

Collectively, ARG1 and E-Ras expression was detectable in freshly isolated HSCs (d0) and in addition in the same cellular compartments of HSCs. Furthermore, ARG1 and E-Ras co-immunoprecipitated in HSCs, which indicates a possible cellular interaction of E-Ras with ARG1 in the cytosol and at the cell membrane and regulation of ARG1 enzyme reaction with the formation of urea and ornithine.

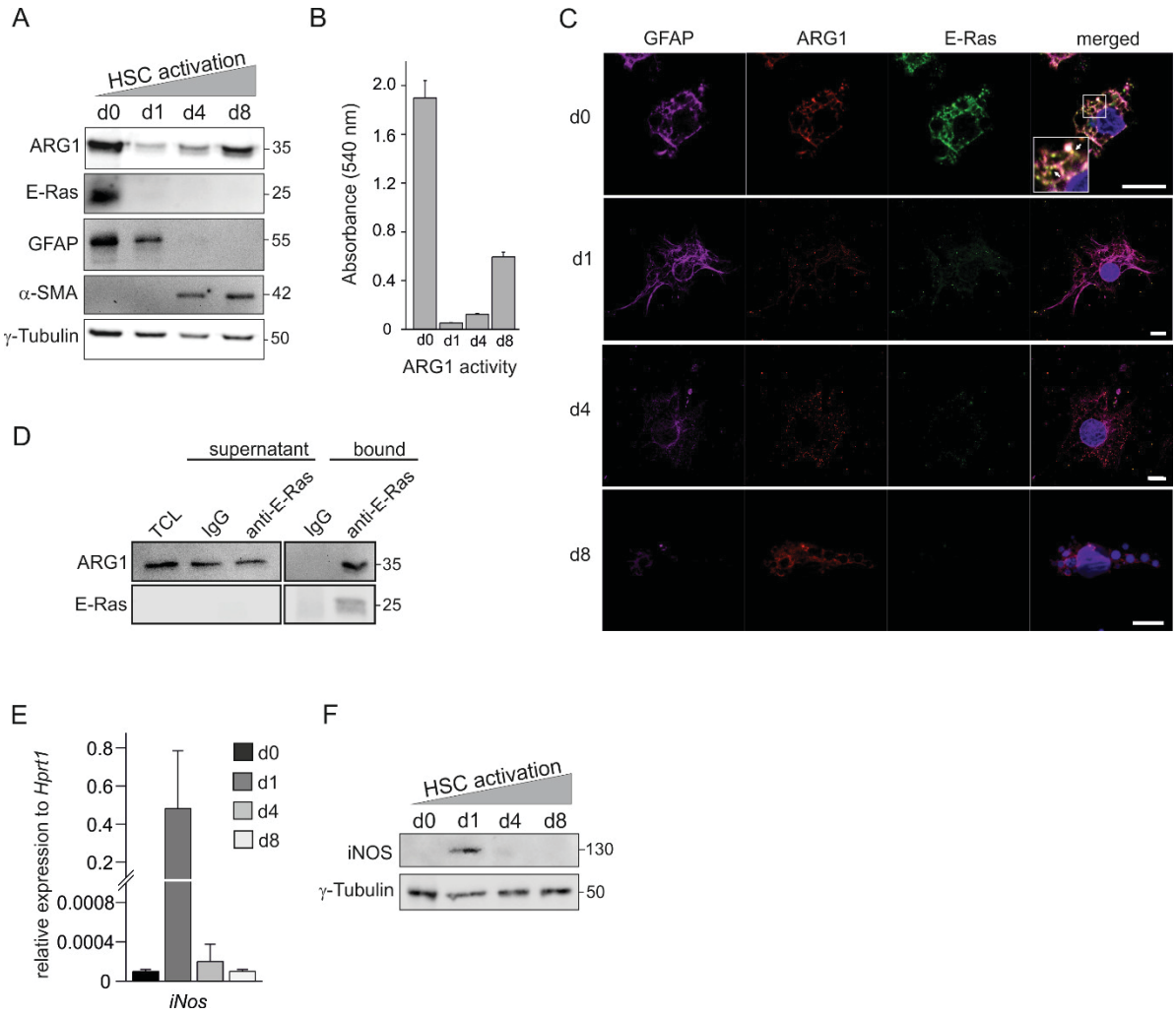


***Figure 12: E-Ras interactions in hepatic stellate cells (HSC).*** (A) Immunoblot analysis of ARG1 and E-Ras from freshly isolated (*d0*) and activated HSCs maintained in monoculture up to 8 days (*d8*). GFAP was used as a marker for quiescent HSCs (*d0*), and α-SMA was used as a marker for activated HSCs (*d8*). γ-tubulin served as loading control. (B) ARG1 activity measurement of TCL from freshly isolated HSCs (*d0*) and activated HSCs maintained in monoculture up to 8 days (*d8*) (N=3) *Error bars* S.D. (C) Confocal imaging of GFAP, ARG1 and E-Ras in HSC monocultures from d0 to d8 shows colocalization of E-Ras and ARG1 on d0. *Scale bar*, 10 µm. (D) Immunoprecipitation (IP) analysis of ARG1 with *rn*E-Ras in HSC cell lysates with monoclonal antibody against E-Ras immobilized on Protein G beads. Proteins retained on the beads were resolved by laemmli buffer and processed for Western blot using a monoclonal antibody against ARG1 and E-Ras. (E) Expression pattern of *iNos* in HSC at different culture time (day 0 to day 8; N=3; *Error bars* S.E.M). (F) Immunoblot analysis of iNOS from freshly isolated (d0) and activated HSCs maintained in monoculture up to 8 days (d1, d4, d8).

## 3.3. Maintenance of HSC quiescence

HSCs are involved in pivotal processes such as liver development, immunoregulation, regeneration, and also liver fibrogenesis. Freshly isolated HSCs start to activate upon *ex vivo* culture and exit the quiescent state as observed after liver injury. The high expression of E-Ras in quiescent HSCs correlates with the activation of the mTORC2, PI3K/AKT, and HIPPO pathway and results in support and homeostasis of the liver stem cell niche integrity (Nakhaei-Rad et al., 2016). Thus, E-Ras expression is postulated to play an important role in the maintenance of quiescence in HSC. However, many scientists try to halt HSC activation from various directions and postulate to have a recipe to maintain HSC quiescence (Deleve et al., 2008; Lin et al., 2018; Rohn et al., 2018; Yoneda et al., 2016). Nevertheless, there is an urgent need to further identify key players that orchestrate HSC activity and to find out how they control HSC activation as positive and negative regulators.

### 3.3.1. Laminin-521 as a gatekeeper for quiescence?

Laminin is the first extracellular matrix protein in the blastocyst, which is supposed to preserve the quiescence by recreating the stem cell niche as well as reliably facilitate self-renewal of stem cells in a chemically defined, feeder-free cell culture system. Recently, the effect of laminin-521 on HSC maintenance was investigated and was supposed to improve HSC adhesion and support the quiescent state of HSCs (Rohn et al., 2018). Therefore, freshly isolated rat HSCs were seeded on uncoated polystyrene (PS) cell culture dishes or PS cell culture dishes coated with laminin-521. Cells were cultured for up to 8 days and were analyzed on day 0 (d0), day 1 (d1), day 4 (d4), and day 8 (d8) by confocal microscopy, immunoblotting, and quantitative real-time PCR. Confocal imaging of laminin-521-coated dishes cultured with HSCs show E-Ras as well as GFAP (used as a marker for quiescence) expression up to day 4. Expression of E-Ras in regularly cultured, polystyrene-based HSCs was only detectable on day 0 as expected and published before (Fig. 13A) (Nakhaei-Rad et al., 2016). GFAP expression could be detected until day 4. Immunoblotting of laminin-521-coated *vs*. polystyrene-based cultured HSCs displayed GFAP expression in both conditions on all days of culture. Expression of α-SMA (used as a marker for activation of HSCs) was detected on day 4 in both conditions. And E-Ras expression was slightly detected on d0 of polystyrene-based cultured HSCs (Fig. 13B). Final mRNA expression data indicate activation of HSCs in both conditions by the expression of *α-SMA* starting from day 4 (Fig. 13C), as well as reduction of *E-Ras* expression and *GFAP* expression from d0 to day 8 (Fig. 13D). The expression of *Desmin*, which is usually strongly upregulated during HSC activation (Niki et al., 1999), was also upregulated in laminin-521-coated, cultured HSCs, while it was up-regulated on d1, followed by downregulation on day 4 and 8 in HSCs cultured on polystyrene dishes (Fig. 13C).

Taken together, HSC culture on laminin-521-coated dishes could support the basement of membrane-like structures as existing in the space of Disse (Rohn et al., 2018). However, HSCs were still activating in laminin-521-coated dishes as displayed by the upregulated expression of α-SMA and down-regulated expression of GFAP in immunoblotting and quantitative mRNA analysis. In addition E-Ras expression was also downregulated in HSCs on laminin-521-coated dishes in all experiments.

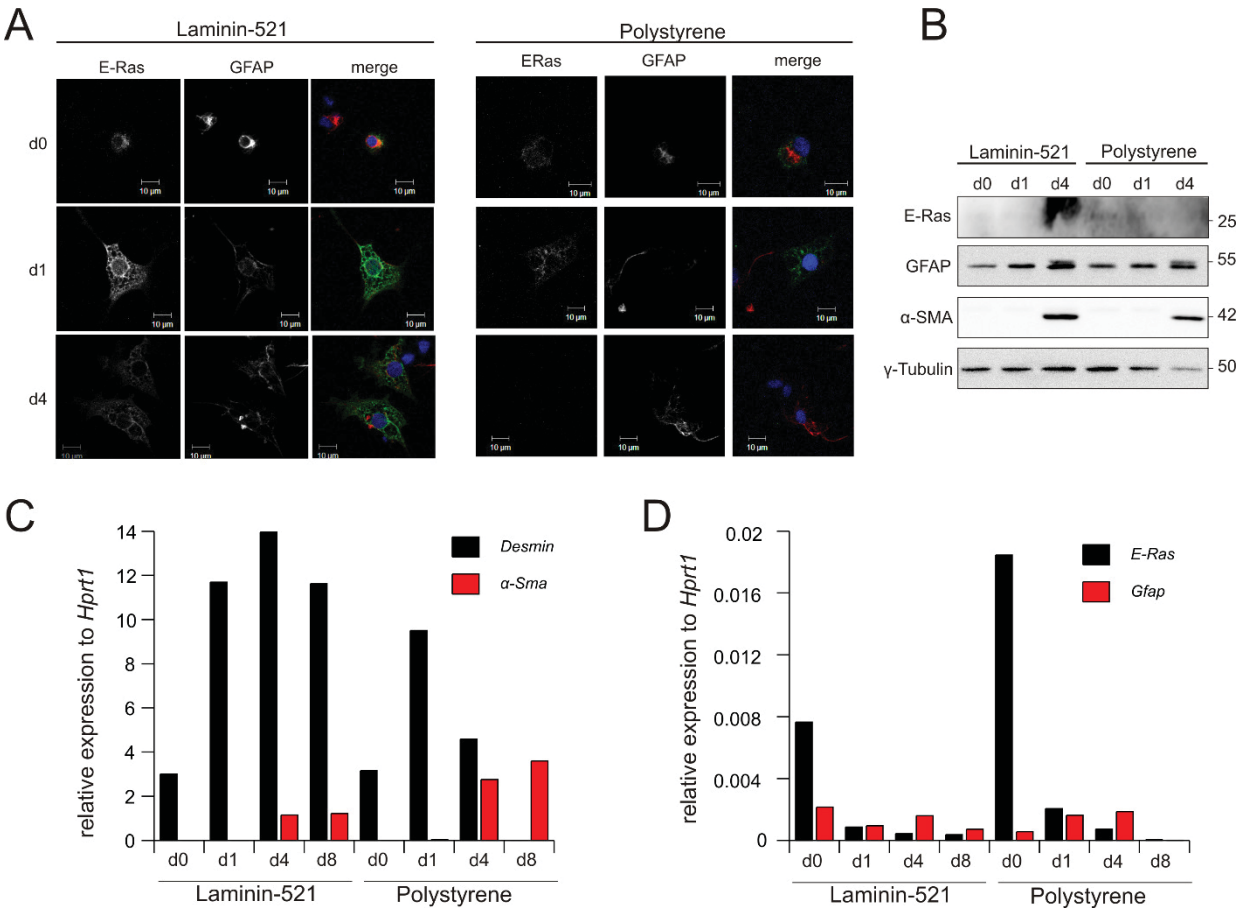


***Figure 13: Laminin-521-coated vs. polystyrene-based culture of hepatic stellate cells (HSCs).*** *(A)* Confocal imaging of E-Ras and GFAP in Laminin-521-coated *vs.* polystyrene-based HSC monocultures from d0 to d8. Scale bar, 10 µm. (B) Immunoblot analysis of E-Ras, GFAP, and α-SMA from freshly isolated (d0) and activated Laminin-521-coated *vs*. polystyrene-based HSCs maintained in monoculture up to 4 days (d8). GFAP was used as a marker for quiescent HSCs (d0), and α-SMA was used as a marker for activated HSCs (d4). γ-tubulin served as loading control. (C) Expression pattern of *Desmin* and *α-SMA* in Laminin-521-coated *vs*. polystyrene-based monocultures of HSCs *(day 0 to day 4; N=1).* (D) Expression pattern of *E-Ras* and *GFAP* in Laminin-521- *vs*. Polystyrene-based monocultures of HSCs *(day 0 to day 4; N=1).*

### 3.3.2. Co-culture of hepatic stellate cells with hepatocytes

HSC culture on laminin-521 was not able to maintain quiescence (Fig. 13). Therefore, the next try was to analyze the characteristics of HSCs in a co-culture transwell system with hepatocytes (HCs). HCs, that occupy about 80 % of the total liver volume, are sandwiched around the liver sinusoids. They self-assemble in culture to form compacted spherical aggregates, or spheroids, that mimic the structure of the liver by forming tight junctions and bile canalicular channels (Abu-Absi et al., 2004). Thus, freshly isolated rat HSCs were regularly seeded on polystyrene culture dishes. 1 day after that, freshly isolated rat HCs were seeded above in transwell format (Fig. 14A). HSCs were then analyzed by confocal microscopy and quantitative real-time PCR on different days of culture. For day 1 analysis (d1) HSCs were kept in co-culture for 5-6h. Mono-culture of HSCs were used as control for the activated status. Confocal imaging of HSCs in co-culture system shows E-Ras expression on all days of culture (Fig. 14B, left green panels). GFAP expression was detected on d1 and d4, very less on d8 of culture (Fig 14B, left red panels). Expression of α-SMA, a marker for activation, was slightly detected on d1 and d4, and clearly detected on d8 of culture (Fig. 14B, left green panels). Mono-cultures showed the typical and well described loss of expression of E-Ras and GFAP, and increase in α-SMA expression. The major difference of HSCs cultured in both conditions can be noticed in the cell morphology. While HSCs cultured in mono-culture system at day8 appear rounded, HSCs in the co-culture system at day 8 appear stellate shaped as detected in quiescent cells in the healthy liver (Wake, 2006). Analysis of mRNA expression revealed almost no alterations of expression for day 1 compared to day 8 for *Desmin* and *α-SMA* in co-cultures of HSCs with HCs. *Desmin* expression in mono-culture of HSCs was slightly down-regulated from day1 to day8, while expression of *α-SMA* slightly increased on day 8 (Fig. 14C). *E-Ras* expression in co-cultures was noticeably upregulated upon culture on day 8, while it was downregulated on mono-cultures. And *GFAP* expression slightly increased in both conditions (Fig. 14D).

In conclusion, based on confocal imaging and quantitative real-time PCR analysis, co-culture of HSCs with HCs in transwell format provided a first attractive system for further experiments to mimic the HSC niche and maintain HSC quiescence. Results of co-cultures indicated that the presence and contributions of multiple liver cells capture the interactions between the cells to recreate the liver niche and maintain HSCs in a quiescent status, which may last longer as seen in mono-culture system or with laminin-521-coated dishes.

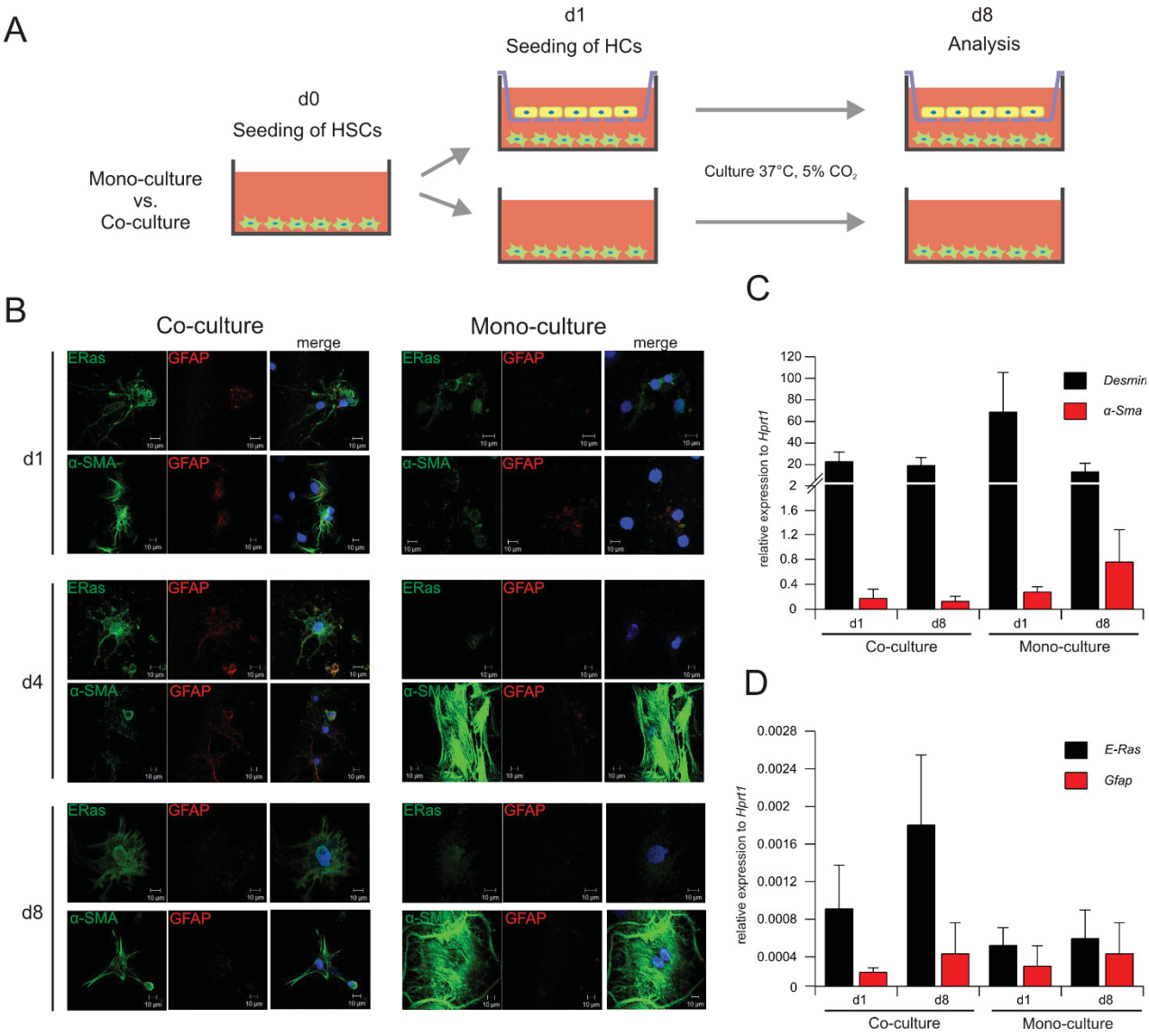


***Figure 14: Analysis of HSCs in mono- and co-culture.*** (A) Scheme of HSC culture system in mono- and co-culture with hepatocytes (HCs) up to day 8. (B) Confocal imaging of E-Ras, GFAP, and α-SMA in HSC co- and mono-culture system for d1, d4 and d8. Scale bar, 10 µm. (C) Expression pattern of *Desmin* and *α-SMA* in HSC co-and mono-culture system *(day 1 and day 8; N=3; Error bars represent SD).* (D) Expression pattern of *E-Ras* and *Gfap* in HSC co-and mono-culture system *(day 1 and day 8; N=3; Error bars represent SD).*

### 3.3.3. Can co-culture with the addition of vitamin A and insulin sustain HSC quiescence?

Co-culture of HSCs with HCs in transwell format provided a first attractive system for further experiments, but did not represent an optimal result for maintenance of quiescence yet. A research group recently published, that the constant addition of vitamin A and insulin are required for HSC quiescence (Yoneda et al., 2016). Vitamin A regulates lipid accumulation and gene transcription, suggesting that vitamin A is involved in the maintenance of HSC quiescence under a physiological condition. Therefore, freshly isolated rat HSCs were regularly seeded on polystyrene culture dishes. One day later, freshly isolated rat HCs were seeded above in transwell format as already described before (Fig. 14A). To provide liver related factors in addition to the reconstruction of the extracellular environment by co-culturing the HSCs, 10 µM retinol and 50 ng/ml insulin was added to co-culture medium and medium was changed every 48h until subsequent analysis (Fig. 15A). As REs are hydrolyzed into retinol and either released into the circulation or re-esterified and stored in cytosolic LDs (Kudo, 1989), crystaline retinol was used for treatment. Confocal imaging of treated HSCs in co-culture system showed besides a constant expression of GFAP up to d8, not detected α-SMA expression in d1 or d8. Expression of E-Ras was slighly detected on d1 and d8 (Fig. 15B, left panels). In contrast, GFAP and E-Ras expression was detectable on d1 of treated HSCs in mono-culture system, but not on d8. Additionally, α-SMA expression was not identified on d1, but was detected on d8 of culture (Fig.15B, right panels). The major difference in HSCs cultured with the addition of vitamn a and insulin was sensed in cell morphology and LD amount. While co-cultured cells sustained in stellate shape form up to day 8 and had many cytosolic auto-fluorescent LDs (Fig. 15B, left panels, blue spots), mono-cultured cells showed less stellate morpholgy on day 8, but also auto-fluorescent LDs.

Taken together, based on initial results of confocal imaging, co-culture of HSCs with HCs and the constant addition of vitamin a and insulin seemed promising for maintenance of HSC quiescence. Results indicated that the presence of liver relevant factors (i.e. vitamin a and insulin) contributes to further mimicry of the liver niche and maintain HSCs in a quiescent status.

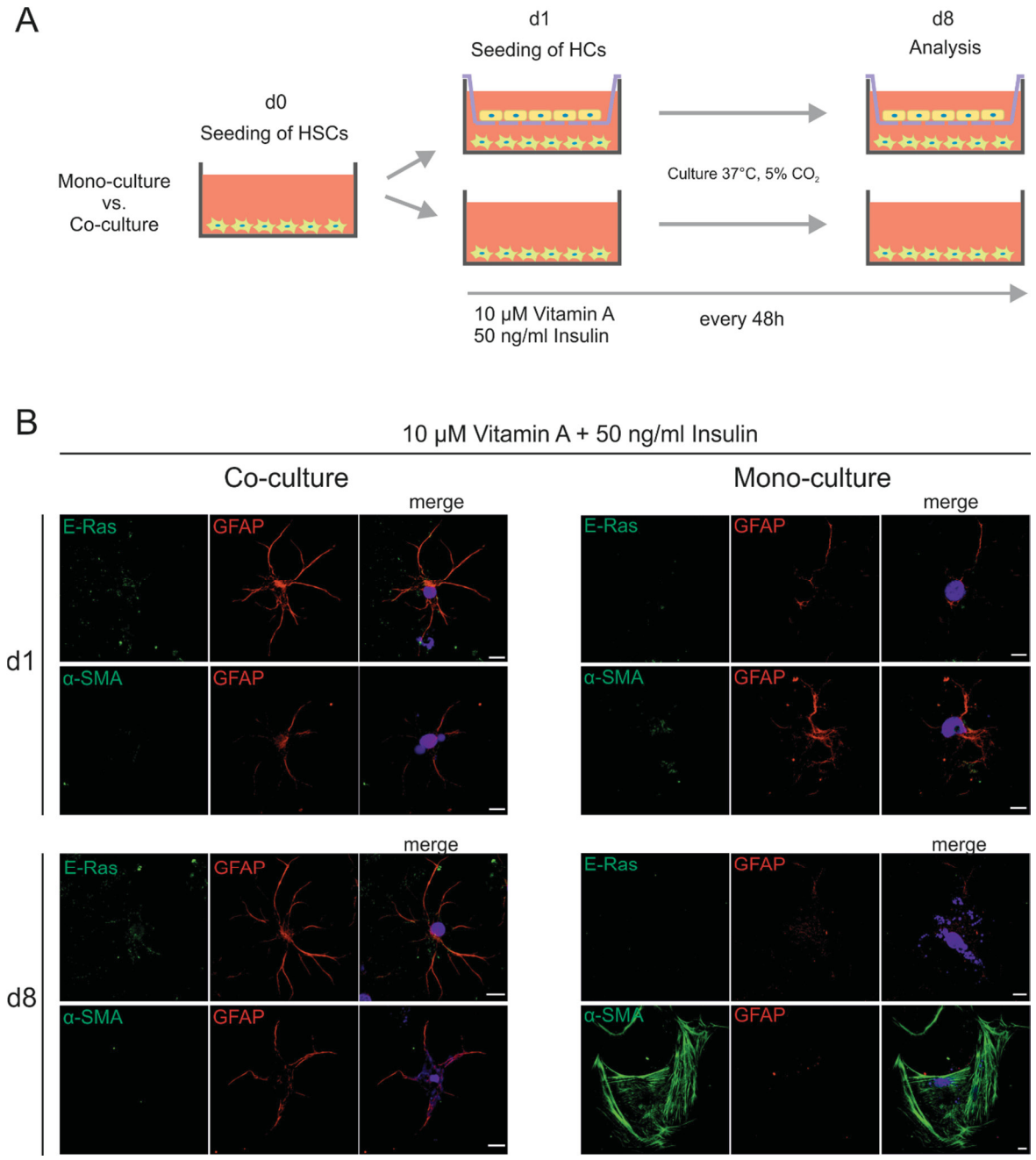


***Figure 15: Co-culture with additional vitamin A and insulin preserves HSC niche and provides liver relevant factors.*** (A) Scheme of HSC culture system in mono- and co-culture with hepatocytes (HCs) up to day 8 with the addition of vitamin A and insulin (B) Confocal imaging of E-Ras, GFAP, and α-SMA in HSC co- and mono-culture system for d1, d4 and d8. Scale bar, 10 µm.

# 4. Discussion

## 4.1. E-Ras and H-Ras activate the mTORC2 pathway via interaction with SIN1

Endogenous E-Ras expression in quiescent HSCs strongly correlates with high levels of AKT phosphorylated at T308 and S473 through PDK1 and mTORC2, respectively (Nakhaei-Rad et al., 2016). E-Ras is proposed to be the regulator of the PI3K-PDK1-AKT-mTORC1 and the mTORC2/AKT axis (Nakhaei-Rad et al., 2016; Y. Yu et al., 2014). These axes control various processes including cell cycle progress, autophagy, apoptosis, lipid synthesis, survival and translation (Nakhaei-Rad et al., 2018; Sabatini, 2017; J. S. Yu & Cui, 2016; Zoncu et al., 2011). Previous studies have shown that quiescent HSCs produce and secrete a significant amount of HGF (Schirmacher et al., 1992), which is modulated by the mTORC1-S6K pathway (Tomiya et al., 2007) and is known to regulate hepatocyte survival (X. Wang et al., 2002). In comparison with mTORC1, the regulation of mTORC2 is less understood (Oh & Jacinto, 2011). As already mentioned, E-Ras is proposed to be an upstream regulator of the mTORC2 pathway, but the mechanism of activation still remains unclear.

***SIN1 RBD can interact with RAS proteins*** - SIN1 possess a RBD and has been proposed to bind and co-localize with the small GTPases, such as H-Ras (Schroder et al., 2007; Y. Yuan et al., 2015), human RAP1 and *Dictyostelium* RasC (Khanna et al., 2016). Nevertheless, overexpression of SIN1 has also been reported to inhibit Ras-dependent activation of AKT and ERK1/2 (Schroder et al., 2007). Pulldown experiments in this study now confirmed the interaction of SIN1 RBD with rat and human E-Ras. In addition, co-immunoprecipitation of endogenous SIN1 with H-Ras$^{G12V}$ and E-Ras$^{WT}$ overexpressed as EYFP-fusion proteins revealed that both RAS proteins physically interact with SIN1. Following these initial interaction experiments, three different SIN1 RBD mutants were designed and analyzed regarding possible responsibility of interaction to RAS proteins. Various interaction methods were performed and showed highest binding affinity between SIN1 RBD$^{WT}$ and RAS proteins (i.e. E-Ras, H-Ras, RIT1). SIN1 RBD mutants (SIN1 RBD$^{D}$, SIN1 RBD$^{EE}$, and SIN1 RBD$^{REE}$) showed decreasing binding affinity to RAS proteins in ascending order of introduced number of amino acid mutations. This mutational analysis correctly proved the predicted region including the correct amino acids within the SIN1 RBD interaction surface, which are responsible for binding to RAS proteins. Besides proving SIN1 as an interaction partner for RAS, it then raised the question whether the RAS-SIN1 interaction can activate the mTORC2 pathway and is in charge for the signal transduction. Studies to date suggest that mTORC2 specifically senses upstream growth factors and therefore regulates proliferation, actin cytoskeleton, and cell survival. However, inconsistent findings have been reported, and the underlying mechanisms are currently unclear (Hung et al., 2012; Oh & Jacinto, 2011). However, RIT1 has been recently identified to

interact with SIN1 and promote mTORC2-mediated AKT phosphorylation (Cai & Andres, 2014), but other GTPases have not been directly described as upstream regulators of the mTOR complex 2.

***mTORC2 pathway activation by E-Ras overexpression*** – Next, possible mTORC2 pathway activation by the detected RAS-SIN1 interaction was analyzed. After transfection of COS7 cells with hyperactive variants of RIT1 and H-Ras, as well as E-Ras, cells were serum starved to inhibit growth factor activation of RAS signaling, followed by PI3K-inhibition to prevent cross-talk activation between mTORC1 and mTORC2 pathway by phosphorylation of AKT and S6K (Liu et al., 2013; Liu et al., 2014; J. Xie & Proud, 2013). Interestingly, mTORC2/AKT axis was mostly activated by overexpression with *rn*E-Ras, followed by the other RAS proteins. mTORC2 pathway activation was investigated by phosphorylation of AKT$^{S473}$. Members of the class O forkhead box transcription factors (FOXO) have important roles in metabolism, cellular proliferation stress resistance, and apoptosis (Y. Wang et al., 2014). Although there was no significant downregulation of p-FOXO1$^{S256}$, E-Ras is certainly proposed as an activator of the mTORC2 pathway via interaction with SIN1, as other cross-talks may phosphorylate FOXO1 to safeguard this important pathway. Phosphorylation of FOXO1 and FOXO3 by AKT effectively prevents them from translocating to the nucleus and activating gene expression programs that promote apoptosis; thus, mTORC2 may favor cell survival through AKT-mediated inhibition of FOXO1 and FOXO3 (Zoncu et al., 2011). FOXO activity is also responsible for stem cell maintenance and lifespan, as well as cell cycle and metabolism. Modest alterations of the transcriptional output can result in profound effects (Accili & Arden, 2004). FOXO can be phosphorylated by several other kinases such as IKK, PKB, JNK, MST1, p38, AMPK and many more. Some of these phosphorylations have an activating, some an inhibitory effect on FOXO1 (Eijkelenboom & Burgering, 2013). Other possible cross-talks to FOXO1 were not investigated within this study, therefore it was not examined which other kinases where responsible for phosphorylation of FOXO1.

***Role of the ERAS-mTORC2 activity in quiescent HSCs*** - E-Ras as well as the mTORC2 pathway was activated and/or upregulated in freshly isolated, quiescent HSCs (Nakhaei-Rad et al., 2016). Thus, E-Ras was proposed but not proved as an upstream regulator of the mTORC2 pathway. After the identification of the RAS-SIN1 interaction by various interaction methods and the subsequent analysis of the mTORC2 activation by E-Ras, it was the aim to investigate whether upregulated E-Ras in quiescent HSCs is responsible for the mTORC2 pathway activation. Immunoblotting of TCL of freshly isolated and cultured HSCs up to day 8 proved ones more what was already observed in 2016: p-AKT$^{S473}$ was upregulated in freshly isolated HSCs and expression levels dropped down during culture induced activation (Nakhaei-Rad et al., 2016). While phosphorylation of p-FOXO$^{S256}$ on d0 was not detected, it was upregulated from d1 to d8 and also showed activation of the mTORC2 pathway. Confocal imaging of freshly isolated HSCs showed colocalization of E-Ras and SIN1 in cytoplasm, especially cytoplasmic region around the nucleus.

SIN1α, SIN1β and SIN1δ isoforms showed cytoplasmic localization, but mostly plasma membrane localization in overexpressed HeLa cells, due to their PH domain, which can bind phosphatidylinositol lipids within biological membranes (Y. Yuan et al., 2015). In this study, it was not analyzed which isoform of SIN1 is present in HSCs. Due to short culture time of freshly isolated HSCs (4-6h) before fixation for confocal imaging, cells are stressed and displayed a more or less round shaped morphology. It is assumed, that because of a different *in vitro* morphology of HSCs compared to *in vivo* morphology, where cells are stellate shaped (Wake, 2006), the cellular distribution and localization of SIN1 could slightly differ. However, E-Ras expression is down-regulated during culture induced activation of HSCs and is therefore not detectable on protein level in confocal imaging upon d1. Thus, colocalization of E-Ras and SIN1 could not be detected in other culture days of HSC mono-cultures. Co-culture with HCs in transwell systems were thought to maintain HSC quiescence as it maintains hepatocyte differentiation (Krause et al., 2009; Thomas et al., 2005). Unfortunately, confocal imaging showed strong background signals in SIN1 and E-Ras channels and did not show colocalization.

However, E-Ras/mTORC2/AKT/FOXO1 axis was proved and shown in *in vitro* analysis and in HSCs and may insure the survival of HSCs in the space of Disse in a healthy liver. SIN1 may play an important role in orchestrating the function of survival, as SIN1 knockout cells are more sensitive to stress-induced apoptosis (Jacinto et al., 2006; Paramo, 2014). Nevertheless, further experiments are needed to demonstrate the interaction and the resulting activation of the mTORC2 pathway *in vivo*. The knockout of E-Ras does not seem lethal (Takahashi et al., 2003). Hydrodynamic injections into the tail vein of animals is used as a tool to analyze promoters and enhancers of the liver (Kim & Ahituv, 2013). Therefore, possible knockdown and/or knockout experiments of E-Ras with lentiviruses via hydrodynamic injection with subsequent analysis of the mTORC2 pathway could help to shed more light into the liver-related role and function of E-Ras-SIN1 interaction, as hepatic mTORC2 pathway plays a critical role in survival and glucose metabolism (M. Yuan et al., 2012). In addition, these experiments could show and support the relevance of E-Ras in the process of liver regeneration.

## 4.2. E-Ras interacts with Arginase-1 and regulates its activity in quiescent hepatic stellate cells

E-Ras expression seems to be critical for maintenance of growth and tumor-like properties in undifferentiated mouse embryonic stem cells and some tumor cell lines. It further seems to have a major effect on the fate of HSCs as it is also expressed in freshly isolated, quiescent HSCs of a healthy liver. E-Ras controls distinct pathways, including PI3K/AKT and MST/YAP, and is critical for maintenance of HSC quiescence in the liver (Nakhaei-Rad et al., 2016; Takahashi et al., 2003). Other than that, little is known about E-Ras interaction partners or E-Ras effectors.

***E-Ras Nex serves as a binding site*** - E-Ras possesses a unique 38-amino acid N-terminal extension. This amino acid sequence, in comparison between E-Ras and other RAS proteins, displays an additional region upstream of its G domain, which is unique for E-Ras in different organisms. As it was already proposed in 2016, this extension could serve as a potential binding site for interaction partners, especially as the human form of E-Ras N-terminus exhibits a PxxP motive (Nakhaei-Rad et al., 2016).
In this study, we found a high number potential interaction partners for E-Ras that could be responsible for several HSC functions, including nitric oxide and urea rates. A total of 76 proteins, including ARG1, NPM1, VIM and LMNB1, were detected in proteome analysis as possible binding partners for rat and human E-Ras. Results obtained from mass spectrometry of identified interaction partners were statistically not significant. In most cases, p-values were higher than 0.05, probably due to pulldown analysis with a very short single domain (N-terminus) of E-Ras (aa 1-38) instead of FL. Nevertheless, subsequent interaction experiments proved interaction affinity between selected interaction partners and E-Ras Nex as well as FL. Additionally, proteome analysis was only conducted to initially obtain a few possible interaction hits within a huge pool of proteins.
As E-Ras is expressed in liver residing, quiescent hepatic stellate cells (HSC), we focused on identified interaction partners and proteins also expressed in HSCs or at least in liver cells. NPM1 is an abundant nucleolar phosphoprotein involved in multiple cellular functions. It is overexpressed in liver cancer cells and is upregulated during HSCs activation (Ji et al., 2012; Xu et al., 2014). LMNB1 possesses a transcriptional coregulatory activity and plays an important role in DNA replication, cellular aging, and stress responses. It is also upregulated during HSC activation (Ji et al., 2012; Sun et al., 2010). VIM is used as a mesodermal marker in HSCs and is upregulated during HSC activation (Niki et al., 1999). ARG1 is known to be expressed in the liver, mainly in macrophages, but also in nuclei of other liver cells (Dounce & Beyer, 1948; Mattila et al., 2013). For the first time, we showed ARG1 expression in HSCs. The cytoplasmic extracts of murine and human macrophages showed high levels of arginase activity (Di Costanzo et al., 2005). ARG1 regulates ureagenesis, but is also a counter actor for nitric oxide synthetase (iNOS), which is responsible for nitric oxide (NO) production (Cederbaum et al., 2004; Durante et al.,

2007; Janne et al., 1991; Lange et al., 2004; Mezl & Knox, 1977). E-Ras is known to be mainly expressed in heavy and light membrane fractions, but also partly in the cytoplasm of liver residing, quiescent hepatic stellate cells (Nakhaei-Rad et al., 2016). Therefore, it was proposed that all four identified interaction proteins (ARG1, NPM1, LMNB1, and VIM) could interact with E-Ras as it was initially found in proteome analysis.

To shed light into the possible role of interaction between E-Ras and the identified proteins, we analyzed expression profiles of ARG1, NPM1, VIM and LMNB1 in quiescent *versus* activated rat HSCs by quantitative real-time PCR and immunoblot. Freshly isolated primary HSCs were cultivated on plastic dishes for up to 8 days, where they become activated upon ex vivo culture and undergo myofibroblast transition (Kordes et al., 2013). For the first time we describe ARG1 to be found in HSCs, especially detected in quiescent and to a lesser extend in cultured, activated HSCs. The mRNA expression data was concomitant with protein expression detected in cultures HSCs. In contrast, mRNA levels of NPM1 and VIM were upregulated during HSC activation as it is stated in literature (Ji et al., 2012; Niki et al., 1999; Xu et al., 2014). In contrast, expression of LMNB1 was very low compared to other genes. Besides the fact that ARG1 as well as E-Ras mRNA and protein levels are upregulated in freshly isolated HSCs, we aimed to elucidate whether they are located in the same cellular compartment. In this subcellular fractionation, E-Ras was, as already described before mostly found in the heavy (plasma membrane and rough endoplasmic reticulum) and light membrane fraction (Golgi apparatus, smooth endoplasmic reticulum, and various organelles), as well as in the cytoplasm (Nakhaei-Rad et al., 2016; Taha et al., 2014). Interestingly, ARG1 was found in all HSC fractions including the nuclei (Dounce & Beyer, 1948) and the membrane fractions. As it can be seen in subsequent liposome assay, ARG1 seemed to bind to the membrane by containing positively charged residues on the protein surface, which could be responsible for recruitment to the membrane (Jiang et al., 2006) and hydrolyzing L-arginine to urea and ornithine. As expected, NPM1 was found in all fractions except the cytoplasmic fraction. After expression analysis of all four proteins in HSCs by quantitative real-time PCR and/or fractionation, it was the aim to investigate whether these proteins can interact with E-Ras in freshly isolated HSCs in addition to HeLa cell lysates. Immunoblotting revealed interaction of all for proteins (i.e. ARG1, NPM1, VIM and LMNB1) with endogenous E-Ras and therefore confirmed the previous proteome analysis conducted in HeLa cell lysates.

As we showed ARG1 expression in HSCs for the first time, we further focused on interaction analysis between E-Ras and ARG1. In addition, ARG1 is responsible for urea production and is the counter actor of iNOS, which is responsible for NO production. Thus, it caught our interest to investigate if a possible interaction of E-Ras and ARG1 could be responsible to change the equilibrium between ARG1 and iNOS. To gain insights into the binding specificity of E-Ras and prove what we could observe in proteome and initial pulldown analysis of HSCs, we performed another pulldown and IP experiment. Both experiments

verified the previous analysis showing ARG1 as an interaction partner for rat as well as human E-Ras. The subsequent kinetic measurements showed interaction between ARG1 and E-Ras Nex in µM range and even nM range between ARG1 and E-Ras FL. Competition assay using ARG1, E-Ras FL and E-Ras Nex proved that the N-terminus alone was able to pull ARG1 from the liposome-based membrane. Following liposome sedimentation assay also proved this. In conclusion, E-Ras Nex seems enough to interact with ARG1 by a still unknown process, but interaction affinity is much higher to the full-length protein. The identified PxxP motif within the unique N-terminus of E-Ras could play a role in interaction process as it is usually sufficient for SH3 domain-mediated binding to other proteins (Wuertenberger & Groemping, 2015), but this needs to be further analyzed. However, previous studies showed that the N-terminal extension of E-Ras is critical for PI3K-AKT-mTORC activation and N-terminal truncated E-Ras variants had remarkably lower signaling activity (Nakhaei-Rad et al., 2015). One explanation might be the role of the unique N-terminus in lateral segregation of E-Ras across the membrane, that consequently specifies association with and activation of its effectors in a manner reminiscent to microdomain localization of H-Ras (Jaumot et al., 2002).

***E-Ras potentiates ARG1 activity*** - ARG1 is known to play a role in hepatic ureagenesis and is important in eliminating nitrogen formed during amino acid and nucleotide metabolism (Cederbaum et al., 2004). To ensure that our experiments obtained with purified ARG1 protein only address catalytically active ARG1, we aimed to measure its activity. First, our Michaelis-Menten kinetics identified human ARG1, heterologously purified from *E. coli*, as a highly active enzyme with similar Michaelis constant as stated in literature (Garganta & Bond, 1986; Hirsch-Kolb et al., 1970; Muszynska & Ber, 1978). Further ARG1 activity measurements indicated increased urea formation in the presence of *hs*E-Ras. Thus, in quiescent HSCs, E-Ras is proposed as a regulator of the catalytic activity of ARG1. The interaction between E-Ras and ARG1 could play a role in balancing the equilibrium between ornithine, urea and NO formation, serving as precursors for growth and proliferation and furthermore helping the hepatoarterial blood supply, as NO is a known vasodilator for smooth muscle cells (Caldwell et al., 2015; Lange et al., 2004). To gain further insights in the regulation and interaction of ARG1 and E-Ras in a liver based context, we further analyzed HSCs.

***Role of the E-Ras – ARG1 interaction in HSCs*** - Endogenous expression of E-Ras in HSCs strongly correlated with high levels of ARG1 expression. Moreover, activity analysis of HSCs (d0 to d8) correlated with detected ARG1 protein levels and ARG1 and E-Ras colocalized in HSCs on d0. In contrast, iNOS expression was highly present on d1, which is probably due to the high oxidative stress level after cell isolation. Whenever an organ is injured by various causes, a repair process is initiated to recover to the normal condition. During liver injury HSCs are activated by cytokines that originate from damaged hepatocytes and Kupffer cells (Dong et al., 1998). Oxygen radicals are associated with cell damage by

lipid peroxidation and DNA fragmentation, causing oxidative stress. Oxidative stress is related to several liver diseases such as alcoholic liver disease, chronic hepatitis C and liver cancer (Galicia-Moreno & Gutierrez-Reyes, 2014; Ivanov et al., 2017). Upon oxidative stress hepatocytes increase iNOS (inducible form of NOS) expression (Kuo et al., 1997). Most likely iNOS expression increases in other cells as well, as variety of cells, including vascular smooth muscle cells, hepatocytes, and HSCs, express the iNOS. Whereas endothelial cells (eNOS) and neuronal cells (nNOS) express constitutive NOS forms (Rockey & Chung, 1995; Wiest & Groszmann, 1999). Isolating and culturing HSCs *in vitro* causes not only activation of the cells, but also oxidative stress, and oxidative stress in turn causes activation of HSCs (K. S. Lee et al., 2001).

It has been shown, that constitutively active Ras mutants and different members of the MAPK family play a role in modulating iNOS and arginase expression (Jin et al., 2015). ARG1 and iNOS could probably compete with each other, affecting the NO concentration and therefore could have an impact on the immune suppressive functions in HSCs (Bhatt et al., 2014; Chen et al., 2006). Furthermore, it has been shown that reactive oxygen species (ROS) cause ROS-induced activation and proliferation of HSCs in the early phase of liver injury leading to hepatic fibrosis in vivo. Balanced NO radicals can react with ROS species and therefore prevent HSC proliferation and activation, by scavenging superoxide anions (Svegliati-Baroni et al., 2001). The importance to understand the arginine metabolism of HSC phenotypes is therefore fundamental in order to find new possibilities to manipulate immune responses in infection, autoimmune diseases, chronic inflammatory conditions, and cancer (Munder, 2009; Raber et al., 2012). Further studies are needed to provide a better insight in the role of interaction between E-Ras and ARG1 in liver, especially in HSCs, as they are responsible for liver regeneration and homeostasis of the liver stem cell niche.

## 4.3. Co-culture, vitamin A and insulin are required for the maintenance of HSC quiescence

Quiescent HSCs are characterized by the accumulation of vitamin A droplets (lipid droplets, LDs), the expression of quiescent marker such as GFAP and a stellate shaped morphology. Upon liver injury or inflammation transdifferentiation of HSCs from the quiescent phenotype to activated, myofibroblast-like phenotype is coincident with the disappearance of LDs, decrease in GFAP expression level, and increase of expression of α-SMA and collagen type I (Kordes et al., 2013; Nakhaei-Rad et al., 2016; Sawitza et al., 2009). In addition, forced expression of PPAR-γ and C/EBP-α in activated HSCs has been demonstrated to result in the reappearance of morphologic features of quiescent HSCs and inhibition of functional parameters for HSC activation such as increased DNA synthesis and expression of α- SMA,

collagen type I and TGF-β (Hazra et al., 2004; Huang et al., 2004; She et al., 2005). Despite these findings suggesting that the accumulation of LDs and the expression of GFAP, PPAR-γ and C/EBP-α are required for maintenance of the quiescent phenotype of HSCs, factors that induce these events have not been determined.

***Laminin-521 is not the promising gatekeeper for quiescence*** - The aim of the present study was to find culture conditions which could sustain HSC quiescence with the continuous expression of E-Ras, as E-Ras expression seems to play a pivotal role in maintenance of HSC quiescence (Nakhaei-Rad et al., 2016). First, HSC signaling was analyzed by coating laminin-521, an extracellular matrix protein, to cell culture dishes and was compared to regular, non-coated dishes. Laminin-521 is reported to enable self-renewal of embryonic stem cells (Rodin et al., 2014) and maintain differentiation potential of mouse and human satellite cell-derived myoblasts (Penton et al., 2016). HSCs are considered as liver-resident mesenchymal cells and share some factors with other stem cells, such as the expression of nestin, CD29, PDGFRβ, and CD133 (Kordes et al., 2013; Kordes et al., 2007). Usage of laminin-521-based culture condition could help to obtain a more homogenous cell distribution and better attachment to the culture dishes as it may support the mimicry of the basement of membrane-like liver structures existing in the space of Disse (Friedman et al., 1989; Kordes & Häussinger, 2013; Rohn et al., 2018). However, in contrast to the recent publication about laminin-521-based HSC culture, it was not possible to detect maintenance of HSC quiescence by using laminin-521 coated dishes (Rohn et al., 2018). Expression of α-SMA, a marker for activation, was detected upon day 4 of culture in confocal imaging, quantitative real-time PCR and immunoblotting. Cells displayed a myofibroblast-like morphology under the microscope. Thus, laminin-521 based culture condition was not further analyzed.

***Co-culture of HSCs and HCs*** - Next, an improved co-culture system was developed in which rat primary HSCs were cultivated in the presence of rat HCs. Both parenchymal and nonparenchymal cells are primary cells from the same species, providing reasonable assurance that the information obtained from this co-culture model is more accurate and applicable to the native tissue/organ development. It was reported, that co-culture of hepatocytes with HSCs in the transwell, where the hepatocyte is in intricate contact with spiny extensions of the hepatic stellate cell, its nearest cell neighbor, keep the hepatocyte morphologically and functionally differentiated (Higashiyama et al., 2004; Krause et al., 2009). In this study, HSCs and HCs were cultured vice versa: freshly isolated HSCs were seeded on regular polystyrene culture dishes and one day later HCs were seeded above in transwell systems. Compared to laminin-521-based culture and regular mono-culture, HSCs in co-culture displayed a phenotype similar to quiescent HSCs. Thus, co-culture demonstrated for the first time that primary isolated quiescent HSCs maintain HSC function and structure through cell contact and soluble factors of HCs. One explanation for this effect may be the presentation of cadherins, providing for homoadhesive

cell to cell contacts (Kmiec, 2001). However, results from this co-culture conditions were not completely satisfying, as the expression of GFAP in confocal imaging was not detected upon day 4 and expression of α-SMA displayed activation of HSCs even though the morphology differed compared to mono-culture.

***Co-culture with the addition of liver relevant factors*** – Co-culture of HSCs with HCs already displayed a good basic for further investigations how to maintain HSC quiescence. Insulin has been reported to be a profibrotic growth factor and to trigger activation of HSCs (Lin et al., 2009; Svegliati-Baroni et al., 1999; F. Zhang et al., 2014). Upon liver injury, the concentration of insulin is increased while the concentration of vitamin A is decreased (Charlton et al., 2006; Chaves et al., 2015; Nkontchou et al., 2010). However, the expression of quiescent markers was not sustained and the expression of activation markers was not suppressed by the treatment with vitamin A alone or insulin alone in the recent publication (Yoneda et al., 2016). Hepatocytes as well as hepatoma cells preserve/regain functionality and structure when cultured with vitamin A (Alisi et al., 2003; Falasca et al., 1999). The commercial culture medium used here contains 0.3 µM vitamin A, therefore medium was supplemented with a total concentration of 10 µM. The antiproliferative and differentiative action of vitamin A has been well investigated (Fields et al., 2007); more recently unsaturated fatty acids have been recognized as important signals in diverse processes such as differentiation, development and proliferation (Edwards & O'Flaherty, 2008; Tontonoz & Spiegelman, 2008). It was reported, that combined treatment of vitamin A with insulin maintained HSC quiescence and inhibited the transdifferentiation to activated HSCs, suggesting that the presence of both liver-relevant factors, vitamin A and insulin, is important for the maintenance of HSC quiescence (Yoneda et al., 2016). As displayed in the confocal imaging, co-culture with vitamin a and insulin closely resemble primary HSCs at the transcriptional, cellular, and functional levels and possess a gene expression profile intermediate between that of quiescent and activated HSCs. The morphology of HSCs remains stellate shaped throughout eight days of culture (Wake, 2006). Furthermore, the accumulation of lipid droplets and expression of GFAP and inhibition of the transdifferentiation to activated HSCs were sustained by combined treatment of vitamin A with insulin, suggesting that the quiescence of HSCs is regulated by both the vitamin A/JAK2/STAT5 signaling pathway and insulin signaling pathway.

In conclusion, the present study demonstrated that treatment of co-cultured HSCs with vitamin A maintained the quiescence of HSCs in combination with insulin. For future analysis, which is needed to prove this initial observations, one could think about to omit FBS in culture medium, as TGFβ is considered as a trigger for transdifferentiation of quiescent HSCs to activated HSCs. Additionally, previous coating of cell culture dishes with laminin-521 in combination with co-culture and the addition

of vitamin A and insulin could be used to obtain a more homogenous cell distribution and a better attachment to the culture dishes and maintain HSC quiescence.

## 4.4. Final remarks and outlook

Collectively, this doctoral thesis shed light on the RAS- and RHO dependent intracellular signaling pathways that may drive the fate decisions of HSCs, maintain the quiescence of HSCs and induce HSC activation, proliferation, contraction and migration (Fig. 16). Herein, the central focus was the RAS family member E-Ras, as its expression is thought to play a crucial role in the fate of HSCs.

According to the past obtained data, the MST/YAP, PI3K/AKT, and mTORC2/AKT pathways were suggested to be active in qHSCs, whereas the classical RAS/RAF/MEK/ERK pathway was active in aHSCs (Nakhaei-Rad et al., 2016) (Fig 16). In this doctoral study E-Ras was identified to interact and bind to SIN1, a complex member of mTORC2. Further data also revealed RIT1 and H-Ras as binding and interaction partner of SIN1, but compared to E-Ras, these two proteins did not seem to activate the mTORC2 pathway in cell-based conditions. Initial experiments in HSCs showed colocalization of E-Ras and SIN1, along with upregulated E-Ras, SIN1, $pSIN1^{T86}$, and $pAKT^{S473}$ expression in freshly isolated HSCs, counting for a possible relevance of the detected E-Ras-SIN1 interaction. Future *in vivo* analysis could be used to prove and further analyze the E-Ras-SIN1 interaction and subsequent mTORC2 activation in HSCs to gain knowledge about the importance and function of interaction for liver regeneration and HSC survival under physiological conditions. Additionally to the detected E-Ras/SIN1/mTORC2/AKT axis that my ensure survival in HSCs, ARG1, the final enzyme in the urea cycle, was found to interact and bind to E-Ras FL and E-Ras Nex. Addition of E-Ras increased ARG1 enzyme activity. This interaction may be responsible for the correct balance of produced urea, ornithine, and NO, as ARG1 and iNOS compete with each other and enable or prevent growth, proliferation and activation of HSCs. Further studies could analyze whether an overexpression of E-Ras could help to maintain HSC quiescence by regulating NO, ornithine and urea levels. Finally, this doctoral thesis analyzed whether different cell culture conditions can maintain the HSC quiescence. So far, co-culture of HSCs with HCs and the addition of vitamin A and insulin obtained the best results. HSCs displayed a stellate shaped morphology after eight days of culture, detectable expression of GFAP, no expression of α-SMA, and unfortunately no expression of E-Ras as well. One could argue now, that these cells display a phenotype in-between quiescent and activated and therefore E-Ras expression is not detected. Or one could say, as E-Ras is proposed to maintain quiescence, but is not detected here, HSCs are not completely quiescent. However, further studied are needed to analyze the supplemented co-culture on protein and mRNA level and prove what could initially be demonstrated here.

Even though this doctoral thesis obtained a few results of the E-Ras interactions (Fig. 16), the complete E-Ras signaling network, especially in HSCs, still remains elusive and future studies are needed. In particular, *in vivo* experiments to understand upstream regulators, functions and interactions, and the downstream network of E-Ras.

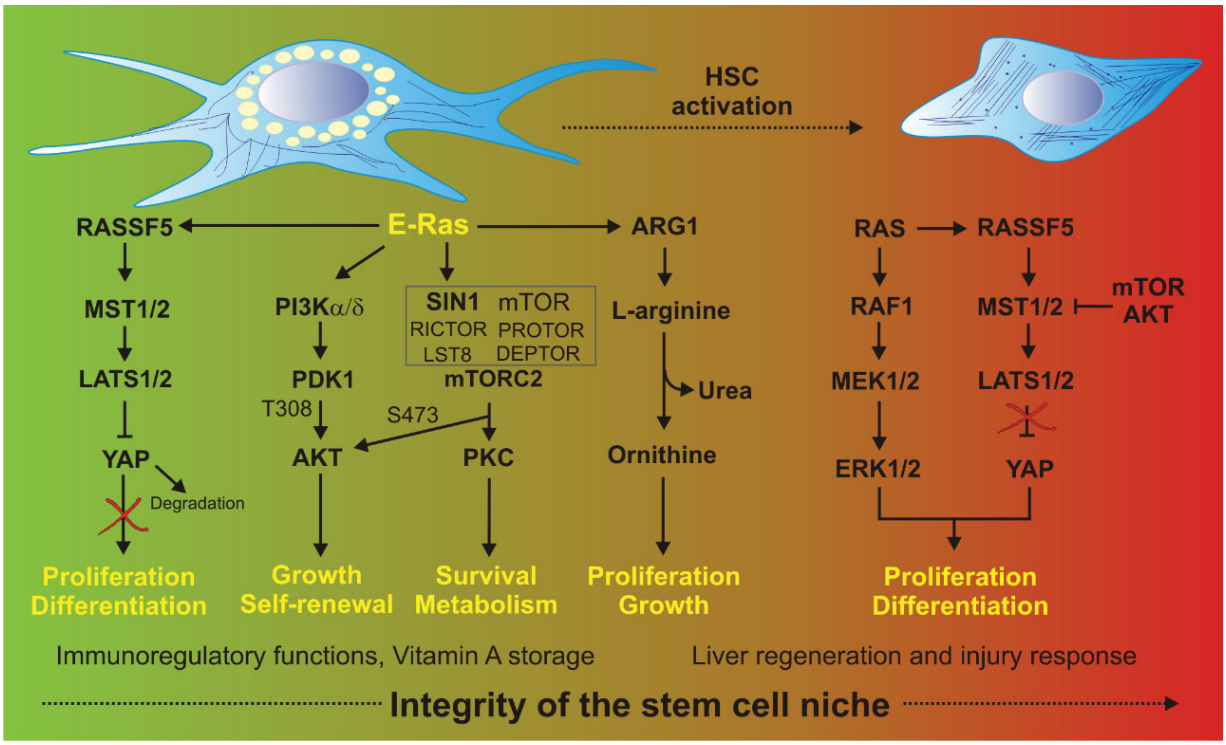


***Figure 16: Schematic view of the proposed signaling network model in HSCs.*** Reciprocal RAS-dependent signaling pathways in qHSCs and aHSCs (modified from (Nakhaei-Rad et al., 2016)).

# 5. Summary

Hepatic stellate cells (HSCs) are non-parenchymal liver cells located in the space of Disse. They play a central role in metabolism, storage of vitamin A and are involved in liver development, immunoregulation, homeostasis, and regeneration. In a healthy liver, HSCs are in a quiescent, non-proliferating state. After liver injury, HSCs develop into proliferating, activated, myofibroblast-like cells and gain the ability to migrate, contract, and differentiate into other liver cell types and therefore, contribute to liver regeneration. However, during sustained liver injury, HSCs promote liver fibrosis *via* excessive extracellular matrix production. Consequently, additional investigations on the key signaling network are necessary to further understand how HSCs maintain the quiescence and orchestrate their plasticity toward liver regeneration or fibrosis.

Members of the RAS and RHO families are central in a network controlling intracellular signaling pathways, which adopt the cellular responses upon integration of external stimuli from the neighboring cells and the microenvironment. The functions and activity of RAS- and RHO-dependent signaling pathways in the fate of HSCs are poorly understood. This doctoral thesis provides new insights into the signaling interaction network of E-Ras, as well as an investigation on how to maintain HSC quiescence in cell culture after cell isolation.

Comprehensive biochemical studies identified E-Ras interaction with SIN1, a complex member of mTORC2, and subsequent pathway activation of the mTORC2/AKT axis in cell-based experiments. Cytoplasmic colocalization of E-Ras and SIN1, along with high phosphorylation levels of p-AKT$^{S473}$ in quiescent HSCs, give evidence, that E-Ras may activate the mTORC2 pathway in HSCs. Furthermore, cytosolic Arginase-1 (ARG1), the final enzyme in the urea cycle, was identified as a binding protein for human and rat E-Ras. ARG1 shows the highest activity in quiescent HSCs where it colocalizes with E-Ras at the plasma and endomembranes. E-Ras interaction with ARG1 may balance the equilibrium between the formation of ornithine, as a precursor for growth, and nitric oxide (NO), a vasodilator in vascular smooth muscle cells of the liver, and thus affect the hepatoarterial blood flow. Finally, co-culture of freshly isolated HSCs with rat hepatocytes (HCs) in a transwell system with the regular addition of vitamin A and insulin was detected to maintain HSC quiescence. HSCs displayed a stellate shaped morphology after eight days of supplemented co-culture, detectable expression of the quiescence marker GFAP, and no expression of the activation marker α-SMA.

# 6. Zusammenfassung

Hepatische Sternzellen (HSCs) sind nicht-parenchymale, im Dissé'schen Raum der Leber ansässige Zellen. Sie sind für den Metabolismus und die Speicherung von Vitamin A von zentraler Bedeutung und sind wesentlich an der Entwicklung, Immunregulation, Homöostase und Regeneration der Leber beteiligt. In gesundem Lebergewebe befinden sich die HSCs in einem ruhenden, nicht-proliferierenden Zustand (qHSCs). Nach Leberschädigung aktivieren die HSCs (aHSCs) und erlangen die Fähigkeit zu proliferieren, migrieren, kontrahieren, sowie in andere hepatische Zelltypen zu differenzieren, womit sie wesentlich an der Leberregeneration beteiligt sind. Bei einer anhaltenden Leberschädigung begünstigen HSCs jedoch durch eine übermäßige Produktion an extrazellulärer Matrix die Entstehung einer Fibrose. Folglich sind weitergehende Untersuchungen der zugrundeliegenden (patho)-biochemischen Signalkaskaden notwendig, welche für die Aufrechterhaltung ruhender HSCs und deren Aktivierung im Rahmen regenerativer und fibrotischer Prozesse in der Leber ausschlaggebend sind.

Die Mitglieder der RAS- und RHO-Proteinfamilien spielen eine zentrale Rolle für die Kontrolle intrazellulärer Signalwege. Sie vermitteln intrazelluläre Reaktionen entsprechend äußerer Reize benachbarter Zellen und der Mikroumgebung. Jedoch sind die Funktionen der RAS- und RHO-abhängigen Signalwege in Bezug auf das Schicksal der HSCs kaum verstanden. Diese Doktorarbeit gibt neue Einblicke in das Signal- und Interaktionsnetzwerk von E-Ras und zeigt und untersucht Zellkulturbedingungen, welche zur Aufrecht-erhaltung der HSC Quieszenz führen. Umfassende biochemische Untersuchungen zeigten eine Interaktion zwischen E-Ras und SIN1, einem Komplexpartner von mTORC2, sowie eine daraus resultierende Aktivierung des mTORC2/AKT Signalweges in zell-basierten Experimenten. Eine cytoplasmatische Kolokalisation von E-Ras und SIN1 und eine hohe Phosphorylierung von p-AKT$^{S473}$ in qHSCs zeugen von einer E-Ras-vermittelten Aktivierung des mTORC2-Weges in HSCs. Des Weiteren wurde die cytosolische Arginase-1 (ARG1), das finale Enzym im Harnstoffzyklus, als Bindungs-partner von Humanem und Ratten E-Ras identifiziert. In ruhenden HSCs wurde eine hohe ARG1 Enzymaktivität gezeigt, sowie eine Kolokalisation beider Proteine an der Plasma- und Endomembran. Die Interaktion von E-Ras und ARG1 könnte für ein ausgewogenes Gleichgewicht zwischen gebildetem Ornithin, als Vorstufe für Wachstum, und Stickoxid (NO), für die Gefäßerweiterung in vaskulären glatten Muskelzellen der Leber, dienen und somit den hepatoarteriellen Blutfluss beeinflussen. Zu guter Letzt konnte gezeigt werden, dass die Ko-kultur von HSCs mit Hepatozyten in einem Transwell System mit regelmäßiger Zugabe von Vitamin A und Insulin eine Aufrechterhaltung der Quieszenz bedingt. Hierbei zeigten HSCs nach insgesamt acht Ko-Kulturtagen eine sternzell-förmige Morphologie, sowie vermehrte Expression von GFAP, aber nicht von α-SMA.

# 7. References


Abdel-Misih, S. R., & Bloomston, M. (2010). Liver anatomy. *Surg Clin North Am, 90*(4), 643-653. doi: 10.1016/j.suc.2010.04.017

Abu-Absi, S. F., Hansen, L. K., & Hu, W. S. (2004). Three-dimensional co-culture of hepatocytes and stellate cells. *Cytotechnology, 45*(3), 125-140. doi: 10.1007/s10616-004-7996-6

Accili, D., & Arden, K. C. (2004). FoxOs at the crossroads of cellular metabolism, differentiation, and transformation. *Cell, 117*(4), 421-426.

Ahearn, I. M., Haigis, K., Bar-Sagi, D., & Philips, M. R. (2012). Regulating the regulator: post-translational modification of RAS. *Nat Rev Mol Cell Biol, 13*(1), 39-51. doi: 10.1038/nrm3255

Alisi, A., Leoni, S., Piacentani, A., & Conti Devirgiliis, L. (2003). Retinoic acid modulates the cell-cycle in fetal rat hepatocytes and HepG2 cells by regulating cyclin-cdk activities. *Liver Int, 23*(3), 179-186.

Amin, E., Dubey, B. N., Zhang, S. C., Gremer, L., Dvorsky, R., Moll, J. M., . . . Ahmadian, M. R. (2013). Rho-kinase: regulation, (dys)function, and inhibition. *Biol Chem, 394*(11), 1399-1410. doi: 10.1515/hsz-2013-0181

Aoyama. (2010). Resistance to chemotherapeutic agents and promotion of transforming activity mediated by embryonic stem cell-expressed Ras (ERas) signal in neuroblastoma cells. *International Journal of Oncology, 37*(4). doi: 10.3892/ijo_00000752

Aspenstrom, P. (2018). Activated Rho GTPases in Cancer-The Beginning of a New Paradigm. *Int J Mol Sci, 19*(12). doi: 10.3390/ijms19123949

Aspenstrom, P., Ruusala, A., & Pacholsky, D. (2007). Taking Rho GTPases to the next level: the cellular functions of atypical Rho GTPases. *Exp Cell Res, 313*(17), 3673-3679. doi: 10.1016/j.yexcr.2007.07.022

Banerjee, B., Koner, D., Lal, P., & Saha, N. (2017). Unique mitochondrial localization of arginase 1 and 2 in hepatocytes of air-breathing walking catfish, Clarias batrachus and their differential expression patterns under hyper-ammonia stress. *Gene, 622*, 13-22. doi: 10.1016/j.gene.2017.04.025

Bansal, M. B. (2016). Hepatic stellate cells: fibrogenic, regenerative or both? Heterogeneity and context are key. *Hepatol Int, 10*(6), 902-908. doi: 10.1007/s12072-016-9758-x

Baummann, U., Miller, A. J. W., & Brown, R. M. (2008). Structure Function and Repair of the Liver. In D. Kelly (Ed.), *Diseases of the Liver and Biliary System in Children*: Blackwell.

Berg, T., Rountree, C. B., Lee, L., Estrada, J., Sala, F. G., Choe, A., . . . Wang, K. S. (2007). Fibroblast growth factor 10 is critical for liver growth during embryogenesis and controls hepatoblast survival via beta-catenin activation. *Hepatology, 46*(4), 1187-1197. doi: 10.1002/hep.21814

Bhatt, S., Qin, J., Bennett, C., Qian, S., Fung, J. J., Hamilton, T. A., & Lu, L. (2014). All-trans retinoic acid induces arginase-1 and inducible nitric oxide synthase-producing dendritic cells with T cell inhibitory function. *J Immunol, 192*(11), 5098-5108. doi: 10.4049/jimmunol.1303073

Blaner, W. S., O'Byrne, S. M., Wongsiriroj, N., Kluwe, J., D'Ambrosio, D. M., Jiang, H., . . . Libien, J. (2009). Hepatic stellate cell lipid droplets: A specialized lipid droplet for retinoid storage. *Biochimica et Biophysica Acta (BBA) - Molecular and Cell Biology of Lipids, 1791*(6), 467-473. doi: 10.1016/j.bbalip.2008.11.001

Bos, J. L. (1989). ras oncogenes in human cancer: a review. *Cancer Res, 49*(17), 4682-4689.

Bourne, H. R., Sanders, D. A., & McCormick, F. (1990). The GTPase superfamily: a conserved switch for diverse cell functions. *Nature, 348*(6297), 125-132. doi: 10.1038/348125a0

Bourne, H. R., Sanders, D. A., & McCormick, F. (1991). The GTPase superfamily: conserved structure and molecular mechanism. *Nature, 349*(6305), 117-127. doi: 10.1038/349117a0

Bratt, J. M., Zeki, A. A., Last, J. A., & Kenyon, N. J. (2011). Competitive metabolism of L-arginine: arginase as a therapeutic target in asthma. *J Biomed Res, 25*(5), 299-308. doi: 10.1016/S1674-8301(11)60041-9

Brown, E. J., Albers, M. W., Shin, T. B., Ichikawa, K., Keith, C. T., Lane, W. S., & Schreiber, S. L. (1994). A mammalian protein targeted by G1-arresting rapamycin-receptor complex. *Nature, 369*(6483), 756-758. doi: 10.1038/369756a0

Burt, A. D., & Day, C. P. (2003). Pathophysiology of the liver. In R. MacSween (Ed.), *Pathology of the Liver* (pp. 67–105). New York: Churchill Livingstone.

Buss, J. E., & Sefton, B. M. (1986). Direct identification of palmitic acid as the lipid attached to p21ras. *Mol Cell Biol, 6*(1), 116-122.

Cai, W., & Andres, D. A. (2014). mTORC2 is required for rit-mediated oxidative stress resistance. *PLoS One, 9*(12), e115602. doi: 10.1371/journal.pone.0115602

Caldwell, R. B., Toque, H. A., Narayanan, S. P., & Caldwell, R. W. (2015). Arginase: an old enzyme with new tricks. *Trends Pharmacol Sci, 36*(6), 395-405. doi: 10.1016/j.tips.2015.03.006

Cameron, A. J., Linch, M. D., Saurin, A. T., Escribano, C., & Parker, P. J. (2011). mTORC2 targets AGC kinases through Sin1-dependent recruitment. *Biochem J, 439*(2), 287-297. doi: 10.1042/BJ20110678

Carloni, V., Defranco, R. M., Caligiuri, A., Gentilini, A., Sciammetta, S. C., Baldi, E., . . . Pinzani, M. (2002). Cell adhesion regulates platelet-derived growth factor-induced MAP kinase and PI-3 kinase activation in stellate cells. *Hepatology, 36*(3), 582-591. doi: 10.1053/jhep.2002.35277

Castellano, E., & Santos, E. (2011). Functional Specificity of Ras Isoforms: So Similar but So Different. *Genes & Cancer, 2*(3), 216-231. doi: 10.1177/1947601911408081

Castilho-Fernandes, A., de Almeida, D. C., Fontes, A. M., Melo, F. U., Picanco-Castro, V., Freitas, M. C., . . . Covas, D. T. (2011). Human hepatic stellate cell line (LX-2) exhibits characteristics of bone marrow-derived mesenchymal stem cells. *Exp Mol Pathol, 91*(3), 664-672. doi: 10.1016/j.yexmp.2011.09.002

Cederbaum, S. D., Yu, H., Grody, W. W., Kern, R. M., Yoo, P., & Iyer, R. K. (2004). Arginases I and II: do their functions overlap? *Mol Genet Metab, 81 Suppl 1*, S38-44. doi: 10.1016/j.ymgme.2003.10.012

Chardin, P., Boquet, P., Madaule, P., Popoff, M. R., Rubin, E. J., & Gill, D. M. (1989). The mammalian G protein rhoC is ADP-ribosylated by Clostridium botulinum exoenzyme C3 and affects actin microfilaments in Vero cells. *EMBO J, 8*(4), 1087-1092.

Charest, P. G., Shen, Z., Lakoduk, A., Sasaki, A. T., Briggs, S. P., & Firtel, R. A. (2010). A Ras Signaling Complex Controls the RasC-TORC2 Pathway and Directed Cell Migration. *Developmental Cell, 18*(5), 737-749. doi: 10.1016/j.devcel.2010.03.017

Charlton, M. R., Pockros, P. J., & Harrison, S. A. (2006). Impact of obesity on treatment of chronic hepatitis C. *Hepatology, 43*(6), 1177-1186. doi: 10.1002/hep.21239

Chaves, G. V., Peres, W. A., Goncalves, J. C., & Ramalho, A. (2015). Vitamin A and retinol-binding protein deficiency among chronic liver disease patients. *Nutrition, 31*(5), 664-668. doi: 10.1016/j.nut.2014.10.016

Chen, C. H., Kuo, L. M., Chang, Y., Wu, W., Goldbach, C., Ross, M. A., . . . Qian, S. (2006). In vivo immune modulatory activity of hepatic stellate cells in mice. *Hepatology, 44*(5), 1171-1181. doi: 10.1002/hep.21379

Coleman, M. L., Marshall, C. J., & Olson, M. F. (2004). RAS and RHO GTPases in G1-phase cell-cycle regulation. *Nature Reviews Molecular Cell Biology, 5*(5), 355-366. doi: 10.1038/nrm1365

Colicelli, J. (2004). Human RAS superfamily proteins and related GTPases. *Sci STKE, 2004*(250), RE13. doi: 10.1126/stke.2502004re13

Corraliza, I. M., Campo, M. L., Soler, G., & Modolell, M. (1994). Determination of arginase activity in macrophages: a micromethod. *J Immunol Methods, 174*(1-2), 231-235.

Cota, D. (2014). mTORC2, the "other" mTOR, is a new player in energy balance regulation. *Mol Metab, 3*(4), 349-350. doi: 10.1016/j.molmet.2014.04.002

De Minicis, S., Seki, E., Uchinami, H., Kluwe, J., Zhang, Y., Brenner, D. A., & Schwabe, R. F. (2007). Gene Expression Profiles During Hepatic Stellate Cell Activation in Culture and In Vivo. *Gastroenterology, 132*(5), 1937-1946. doi: 10.1053/j.gastro.2007.02.033

de Souza, I. C. C., Meira Martins, L. A., de Vasconcelos, M., de Oliveira, C. M., Barbé-Tuana, F., Andrade, C. B., . . . Guma, F. C. R. (2015). Resveratrol Regulates the Quiescence-Like Induction of Activated Stellate Cells by Modulating the PPARγ/SIRT1 Ratio. *Journal of Cellular Biochemistry*, n/a-n/a. doi: 10.1002/jcb.25181

Dechene, A., Sowa, J. P., Gieseler, R. K., Jochum, C., Bechmann, L. P., El Fouly, A., . . . Canbay, A. (2010). Acute liver failure is associated with elevated liver stiffness and hepatic stellate cell activation. *Hepatology, 52*(3), 1008-1016. doi: 10.1002/hep.23754

Deleve, L. D., Wang, X., & Guo, Y. (2008). Sinusoidal endothelial cells prevent rat stellate cell activation and promote reversion to quiescence. *Hepatology, 48*(3), 920-930. doi: 10.1002/hep.22351

Delgado, J. P., Vanneaux, V., Branger, J., Touboul, T., Sentilhes, L., Mainot, S., . . . Weber, A. (2009). The role of HGF on invasive properties and repopulation potential of human fetal hepatic progenitor cells. *Exp Cell Res, 315*(19), 3396-3405. doi: 10.1016/j.yexcr.2009.07.007

Di Costanzo, L., Sabio, G., Mora, A., Rodriguez, P. C., Ochoa, A. C., Centeno, F., & Christianson, D. W. (2005). Crystal structure of human arginase I at 1.29-A resolution and exploration of inhibition in the immune response. *Proc Natl Acad Sci U S A, 102*(37), 13058-13063. doi: 10.1073/pnas.0504027102

Dixon, L. J., Barnes, M., Tang, H., Pritchard, M. T., & Nagy, L. E. (2013). Kupffer cells in the liver. *Compr Physiol, 3*(2), 785-797. doi: 10.1002/cphy.c120026

Dong, W., Simeonova, P. P., Gallucci, R., Matheson, J., Fannin, R., Montuschi, P., . . . Luster, M. I. (1998). Cytokine expression in hepatocytes: role of oxidant stress. *J Interferon Cytokine Res, 18*(8), 629-638. doi: 10.1089/jir.1998.18.629

Dounce, A. L., & Beyer, G. T. (1948). The arginase activity of isolated cell nuclei. *J Biol Chem, 174*(3), 859-872.

Duester, G. (2008). Retinoic Acid Synthesis and Signaling during Early Organogenesis. *Cell, 134*(6), 921-931. doi: 10.1016/j.cell.2008.09.002

Durante, W., Johnson, F. K., & Johnson, R. A. (2007). Arginase: a critical regulator of nitric oxide synthesis and vascular function. *Clin Exp Pharmacol Physiol, 34*(9), 906-911. doi: 10.1111/j.1440-1681.2007.04638.x

Edwards, I. J., & O'Flaherty, J. T. (2008). Omega-3 Fatty Acids and PPARgamma in Cancer. *PPAR Res, 2008*, 358052. doi: 10.1155/2008/358052

Eijkelenboom, A., & Burgering, B. M. (2013). FOXOs: signalling integrators for homeostasis maintenance. *Nat Rev Mol Cell Biol, 14*(2), 83-97. doi: 10.1038/nrm3507

Enzan, H., Himeno, H., Hiroi, M., Kiyoku, H., Saibara, T., & Onishi, S. (1997). Development of hepatic sinusoidal structure with special reference to the Ito cells. *Microsc Res Tech, 39*(4), 336-349. doi: 10.1002/(SICI)1097-0029(19971115)39:4<336::AID-JEMT4>3.0.CO;2-F

Falasca, L., Marcellini, P., Ara, C., Rufo, A., & Devirgiliis, L. C. (1999). Growth inhibition and induction of specific hepatic phenotype expression by retinoic acid in HEPG2 cells. *Anticancer Res, 19*(4B), 3283-3292.

Ferrell, J. E., Jr. (2000). What do scaffold proteins really do? *Sci STKE, 2000*(52), pe1. doi: 10.1126/stke.2000.52.pe1

Fields, A. L., Soprano, D. R., & Soprano, K. J. (2007). Retinoids in biological control and cancer. *J Cell Biochem, 102*(4), 886-898. doi: 10.1002/jcb.21530

Friedman, S. L. (2008). Hepatic stellate cells: protean, multifunctional, and enigmatic cells of the liver. *Physiol Rev, 88*(1), 125-172. doi: 10.1152/physrev.00013.2007

Friedman, S. L., Roll, F. J., Boyles, J., Arenson, D. M., & Bissell, D. M. (1989). Maintenance of differentiated phenotype of cultured rat hepatic lipocytes by basement membrane matrix. *J Biol Chem, 264*(18), 10756-10762.

Friedman, S. L., Wei, S., & Blaner, W. S. (1993). Retinol release by activated rat hepatic lipocytes: regulation by Kupffer cell-conditioned medium and PDGF. *Am J Physiol, 264*(5 Pt 1), G947-952. doi: 10.1152/ajpgi.1993.264.5.G947

Galicia-Moreno, M., & Gutierrez-Reyes, G. (2014). The role of oxidative stress in the development of alcoholic liver disease. *Rev Gastroenterol Mex, 79*(2), 135-144. doi: 10.1016/j.rgmx.2014.03.001

Gard, A. L., White, F. P., & Dutton, G. R. (1985). Extra-neural glial fibrillary acidic protein (GFAP) immunoreactivity in perisinusoidal stellate cells of rat liver. *J Neuroimmunol, 8*(4-6), 359-375.

Garganta, C. L., & Bond, J. S. (1986). Assay and kinetics of arginase. *Analytical Biochemistry, 154*(2), 388-394. doi: https://doi.org/10.1016/0003-2697(86)90003-5

Geffers, I., Serth, K., Chapman, G., Jaekel, R., Schuster-Gossler, K., Cordes, R., . . . Gossler, A. (2007). Divergent functions and distinct localization of the Notch ligands DLL1 and DLL3 in vivo. *J Cell Biol, 178*(3), 465-476. doi: 10.1083/jcb.200702009

Getz, G. S., & Reardon, C. A. (2006). Arginine/arginase NO NO NO. *Arterioscler Thromb Vasc Biol, 26*(2), 237-239. doi: 10.1161/01.ATV.0000202014.54609.9d

Guertin, D. A., Stevens, D. M., Saitoh, M., Kinkel, S., Crosby, K., Sheen, J. H., . . . Sabatini, D. M. (2009). mTOR complex 2 is required for the development of prostate cancer induced by Pten loss in mice. *Cancer Cell, 15*(2), 148-159. doi: 10.1016/j.ccr.2008.12.017

Gumucio, J. J. (1989). Hepatocyte heterogeneity: the coming of age from the description of a biological curiosity to a partial understanding of its physiological meaning and regulation. *Hepatology, 9*(1), 154-160.

Haga, R. B., & Ridley, A. J. (2016). Rho GTPases: Regulation and roles in cancer cell biology. *Small GTPases, 7*(4), 207-221. doi: 10.1080/21541248.2016.1232583

Harvey, J. J. (1964). An Unidentified Virus Which Causes the Rapid Production of Tumours in Mice. *Nature, 204*, 1104-1105.

Häussinger, D., Sies, H., & Gerok, W. (1985). Functional hepatocyte heterogeneity in ammonia metabolism. The intercellular glutamine cycle. *J Hepatol, 1*(1), 3-14.

Hazra, S., Xiong, S., Wang, J., Rippe, R. A., Krishna, V., Chatterjee, K., & Tsukamoto, H. (2004). Peroxisome proliferator-activated receptor gamma induces a phenotypic switch from activated to quiescent hepatic stellate cells. *J Biol Chem, 279*(12), 11392-11401. doi: 10.1074/jbc.M310284200

Hellemans, K., Verbuyst, P., Quartier, E., Schuit, F., Rombouts, K., Chandraratna, R. A., . . . Geerts, A. (2004). Differential modulation of rat hepatic stellate phenotype by natural and synthetic retinoids. *Hepatology, 39*(1), 97-108. doi: 10.1002/hep.20015

Hendriks, H. F., Blaner, W. S., Wennekers, H. M., Piantedosi, R., Brouwer, A., de Leeuw, A. M., . . . Knook, D. L. (1988). Distributions of retinoids, retinoid-binding proteins and related parameters in different types of liver cells isolated from young and old rats. *Eur J Biochem, 171*(1-2), 237-244.

Herrmann, C. (2003). RAS-effector interactions: after one decade. *Current Opinion in Structrual Biology, 13*(1), 122-129.

Higashiyama, S., Noda, M., Muraoka, S., Uyama, N., Kawada, N., Ide, T., . . . Yagi, K. (2004). Maintenance of hepatocyte functions in coculture with hepatic stellate cells. *Biochemical Engineering Journal, 20*(2-3), 113-118. doi: https://doi.org/10.1016/j.bej.2003.07.002.

Hirsch-Kolb, H., Heine, J. P., Kolb, H. J., & Greenberg, D. M. (1970). Comparative physical-chemical studies of mammalian arginases. *Comp Biochem Physiol, 37*(3), 345-359.

Huang, G. C., Zhang, J. S., & Tang, Q. Q. (2004). Involvement of C/EBP-alpha gene in in vitro activation of rat hepatic stellate cells. *Biochem Biophys Res Commun, 324*(4), 1309-1318. doi: 10.1016/j.bbrc.2004.09.196

Hung, C. M., Garcia-Haro, L., Sparks, C. A., & Guertin, D. A. (2012). mTOR-dependent cell survival mechanisms. *Cold Spring Harb Perspect Biol, 4*(12). doi: 10.1101/cshperspect.a008771

Ichise, T., Yoshida, N., & Ichise, H. (2010). H-, N- and Kras cooperatively regulate lymphatic vessel growth by modulating VEGFR3 expression in lymphatic endothelial cells in mice. *Development, 137*(6), 1003-1013. doi: 10.1242/dev.043489

Ikink, G. J., Boer, M., Bakker, E. R. M., Vendel-Zwaagstra, A., Klijn, C., Ten Hoeve, J., . . . Hilkens, J. (2018). Insertional mutagenesis in a HER2-positive breast cancer model reveals ERAS as a

driver of cancer and therapy resistance. *Oncogene, 37*(12), 1594-1609. doi: 10.1038/s41388-017-0031-0

Illenberger, D., Schwald, F., Pimmer, D., Binder, W., Maier, G., Dietrich, A., & Gierschik, P. (1998). Stimulation of phospholipase C-beta2 by the Rho GTPases Cdc42Hs and Rac1. *EMBO J, 17*(21), 6241-6249. doi: 10.1093/emboj/17.21.6241

Iredale, J. P., Thompson, A., & Henderson, N. C. (2013). Extracellular matrix degradation in liver fibrosis: Biochemistry and regulation. *Biochim Biophys Acta, 1832*(7), 876-883. doi: 10.1016/j.bbadis.2012.11.002

Ivanov, A. V., Valuev-Elliston, V. T., Tyurina, D. A., Ivanova, O. N., Kochetkov, S. N., Bartosch, B., & Isaguliants, M. G. (2017). Oxidative stress, a trigger of hepatitis C and B virus-induced liver carcinogenesis. *Oncotarget, 8*(3), 3895-3932. doi: 10.18632/oncotarget.13904

Jacinto, E., Facchinetti, V., Liu, D., Soto, N., Wei, S., Jung, S. Y., . . . Su, B. (2006). SIN1/MIP1 maintains rictor-mTOR complex integrity and regulates Akt phosphorylation and substrate specificity. *Cell, 127*(1), 125-137. doi: 10.1016/j.cell.2006.08.033

Jaffe, A. B., & Hall, A. (2005). Rho GTPases: biochemistry and biology. *Annu Rev Cell Dev Biol, 21*, 247-269. doi: 10.1146/annurev.cellbio.21.020604.150721

Janne, J., Alhonen, L., & Leinonen, P. (1991). Polyamines: from molecular biology to clinical applications. *Ann Med, 23*(3), 241-259.

Jaumot, M., Yan, J., Clyde-Smith, J., Sluimer, J., & Hancock, J. F. (2002). The linker domain of the Ha-Ras hypervariable region regulates interactions with exchange factors, Raf-1 and phosphoinositide 3-kinase. *J Biol Chem, 277*(1), 272-278. doi: 10.1074/jbc.M108423200

JeBailey, L., Rudich, A., Huang, X., Di Ciano-Oliveira, C., Kapus, A., & Klip, A. (2004). Skeletal muscle cells and adipocytes differ in their reliance on TC10 and Rac for insulin-induced actin remodeling. *Mol Endocrinol, 18*(2), 359-372. doi: 10.1210/me.2003-0294

Jenkinson, C. P., Grody, W. W., & Cederbaum, S. D. (1996). Comparative properties of arginases. *Comp Biochem Physiol B Biochem Mol Biol, 114*(1), 107-132.

Ji, J., Yu, F., Ji, Q., Li, Z., Wang, K., Zhang, J., . . . Ji, Y. (2012). Comparative proteomic analysis of rat hepatic stellate cell activation: A comprehensive view and suppressed immune response. *Hepatology, 56*(1), 332-349. doi: 10.1002/hep.25650

Jiang, M., Ding, Y., Su, Y., Hu, X., Li, J., & Zhang, Z. (2006). Arginase-flotillin interaction brings arginase to red blood cell membrane. *FEBS Lett, 580*(28-29), 6561-6564. doi: 10.1016/j.febslet.2006.11.003

Jin, Y., Liu, Y., & Nelin, L. D. (2015). Extracellular signal-regulated kinase mediates expression of arginase II but not inducible nitric-oxide synthase in lipopolysaccharide-stimulated macrophages. *J Biol Chem, 290*(4), 2099-2111. doi: 10.1074/jbc.M114.599985

Jones, P. L., Schmidhauser, C., & Bissell, M. J. (1993). Regulation of gene expression and cell function by extracellular matrix. *Crit Rev Eukaryot Gene Expr, 3*(2), 137-154.

Kaizaki, R., Yashiro, M., Shinto, O., Yasuda, K., Matsuzaki, T., Sawada, T., & Hirakawa, K. (2009). Expression of ERas oncogene in gastric carcinoma. *Anticancer Res, 29*(6), 2189-2193. doi: 29/6/2189 [pii]

Kamimura, Y., Xiong, Y., Iglesias, P. A., Hoeller, O., Bolourani, P., & Devreotes, P. N. (2008). PIP3-independent activation of TorC2 and PKB at the cell's leading edge mediates chemotaxis. *Curr Biol, 18*(14), 1034-1043. doi: 10.1016/j.cub.2008.06.068

Kanzaki, M., & Pessin, J. E. (2003). Insulin signaling: GLUT4 vesicles exit via the exocyst. *Curr Biol, 13*(14), R574-576.

Khanna, A., Lotfi, P., Chavan, A. J., Montano, N. M., Bolourani, P., Weeks, G., . . . Charest, P. G. (2016). The small GTPases Ras and Rap1 bind to and control TORC2 activity. *Sci Rep, 6*, 25823. doi: 10.1038/srep25823

Kiernan, F. (1833). The anatomy and physiology of the liver *Phil. Trans. R. Soc. Lond., 123*, 711 – 770.

Kim, M. J., & Ahituv, N. (2013). The hydrodynamic tail vein assay as a tool for the study of liver promoters and enhancers. *Methods Mol Biol, 1015*, 279-289. doi: 10.1007/978-1-62703-435-7_18

Kirsten, W. H., & Mayer, L. A. (1967). Morphologic responses to a murine erythroblastosis virus. *J Natl Cancer Inst, 39*(2), 311-335.

Kisseleva, T., Cong, M., Paik, Y., Scholten, D., Jiang, C., Benner, C., . . . Brenner, D. A. (2012). Myofibroblasts revert to an inactive phenotype during regression of liver fibrosis. *Proc Natl Acad Sci U S A, 109*(24), 9448-9453. doi: 10.1073/pnas.1201840109

Kmiec, Z. (2001). Cooperation of liver cells in health and disease. *Adv Anat Embryol Cell Biol, 161*, III-XIII, 1-151.

Kordes, C., & Häussinger, D. (2013). Hepatic stem cell niches. *Journal of Clinical Investigation, 123*(5), 1874-1880. doi: 10.1172/jci66027

Kordes, C., Sawitza, I., Götze, S., & Häussinger, D. (2013). Hepatic Stellate Cells Support Hematopoiesis and are Liver-Resident Mesenchymal Stem Cells. *Cellular Physiology and Biochemistry, 31*(2-3), 290-304. doi: 10.1159/000343368

Kordes, C., Sawitza, I., Götze, S., Herebian, D., & Häussinger, D. (2014). Hepatic stellate cells contribute to progenitor cells and liver regeneration. *Journal of Clinical Investigation, 124*(12), 5503-5515. doi: 10.1172/jci74119

Kordes, C., Sawitza, I., & Häussinger, D. (2008). Canonical Wnt signaling maintains the quiescent stage of hepatic stellate cells. *Biochemical and Biophysical Research Communications, 367*(1), 116-123. doi: 10.1016/j.bbrc.2007.12.085

Kordes, C., Sawitza, I., Müller-Marbach, A., Ale-Agha, N., Keitel, V., Klonowski-Stumpe, H., & Häussinger, D. (2007). CD133+ hepatic stellate cells are progenitor cells. *Biochemical and Biophysical Research Communications, 352*(2), 410-417. doi: 10.1016/j.bbrc.2006.11.029

Krause, P., Saghatolislam, F., Koenig, S., Unthan-Fechner, K., & Probst, I. (2009). Maintaining hepatocyte differentiation in vitro through co-culture with hepatic stellate cells. *In Vitro Cell Dev Biol Anim, 45*(5-6), 205-212. doi: 10.1007/s11626-008-9166-1

Krebs, H. A., & Henseleit, K. (1932). Untersuchungen uber die Harnstoffbildung im Tierkörper *Hoppe-Seyler´s Zeitschrift für physiologische Chemie* (Vol. 210, pp. 33).

Kubota, E., Kataoka, H., Aoyama, M., Mizoshita, T., Mori, Y., Shimura, T., . . . Joh, T. (2010). Role of ES cell-expressed Ras (ERas) in tumorigenicity of gastric cancer. *Am J Pathol, 177*(2), 955-963. doi: 10.2353/ajpath.2010.091056

Kudo, S. (1989). The morphology of release of vitamin A-containing lipid droplets by hepatocytes in rat liver. *Anat Rec, 225*(1), 11-20. doi: 10.1002/ar.1092250103

Kuo, P. C., Abe, K. Y., & Schroeder, R. A. (1997). Oxidative stress increases hepatocyte iNOS gene transcription and promoter activity. *Biochem Biophys Res Commun, 234*(2), 289-292. doi: 10.1006/bbrc.1997.6562

Lakner, A. M. (2010). Daily genetic profiling indicates JAK/STAT signaling promotes early hepatic stellate cell transdifferentiation. *World Journal of Gastroenterology, 16*(40), 5047. doi: 10.3748/wjg.v16.i40.5047

Lamers, W. H., Hilberts, A., Furt, E., Smith, J., Jonges, G. N., van Noorden, C. J., . . . Moorman, A. F. (1989). Hepatic enzymic zonation: a reevaluation of the concept of the liver acinus. *Hepatology, 10*(1), 72-76.

Lange, P. S., Langley, B., Lu, P., & Ratan, R. R. (2004). Novel roles for arginase in cell survival, regeneration, and translation in the central nervous system. *J Nutr, 134*(10 Suppl), 2812S-2817S; discussion 2818S-2819S. doi: 10.1093/jn/134.10.2812S

Lau, K. S., & Haigis, K. M. (2009). Non-redundancy within the RAS oncogene family: insights into mutational disparities in cancer. *Mol Cells, 28*(4), 315-320. doi: 10.1007/s10059-009-0143-7

Lee, K. S., Lee, S. J., Park, H. J., Chung, J. P., Han, K. H., Chon, C. Y., . . . Moon, Y. M. (2001). Oxidative stress effect on the activation of hepatic stellate cells. *Yonsei Med J, 42*(1), 1-8. doi: 10.3349/ymj.2001.42.1.1

Lee, S. (2005). TOR Complex 2 Integrates Cell Movement during Chemotaxis and Signal Relay in Dictyostelium. *Molecular Biology of the Cell, 16*(10), 4572-4583. doi: 10.1091/mbc.E05-04-0342

Leon, J., Guerrero, I., & Pellicer, A. (1987). Differential expression of the ras gene family in mice. *Mol Cell Biol, 7*(4), 1535-1540.

Lin, J., Zheng, S., Attie, A. D., Keller, M. P., Bernlohr, D. A., Blaner, W. S., . . . Chen, A. (2018). Perilipin 5 and liver fatty acid binding protein function to restore quiescence in mouse hepatic stellate cells. *J Lipid Res, 59*(3), 416-428. doi: 10.1194/jlr.M077487

Lin, J., Zheng, S., & Chen, A. (2009). Curcumin attenuates the effects of insulin on stimulating hepatic stellate cell activation by interrupting insulin signaling and attenuating oxidative stress. *Lab Invest, 89*(12), 1397-1409. doi: 10.1038/labinvest.2009.115

Liu, P., Gan, W., Inuzuka, H., Lazorchak, A. S., Gao, D., Arojo, O., . . . Wei, W. (2013). Sin1 phosphorylation impairs mTORC2 complex integrity and inhibits downstream Akt signalling to suppress tumorigenesis. *Nature Cell Biology, 15*(11), 1340-1350. doi: 10.1038/ncb2860

Liu, P., Guo, J., Gan, W., & Wei, W. (2014). Dual phosphorylation of Sin1 at T86 and T398 negatively regulates mTORC2 complex integrity and activity. *Protein Cell, 5*(3), 171-177. doi: 10.1007/s13238-014-0021-8

Loewith, R., Jacinto, E., Wullschleger, S., Lorberg, A., Crespo, J. L., Bonenfant, D., . . . Hall, M. N. (2002). Two TOR complexes, only one of which is rapamycin sensitive, have distinct roles in cell growth control. *Mol Cell, 10*(3), 457-468.

Lorenz, L., Axnick, J., Buschmann, T., Henning, C., Urner, S., Fang, S., . . . Lammert, E. (2018). Mechanosensing by β1 integrin induces angiocrine signals for liver growth and survival. *Nature, 562*(7725), 128-132. doi: 10.1038/s41586-018-0522-3

Mannaerts, I., Leite, S. B., Verhulst, S., Claerhout, S., Eysackers, N., Thoen, L. F. R., . . . van Grunsven, L. A. (2015). The Hippo pathway effector YAP controls mouse hepatic stellate cell activation. *Journal of Hepatology, 63*(3), 679-688. doi: 10.1016/j.jhep.2015.04.011

Marshall, C. J. (1996). Ras effectors. *Curr Opin Cell Biol, 8*(2), 197-204.

Martinez-Hernandez, A., & Amenta, P. S. (1993). The hepatic extracellular matrix. I. Components and distribution in normal liver. *Virchows Arch A Pathol Anat Histopathol, 423*(1), 1-11.

Matsumoto, K., Miki, R., Nakayama, M., Tatsumi, N., & Yokouchi, Y. (2008). Wnt9a secreted from the walls of hepatic sinusoids is essential for morphogenesis, proliferation, and glycogen accumulation of chick hepatic epithelium. *Dev Biol, 319*(2), 234-247. doi: 10.1016/j.ydbio.2008.04.021

Mattila, J. T., Ojo, O. O., Kepka-Lenhart, D., Marino, S., Kim, J. H., Eum, S. Y., . . . Flynn, J. L. (2013). Microenvironments in tuberculous granulomas are delineated by distinct populations of macrophage subsets and expression of nitric oxide synthase and arginase isoforms. *J Immunol, 191*(2), 773-784. doi: 10.4049/jimmunol.1300113

Mezl, V. A., & Knox, W. E. (1977). Metabolism of arginine in lactating rat mammary gland. *Biochem J, 166*(1), 105-113.

Mi, H., Huang, X., Muruganujan, A., Tang, H., Mills, C., Kang, D., & Thomas, P. D. (2017). PANTHER version 11: expanded annotation data from Gene Ontology and Reactome pathways, and data analysis tool enhancements. *Nucleic Acids Res, 45*(D1), D183-D189. doi: 10.1093/nar/gkw1138

Michalopoulos, G. K. (2010). Liver Regeneration after Partial Hepatectomy: Critical Analysis of Mechanistic Dilemmas. *Am J Pathol, 176*(1), 2-13. doi: 10.2353/ajpath.2010.090675

Michalopoulos, G. K., & DeFrances, M. C. (1997). Liver regeneration. *Science, 276*(5309), 60-66.

Mitin, N., Roberts, P. J., Chenette, E. J., & Der, C. J. (2012). Posttranslational lipid modification of Rho family small GTPases. *Methods Mol Biol, 827*, 87-95. doi: 10.1007/978-1-61779-442-1_6

Munder, M. (2009). Arginase: an emerging key player in the mammalian immune system. *Br J Pharmacol, 158*(3), 638-651. doi: 10.1111/j.1476-5381.2009.00291.x

Muszynska, G., & Ber, E. (1978). Circular dichroic properties of rat liver arginase. *Int J Biochem, 9*(10), 757-759.

Nagai, H., Terada, K., Watanabe, G., Ueno, Y., Aiba, N., Shibuya, T., . . . Sugiyama, T. (2002). Differentiation of liver epithelial (stem-like) cells into hepatocytes induced by coculture with hepatic stellate cells. *Biochem Biophys Res Commun, 293*(5), 1420-1425. doi: 10.1016/s0006-291x(02)00406-0

Nakhaei-Rad, S., Haghighi, F., Nouri, P., Adariani, S. R., Lissy, J., Jasemi, N. S. K., . . . Ahmadian, M. R. (2018). Structural fingerprints, interactions, and signaling networks of RAS family proteins beyond RAS isoforms. *Critical Reviews in Biochemistry and Molecular Biology, 53*(2), 130-156. doi: 10.1080/10409238.2018.1431605

Nakhaei-Rad, S., Nakhaeizadeh, H., Gotze, S., Kordes, C., Sawitza, I., Hoffmann, M. J., . . . Ahmadian, M. R. (2016). The role of embryonic stem cell-expressed RAS (ERAS) in the maintenance of quiescent hepatic stellate cells. *J Biol Chem, 291*(16), 8399-8413. doi: 10.1074/jbc.M115.700088

Nakhaei-Rad, S., Nakhaeizadeh, H., Kordes, C., Cirstea, I. C., Schmick, M., Dvorsky, R., . . . Ahmadian, M. R. (2015). The Function of Embryonic Stem Cell-expressed RAS (E-RAS), a Unique RAS Family Member, Correlates with Its Additional Motifs and Its Structural Properties. *Journal of Biological Chemistry, 290*(25), 15892-15903. doi: 10.1074/jbc.M115.640607

Nanji, A. A., Greenberg, S. S., Tahan, S. R., Fogt, F., Loscalzo, J., Sadrzadeh, S. M., . . . Stamler, J. S. (1995). Nitric oxide production in experimental alcoholic liver disease in the rat: role in protection from injury. *Gastroenterology, 109*(3), 899-907.

Niki, T., Pekny, M., Hellemans, K., Bleser, P. D., Berg, K. V., Vaeyens, F., . . . Geerts, A. (1999). Class VI intermediate filament protein nestin is induced during activation of rat hepatic stellate cells. *Hepatology, 29*(2), 520-527. doi: 10.1002/hep.510290232

Nkontchou, G., Bastard, J. P., Ziol, M., Aout, M., Cosson, E., Ganne-Carrie, N., . . . Beaugrand, M. (2010). Insulin resistance, serum leptin, and adiponectin levels and outcomes of viral hepatitis C cirrhosis. *J Hepatol, 53*(5), 827-833. doi: 10.1016/j.jhep.2010.04.035

Oh, W. J., & Jacinto, E. (2011). mTOR complex 2 signaling and functions. *Cell Cycle, 10*(14), 2305-2316. doi: 10.4161/cc.10.14.16586

Ohata, M., Lin, M., Satre, M., & Tsukamoto, H. (1997). Diminished retinoic acid signaling in hepatic stellate cells in cholestatic liver fibrosis. *Am J Physiol, 272*(3 Pt 1), G589-596. doi: 10.1152/ajpgi.1997.272.3.G589

Omerovic, J., Laude, A. J., & Prior, I. A. (2007). Ras proteins: paradigms for compartmentalised and isoform-specific signalling. *Cellular and Molecular Life Sciences, 64*(19-20), 2575-2589. doi: 10.1007/s00018-007-7133-8

Paramo, B. (2014). *The role of Sin1 in cell survival* (Doctor of Philosophy ), University of Manchester Manchester.

Paterson, H. F., Self, A. J., Garrett, M. D., Just, I., Aktories, K., & Hall, A. (1990). Microinjection of recombinant p21rho induces rapid changes in cell morphology. *J Cell Biol, 111*(3), 1001-1007.

Pellicoro, A., Ramachandran, P., Iredale, J. P., & Fallowfield, J. A. (2014). Liver fibrosis and repair: immune regulation of wound healing in a solid organ. *Nature Reviews Immunology, 14*(3), 181-194. doi: 10.1038/nri3623

Penton, C. M., Badarinarayana, V., Prisco, J., Powers, E., Pincus, M., Allen, R. E., & August, P. R. (2016). Laminin 521 maintains differentiation potential of mouse and human satellite cell-derived myoblasts during long-term culture expansion. *Skelet Muscle, 6*(1), 44. doi: 10.1186/s13395-016-0116-4

Pernow, J., & Jung, C. (2013). Arginase as a potential target in the treatment of cardiovascular disease: reversal of arginine steal? *Cardiovasc Res, 98*(3), 334-343. doi: 10.1093/cvr/cvt036

Poisson, J., Lemoinne, S., Boulanger, C., Durand, F., Moreau, R., Valla, D., & Rautou, P. E. (2017). Liver sinusoidal endothelial cells: Physiology and role in liver diseases. *J Hepatol, 66*(1), 212-227. doi: 10.1016/j.jhep.2016.07.009

Popper, H., & Greenberg, R. (1941). Visualization of Vitamin A in rat organs by fluorescence microscopy. *Arch. Path., 32*, 11-32.

Poschmann, G., Seyfarth, K., Besong Agbo, D., Klafki, H. W., Rozman, J., Wurst, W., . . . Stuhler, K. (2014). High-fat diet induced isoform changes of the Parkinson's disease protein DJ-1. *J Proteome Res, 13*(5), 2339-2351. doi: 10.1021/pr401157k

Qiu, R. G., Chen, J., McCormick, F., & Symons, M. (1995). A role for Rho in Ras transformation. *Proc Natl Acad Sci U S A, 92*(25), 11781-11785.

Raber, P., Ochoa, A. C., & Rodriguez, P. C. (2012). Metabolism of L-arginine by myeloid-derived suppressor cells in cancer: mechanisms of T cell suppression and therapeutic perspectives. *Immunol Invest, 41*(6-7), 614-634. doi: 10.3109/08820139.2012.680634

Rajalingam, K., Schreck, R., Rapp, U. R., & Albert, S. (2007). Ras oncogenes and their downstream targets. *Biochim Biophys Acta, 1773*(8), 1177-1195. doi: 10.1016/j.bbamcr.2007.01.012

Ramadori, G., Neubauer, K., Odenthal, M., Nakamura, T., Knittel, T., Schwogler, S., & Meyer zum Buschenfelde, K. H. (1992). The gene of hepatocyte growth factor is expressed in fat-storing cells of rat liver and is downregulated during cell growth and by transforming growth factor-beta. *Biochem Biophys Res Commun, 183*(2), 739-742.

Ramadori, G., Veit, T., Schwogler, S., Dienes, H. P., Knittel, T., Rieder, H., & Meyer zum Buschenfelde, K. H. (1990). Expression of the gene of the alpha-smooth muscle-actin isoform in rat liver and in rat fat-storing (ITO) cells. *Virchows Arch B Cell Pathol Incl Mol Pathol, 59*(6), 349-357.

Rappaport, A. M., Borowy, Z. J., Lougheed, W. M., & Lotto, W. N. (1954). Subdivision of hexagonal liver lobules into a structural and functional unit; role in hepatic physiology and pathology. *Anat Rec, 119*(1), 11-33.

Rauterberg, J., Voss, B., Pott, G., & Gerlach, U. (1981). Connective tissue components of the normal and fibrotic liver. I. Structure, local distribution and metabolism of connective tissue components in the normal liver and changes in chronic liver diseases. *Klin Wochenschr, 59*(14), 767-779.

Reimann, T., Hempel, U., Krautwald, S., Axmann, A., Scheibe, R., Seidel, D., & Wenzel, K. W. (1997). Transforming growth factor-beta1 induces activation of Ras, Raf-1, MEK and MAPK in rat hepatic stellate cells. *FEBS Lett, 403*(1), 57-60.

Reya, T., Duncan, A. W., Ailles, L., Domen, J., Scherer, D. C., Willert, K., . . . Weissman, I. L. (2003). A role for Wnt signalling in self-renewal of haematopoietic stem cells. *Nature, 423*(6938), 409-414. doi: 10.1038/nature01593

Rockey, D. C., & Chung, J. J. (1995). Inducible nitric oxide synthase in rat hepatic lipocytes and the effect of nitric oxide on lipocyte contractility. *J Clin Invest, 95*(3), 1199-1206. doi: 10.1172/JCI117769

Rodin, S., Antonsson, L., Niaudet, C., Simonson, O. E., Salmela, E., Hansson, E. M., . . . Tryggvason, K. (2014). Clonal culturing of human embryonic stem cells on laminin-521/E-cadherin matrix in defined and xeno-free environment. *Nat Commun, 5*, 3195. doi: 10.1038/ncomms4195

Rohn, F., Kordes, C., Castoldi, M., Gotze, S., Poschmann, G., Stuhler, K., . . . Haussinger, D. (2018). Laminin-521 promotes quiescence in isolated stellate cells from rat liver. *Biomaterials, 180*, 36-51. doi: 10.1016/j.biomaterials.2018.07.008

Rojas, A. M., & Valencia, A. (2014). Evolution of the Ras Superfamily of GTPases. In A. Wittinghofer (Ed.), *Ras Superfamily Small G Proteins: Biology and Mechanisms 1* (pp. 3-23): Springer Vienna.

Roskams, T. (2008). Relationships among stellate cell activation, progenitor cells, and hepatic regeneration. *Clin Liver Dis, 12*(4), 853-860, ix. doi: 10.1016/j.cld.2008.07.014

Sabatini, D. M. (2017). Twenty-five years of mTOR: Uncovering the link from nutrients to growth. *Proc Natl Acad Sci U S A, 114*(45), 11818-11825. doi: 10.1073/pnas.1716173114

Saraste, M., Sibbald, P. R., & Wittinghofer, A. (1990). The P-loop--a common motif in ATP- and GTP-binding proteins. *Trends Biochem Sci, 15*(11), 430-434.

Sarbassov, D. D., Guertin, D. A., Ali, S. M., & Sabatini, D. M. (2005). Phosphorylation and Regulation of Akt/PKB by the Rictor-mTOR Complex. *Science, 307*(5712), 1098-1101. doi: 10.1126/science.1106148

Satoh, T. (2014). Rho GTPases in insulin-stimulated glucose uptake. *Small GTPases, 5*, e28102. doi: 10.4161/sgtp.28102

Sawitza, I., Kordes, C., Gotze, S., Herebian, D., & Haussinger, D. (2015). Bile acids induce hepatic differentiation of mesenchymal stem cells. *Sci Rep, 5*, 13320. doi: 10.1038/srep13320

Sawitza, I., Kordes, C., Reister, S., & Haussinger, D. (2009). The niche of stellate cells within rat liver. *Hepatology, 50*(5), 1617-1624. doi: 10.1002/hep.23184

Scheffzek, K., Ahmadian, M. R., Kabsch, W., Wiesmuller, L., Lautwein, A., Schmitz, F., & Wittinghofer, A. (1997). The Ras-RasGAP complex: structural basis for GTPase activation and its loss in oncogenic Ras mutants. *Science, 277*(5324), 333-338.

Schirmacher, P., Geerts, A., Pietrangelo, A., Dienes, H. P., & Rogler, C. E. (1992). Hepatocyte growth factor/hepatopoietin A is expressed in fat-storing cells from rat liver but not myofibroblast-like cells derived from fat-storing cells. *Hepatology, 15*(1), 5-11.

Schlichting, I., Almo, S. C., Rapp, G., Wilson, K., Petratos, K., Lentfer, A., . . . et al. (1990). Time-resolved X-ray crystallographic study of the conformational change in Ha-Ras p21 protein on GTP hydrolysis. *Nature, 345*(6273), 309-315. doi: 10.1038/345309a0

Schroder, W. A., Buck, M., Cloonan, N., Hancock, J. F., Suhrbier, A., Sculley, T., & Bushell, G. (2007). Human Sin1 contains Ras-binding and pleckstrin homology domains and suppresses Ras signalling. *Cell Signal, 19*(6), 1279-1289. doi: 10.1016/j.cellsig.2007.01.013

Shaw, A. S., & Filbert, E. L. (2009). Scaffold proteins and immune-cell signalling. *Nat Rev Immunol, 9*(1), 47-56. doi: 10.1038/nri2473

She, H., Xiong, S., Hazra, S., & Tsukamoto, H. (2005). Adipogenic transcriptional regulation of hepatic stellate cells. *J Biol Chem, 280*(6), 4959-4967. doi: 10.1074/jbc.M410078200

Shetty, S., Lalor, P. F., & Adams, D. H. (2018). Liver sinusoidal endothelial cells - gatekeepers of hepatic immunity. *Nat Rev Gastroenterol Hepatol, 15*(9), 555-567. doi: 10.1038/s41575-018-0020-y

Sin, Y. Y., Ballantyne, L. L., Mukherjee, K., St Amand, T., Kyriakopoulou, L., Schulze, A., & Funk, C. D. (2013). Inducible arginase 1 deficiency in mice leads to hyperargininemia and altered amino acid metabolism. *PLoS One, 8*(11), e80001. doi: 10.1371/journal.pone.0080001

Sin, Y. Y., Baron, G., Schulze, A., & Funk, C. D. (2015). Arginase-1 deficiency. *J Mol Med (Berl), 93*(12), 1287-1296. doi: 10.1007/s00109-015-1354-3

Sun, S., Xu, M. Z., Poon, R. T., Day, P. J., & Luk, J. M. (2010). Circulating Lamin B1 (LMNB1) biomarker detects early stages of liver cancer in patients. *J Proteome Res, 9*(1), 70-78. doi: 10.1021/pr9002118

Svegliati-Baroni, G., Ridolfi, F., Di Sario, A., Casini, A., Marucci, L., Gaggiotti, G., . . . Folli, F. (1999). Insulin and insulin-like growth factor-1 stimulate proliferation and type I collagen accumulation by human hepatic stellate cells: differential effects on signal transduction pathways. *Hepatology, 29*(6), 1743-1751. doi: 10.1002/hep.510290632

Svegliati-Baroni, G., Saccomanno, S., van Goor, H., Jansen, P., Benedetti, A., & Moshage, H. (2001). Involvement of reactive oxygen species and nitric oxide radicals in activation and proliferation of rat hepatic stellate cells. *Liver, 21*(1), 1-12.

Tabibian, J. H., Masyuk, A. I., Masyuk, T. V., O'Hara, S. P., & LaRusso, N. F. (2013). Physiology of cholangiocytes. *Compr Physiol, 3*(1), 541-565. doi: 10.1002/cphy.c120019

Taha, M. S., Nouri, K., Milroy, L. G., Moll, J. M., Herrmann, C., Brunsveld, L., . . . Ahmadian, M. R. (2014). Subcellular fractionation and localization studies reveal a direct interaction of the fragile X mental retardation protein (FMRP) with nucleolin. *PLoS One, 9*(3), e91465. doi: 10.1371/journal.pone.0091465

Takahashi, K., Mitsui, K., & Yamanaka, S. (2003). Role of ERas in promoting tumour-like properties in mouse embryonic stem cells. *Nature, 423*(6939), 541-545. doi: 10.1038/nature01646

nature01646 [pii]

Takeya, R., & Sumimoto, H. (2003). Molecular mechanism for activation of superoxide-producing NADPH oxidases. *Mol Cells, 16*(3), 271-277.

Tanaka, S., Takasawa, A., Fukasawa, Y., Hasegawa, T., & Sawada, N. (2012). An undifferentiated embryonal sarcoma of the liver containing adipophilin-positive vesicles in an adult with massive sinusoidal invasion. *Int J Clin Exp Pathol, 5*(8), 824-829.

Tatebe, H., Murayama, S., Yonekura, T., Hatano, T., Richter, D., Furuya, T., . . . Shiozaki, K. (2017). Substrate specificity of TOR complex 2 is determined by a ubiquitin-fold domain of the Sin1 subunit. *Elife, 6*. doi: 10.7554/eLife.19594

Teupser, D., Burkhardt, R., Wilfert, W., Haffner, I., Nebendahl, K., & Thiery, J. (2006). Identification of macrophage arginase I as a new candidate gene of atherosclerosis resistance. *Arterioscler Thromb Vasc Biol, 26*(2), 365-371. doi: 10.1161/01.ATV.0000195791.83380.4c

Thomas, R. J., Bhandari, R., Barrett, D. A., Bennett, A. J., Fry, J. R., Powe, D., . . . Shakesheff, K. M. (2005). The effect of three-dimensional co-culture of hepatocytes and hepatic stellate cells on key hepatocyte functions in vitro. *Cells Tissues Organs, 181*(2), 67-79. doi: 10.1159/000091096

Tidyman, W. E., & Rauen, K. A. (2009). The RASopathies: developmental syndromes of Ras/MAPK pathway dysregulation. *Current Opinion in Genetics & Development, 19*(3), 230-236. doi: 10.1016/j.gde.2009.04.001

Tomiya, T., Nishikawa, T., Inoue, Y., Ohtomo, N., Ikeda, H., Tejima, K., . . . Fujiwara, K. (2007). Leucine stimulates HGF production by hepatic stellate cells through mTOR pathway. *Biochem Biophys Res Commun, 358*(1), 176-180. doi: 10.1016/j.bbrc.2007.04.093

Tontonoz, P., & Spiegelman, B. M. (2008). Fat and beyond: the diverse biology of PPARgamma. *Annu Rev Biochem, 77*, 289-312. doi: 10.1146/annurev.biochem.77.061307.091829

Troeger, J. S., Mederacke, I., Gwak, G. Y., Dapito, D. H., Mu, X., Hsu, C. C., . . . Schwabe, R. F. (2012). Deactivation of hepatic stellate cells during liver fibrosis resolution in mice. *Gastroenterology, 143*(4), 1073-1083 e1022. doi: 10.1053/j.gastro.2012.06.036

Tsuchida, T., & Friedman, S. L. (2017). Mechanisms of hepatic stellate cell activation. *Nat Rev Gastroenterol Hepatol, 14*(7), 397-411. doi: 10.1038/nrgastro.2017.38

Tusher, V. G., Tibshirani, R., & Chu, G. (2001). Significance analysis of microarrays applied to the ionizing radiation response. *Proc Natl Acad Sci U S A, 98*(9), 5116-5121. doi: 10.1073/pnas.091062498

von Kupffer, K. W. (1876). Ueber Sternzellen der Leber - Briefliche Mitteilung an Prof. Waldyer. *Arch mikr Anat, 12*, 353-358.

Wake, K. (1971). "Sternzellen" in the liver: perisinusoidal cells with special reference to storage of vitamin A. *Am J Anat, 132*(4), 429-462. doi: 10.1002/aja.1001320404

Wake, K. (2006). Hepatic stellate cells: Three-dimensional structure, localization, heterogeneity and development. *Proc. Jpn. Acad. Ser., 82*, 155-164.

Wang, D., Wu, P., Wang, H., Zhu, L., Zhao, W., & Lu, Y. (2016). SIN1 promotes the proliferation and migration of breast cancer cells by Akt activation. *Biosci Rep, 36*(6). doi: 10.1042/BSR20160192

Wang, D. R., Sato, M., Sato, T., Kojima, N., Higashi, N., & Senoo, H. (2004). Regulation of matrix metallo-proteinase expression by extracellular matrix components in cultured hepatic stellate cells. *Comp Hepatol, 3 Suppl 1*, S20. doi: 10.1186/1476-5926-2-s1-s20

Wang, X., DeFrances, M. C., Dai, Y., Pediaditakis, P., Johnson, C., Bell, A., . . . Zarnegar, R. (2002). A mechanism of cell survival: sequestration of Fas by the HGF receptor Met. *Mol Cell, 9*(2), 411-421.

Wang, Y., Zhou, Y., & Graves, D. T. (2014). FOXO transcription factors: their clinical significance and regulation. *Biomed Res Int, 2014*, 925350. doi: 10.1155/2014/925350

Wennerberg, K., Rossmann, K. L., & Der, C. J. (2005). The Ras superfamily at a glance. *Journal of Cell Science, 118*(5), 843-846. doi: 10.1242/jcs.01660

Wiest, R., & Groszmann, R. J. (1999). Nitric oxide and portal hypertension: its role in the regulation of intrahepatic and splanchnic vascular resistance. *Semin Liver Dis, 19*(4), 411-426. doi: 10.1055/s-2007-1007129

Wittinghofer, A., & Vetter, I. R. (2011). Structure-function relationships of the G domain, a canonical switch motif. *Annu Rev Biochem, 80*, 943-971. doi: 10.1146/annurev-biochem-062708-134043

Wu, G., & Morris, S. M., Jr. (1998). Arginine metabolism: nitric oxide and beyond. *Biochem J, 336 ( Pt 1)*, 1-17.

Wuertenberger, S., & Groemping, Y. (2015). A single PXXP motif in the C-terminal region of srGAP3 mediates binding to multiple SH3 domains. *FEBS Lett, 589*(10), 1156-1163. doi: 10.1016/j.febslet.2015.03.014

Xie, G., Karaca, G., Swiderska-Syn, M., Michelotti, G. A., Krüger, L., Chen, Y., . . . Diehl, A. M. (2013). Cross-talk between Notch and Hedgehog regulates hepatic stellate cell fate in mice. *Hepatology, 58*(5), 1801-1813. doi: 10.1002/hep.26511

Xie, J., & Proud, C. G. (2013). Crosstalk between mTOR complexes. *Nature Cell Biology, 15*(11), 1263-1265. doi: 10.1038/ncb2877

Xu, D. H., Liu, F., Li, X., Chen, X. F., Jing, G. J., Wu, F. Y., . . . Li, Q. F. (2014). Regulatory role of nucleophosmin during the differentiation of human liver cancer cells. *Int J Oncol, 45*(1), 264-272. doi: 10.3892/ijo.2014.2407

Yan, B. C., Gong, C., Song, J., Krausz, T., Tretiakova, M., Hyjek, E., . . . Hart, J. A. (2010). Arginase-1: a new immunohistochemical marker of hepatocytes and hepatocellular neoplasms. *Am J Surg Pathol, 34*(8), 1147-1154. doi: 10.1097/PAS.0b013e3181e5dffa

Yang, G., Murashige, D. S., Humphrey, S. J., & James, D. E. (2015). A Positive Feedback Loop between Akt and mTORC2 via SIN1 Phosphorylation. *Cell Rep, 12*(6), 937-943. doi: 10.1016/j.celrep.2015.07.016

Yang, L., Jung, Y., Omenetti, A., Witek, R. P., Choi, S., Vandongen, H. M., . . . Diehl, A. M. (2008). Fate-mapping evidence that hepatic stellate cells are epithelial progenitors in adult mouse livers. *Stem Cells, 26*(8), 2104-2113. doi: 10.1634/stemcells.2008-0115

Yang, Z., & Ming, X. F. (2013). Arginase: the emerging therapeutic target for vascular oxidative stress and inflammation. *Front Immunol, 4*, 149. doi: 10.3389/fimmu.2013.00149

Yasuda, K., Yashiro, M., Sawada, T., Ohira, M., & Hirakawa, K. (2007). ERas oncogene expression and epigenetic regulation by histone acetylation in human cancer cells. *Anticancer Res, 27*(6B), 4071-4075.

Yin, C., Evason, K. J., Asahina, K., & Stainier, D. Y. R. (2013). Hepatic stellate cells in liver development, regeneration, and cancer. *Journal of Clinical Investigation, 123*(5), 1902-1910. doi: 10.1172/jci66369

Yokoi, Y., Namihisa, T., Kuroda, H., Komatsu, I., Miyazaki, A., Watanabe, S., & Usui, K. (1984). Immunocytochemical detection of desmin in fat-storing cells (Ito cells). *Hepatology, 4*(4), 709-714.

Yoneda, A., Sakai-Sawada, K., Niitsu, Y., & Tamura, Y. (2016). Vitamin A and insulin are required for the maintenance of hepatic stellate cell quiescence. *Exp Cell Res, 341*(1), 8-17. doi: 10.1016/j.yexcr.2016.01.012

Yu, J. S., & Cui, W. (2016). Proliferation, survival and metabolism: the role of PI3K/AKT/mTOR signalling in pluripotency and cell fate determination. *Development, 143*(17), 3050-3060. doi: 10.1242/dev.137075

Yu, Y., Liang, D., Tian, Q., Chen, X., Jiang, B., Chou, B.-K., . . . Wang, G. (2014). Stimulation of Somatic Cell Reprogramming by ERas-Akt-FoxO1 Signaling Axis. *Stem Cells, 32*(2), 349-363. doi: 10.1002/stem.1447

Yuan, M., Pino, E., Wu, L., Kacergis, M., & Soukas, A. A. (2012). Identification of Akt-independent regulation of hepatic lipogenesis by mammalian target of rapamycin (mTOR) complex 2. *J Biol Chem, 287*(35), 29579-29588. doi: 10.1074/jbc.M112.386854

Yuan, Y., Pan, B., Sun, H., Chen, G., Su, B., & Huang, Y. (2015). Characterization of Sin1 Isoforms Reveals an mTOR-Dependent and Independent Function of Sin1gamma. *PLoS One, 10*(8), e0135017. doi: 10.1371/journal.pone.0135017

Zaikina, E. I., Shafigullina, A. K., Titova, A. A., Burganova, G. R., Pevnev, G. O., Mavlikeev, M. O., . . . Kiassov, A. P. (2017). Native and Activated Hepatic Stellate Cells Stimulate Liver Regeneration in Rats After Partial Hepatectomy and 2-Acetylaminofluorene Injection. *BioNanoSci, 7*(1), 246-250. doi: https://doi.org/10.1007/s12668-016-0353-3

Zamecka, E., & Porembska, Z. (1988). Five forms of arginase in human tissues. *Biochem Med Metab Biol, 39*(3), 258-266.

Zhang, F., Zhang, Z., Kong, D., Zhang, X., Chen, L., Zhu, X., . . . Zheng, S. (2014). Tetramethylpyrazine reduces glucose and insulin-induced activation of hepatic stellate cells by inhibiting insulin

receptor-mediated PI3K/AKT and ERK pathways. *Mol Cell Endocrinol, 382*(1), 197-204. doi: 10.1016/j.mce.2013.09.020

Zhang, S. C., Gremer, L., Heise, H., Janning, P., Shymanets, A., Cirstea, I. C., . . . Ahmadian, M. R. (2014). Liposome reconstitution and modulation of recombinant prenylated human Rac1 by GEFs, GDI1 and Pak1. *PLoS One, 9*(7), e102425. doi: 10.1371/journal.pone.0102425

Zhang, S. C., Nouri, K., Amin, E., Taha, M. S., Nakhaeizadeh, H., Nakhaei-Rad, S., . . . Ahmadian, M. R. (2014). Classical Rho Proteins: Biochemistry of Molecular Switch Function and Regulation. In A. Wittinghofer (Ed.), *Ras Superfamily Small G Proteins: Biology and Mechanisms 1* (pp. 327-340): Springer Vienna.

Zhou, T.-B., Drummen, G., & Qin, Y.-H. (2012). The Controversial Role of Retinoic Acid in Fibrotic Diseases: Analysis of Involved Signaling Pathways. *International Journal of Molecular Sciences, 14*(1), 226-243. doi: 10.3390/ijms14010226

Zoncu, R., Efeyan, A., & Sabatini, D. M. (2011). mTOR: from growth signal integration to cancer, diabetes and ageing. *Nat Rev Mol Cell Biol, 12*(1), 21-35. doi: 10.1038/nrm3025

Zong, Y., Panikkar, A., Xu, J., Antoniou, A., Raynaud, P., Lemaigre, F., & Stanger, B. Z. (2009). Notch signaling controls liver development by regulating biliary differentiation. *Development, 136*(10), 1727-1739. doi: 10.1242/dev.029140

# 8. Supplement

## 8.1. Publications

Publications within the dissertation:

Nakhaei-Rad, S., Haghighi, F., Nouri, P., Adariani, S. R., **Lissy, J**., Jasemi, N. S. K., Dvorsky, R., and Ahmadian, M. R. (2018). "Structural fingerprints, interactions, and signaling networks of RAS family proteins beyond RAS isoforms." Critical Reviews in Biochemistry and Molecular Biology **53** (2): 130-156.

**Lissy, J**., Nakhaeizadeh, H., Akbarzadeh, M., Taha, M.S., Jasemi, N. S. K., Nakhaei-Rad, S., Pudewell, S., Kordes, C., Janning, P., Hendgen-Cotta, U., Häussinger, D., and Ahmadian, M. R., "Embryonic stem cell-expressed Ras (E-Ras) interacts with Arginase-1 and regulates its activity in quiescent hepatic stellate cells". (Manuscript ready for submission)

**Lissy, J**., Nakhaeizadeh, H., Dvorsky, R., Konopatzki, R., Jasemi, N. S. K., Pudewell, S., Ahmadian, M.R., "Direct SIN1 interaction with Ras proteins regulates mTORC2". (Manuscript in preparation)

## 8.2. Acknowledgements

I would like to express my deepest thanks to Prof. Dr. Reza Ahmadian, who accepted me in his group. I am thankful for his support, patience, and immense knowledge. I am thankful for allowing me to grow as a researcher and opening new horizons to my scientific life. I greatly appreciate giving me the opportunity to gain confidence and build a strong basis for my future career.

My sincere thanks also goes to my colleagues Marcel Buchholzer, Neda Jasemi Kazemein, Mahyar Akbarzadeh, Oliver Krumbach, Paul Baran and Raphael Konopatzki, who were not only simple colleagues, but great friends. I am really grateful for sharing their knowledge and experiences and also our wonderful collaboration.

I would like to extend my thanks to Dr. Roland Piekorz for his scientific discussion, advice, motivation and never ending optimism. I had the chance to benefit from his knowledge, experience and insightful comments.

I would like to also thank Petra Oprée Jeremic. I couldn't have done it without you. I am so thankful for all your help, support and kindness. You are the BEST!

I am also grateful to: Dr. Doreen Floss, Dr. Jens Moll, Dr. Hossein Nakhaeizadeh, Dr. Saeideh Nakhaei-Rad, Fereshteh Kamrani, and all other colleagues in the institute of biochemistry and molecular biology II for our great friendship and collaboration.

My sincere thanks goes to the German Research Foundation (Deutsche Forschungsgemeinschaft; DFG) for the financial support.

Last but not the least; I would like to thank my lovely family, especially my husband Maik. I cannot express my feeling with words, I love you and I am happy that I can always trust you and count on all of you. You always support me and help me how to be an independent, strong and happy person. Without your help and support I would not be where I am now. And I am happy to soon welcome our little baby girl Louisa!

# Eidesstattliche Erklärung

Hiermit versichere ich, dass die vorliegende Dissertation von mir selbstständig und ohne unzulässige fremde Hilfe unter Beachtung der „Grundsätze zur Sicherung guter wissenschaftlicher Praxis an der Heinrich-Heine-Universität Düsseldorf“ verfasst worden ist.
Die Dissertation wurde in der vorgelegten oder in ähnlicher Form noch bei keiner anderen Institution eingereicht. Ich habe bisher keine erfolglosen Promotionsversuche unternommen.

Düsseldorf, den

_____

(Jana Lissy)